STUDIES OF REGENERATION OF CATALYTIC REFORMING CATALYST

PRESENTED TO CHEMICAL ENGINEERING DEPARTMENT
AHMADU BELLO UNIVERSITY, ZARIA.

BY

TAIWO OLAMIDE OLORI
(M.Sc/ENG/6776/2010-2011)

IN PARTIAL FULFILLMENT OF THE REQUIREMENTS FOR THE AWARD

OF

MASTERS OF SCIENCE DEGREE IN CHEMICAL ENGINEERING

DEPARTMENT OF CHEMICAL ENGINEERING,
AHMADU BELLO UNIVERSITY,
ZARIA, NIGERIA.

AUGUST, 2015

DECLARATION

I, Olori Taiwo Olamide hereby declare that the work in this thesis titled **"Studies Of Regeneration of Catalytic Reforming Catalyst"** was performed by me in the Department of Chemical Engineering, Ahmadu Bello University, Zaria, under the supervision of Dr. P. C. Okonkwo and Professor B. O. Aderemi.

All information derived from literature have been duly acknowledged and a list of reference provided. No part of this work has been presented for another degree or diploma at any institution**.**

_____ _____

Signature Date

CERTIFICATION

This dissertation **"Studies of Regeneration of Catalytic Reforming Catalyst"** meets the regulations governing the award of the degree of Master of the Ahmadu Bello University, and is approved for its contribution to knowledge and literary presentation.

Dr. P. C. Okonkwo	_____	_____
Chairman, Supervisory Committee	Signature	Date
Prof B. O. Aderemi	_____	_____
Member, Supervisory Committee	Signature	Date
Dr. S. M. Waziri	_____	_____
Head, Department of Chemical Engineering, A.B.U Zaria	Signature	Date
Professor Kabir Bala	_____	_____
Dean, Postgraduate School, A.B.U Zaria	Signature	Date

DEDICATION

This work is dedicated to GOD almighty.

ACKNOWLEDGEMENTS

My sincere appreciation goes to God almighty for the wisdom to carry out this research work and for the gift of life. And all praises to HIM. I want to express my profound gratitude to my supervisors, Dr. P. C. Okonkwo and Prof. B. O Aderemi as member, for their patience and understanding, moral and intellectual contributions to the success of this research. You are more than supervisors and lecturers to me; you have trained me to be a relentless and diligent researcher. May God bless you all. I will live to remember these great pools of knowledge.

I will forever remain grateful to my beloved parents Mr and Mrs Ademola Olori for such an upbringing, for their immeasurable support, love and care. The encouragement and supports of my darling, caring wife (Khadijat), my precious daughters (Qaanitah and Qadriyah) and my siblings are immensely appreciated.

My appreciation will be incomplete if I fail to acknowledge some true friends and colleagues Engr. Solomon Bawa, Engr. Akpan, Engr. Wawata, Engr. Amauche, Engr. Awwal, Mr. Oloworise Femi, Engr. Osaze, Mr. Oseke Gbenga, Mr. Omole Kehinde, Mr. Odion Promise, Mr. Jordan and Akor Treasure Roseline, your immense contributions to this work will ever be remembered. May God reward you all bountifully.

ABSTRACT

A study of regeneration of naphtha reforming catalyst was carried out in this work. Two samples of deactivated catalysts were collected at different on-line reforming hours before their usual end of life cycle. The catalyst were characterized using X-ray diffraction (XRD), Xray fluorescence (XRF), Fourier transform infrared spectroscope (FTIR), scanning electron microscopic (SEM) techniques and gas chromatograph/Mass spectrometer (GC/MS). The deactivated catalyst samples were calcined at different temperatures (400 ^{O}C – 800 ^{O}C), air pressures (0.7 – 2.1 kg/cm^2) and times (2 – 8 hours) to obtain ptimum regeneration condition with the addition of dichloropropane to boost the activity of the catalyst. Optimum regeneration temperature, air pressure and time (500 ^{O}C, 1 bar and 4 hours respectively) were obtained via gravimetric method. After regeneration, the FTIR showed the removal of coke (band frequency 2800 -3000 cm^{-1}), the XRD pattern showed that the metal and the support for all the catalysts had similar Bragg angle which coincides at 39 ^{0}, 46 ^{0} and 68 ^{0}, while the support is amorphous, the crystalline nature of platinum enhances the peaks. XRF analyis showed platinum and alumina to be dominant before and after regeneration. The catalytic performance of the catalysts were determined for fresh, deactivated and regenerated catalysts using treated heavy naphtha as substrate at 465 ^{o}C reactor temperature. The results showed low reformate yield for deactivated catalysts (60.47 % and 77.74 %). Nonetheless, a significant improvement in the reformate yield was observed after regeneration of the catalyst from 60.47 % to 76.65 % and 77.74 % to 83.86 %. The regenerated catalyst performance compared favourably. The selectivity of all the catalysts for iso-paraffins were quite impressive. The reformate obtained from regenerated deactivated B catalyst 83.86 % yield contains more of iso-paraffins which are useful for gasoline blend but

unsuitable for production of petrochemical products e.g. kero solvent, benzene, toluene or xylene.

TABLE OF CONTENT

Title Page	i
Declaration	ii
Certification	iii
Dedication	iv
Acknowledgements	v
Abstract	vi
Table of Content	viii
List of Figures	xii
List of Tables	xv
List of Plates	xvii
List of Appendices	xviii
List of Abbreviations and Symbols	xix
CHAPTER ONE	1
1.0 INTRODUCTION	1
1.1 Background Study	1
1.2 Research Problem	3
1.3 Research Scope	4
1.4 Research Aim and Objectives.	4
1.5 Research Justification	5
CHAPTER TWO	6
2.0 LITERATURE REVIEW	6
2.1 Introduction	6
2.2 Platinum/Alumina Base Catalyst	7
2.2.1 Platinum	7

2.2.2 Alumina 8

2.2.3 Platinum/Alumina 8

2.3 Catalyst Reforming 9

2.4 Catalytic Reforming Processes (Regenerative Methods) 13

2.4.1 Semiregenerative Process 14

2.4.2 Cyclic (Fully Regenerative) Process 16

2.4.3 Continuous Regenerative Process 17

2.5 Commercial Reforming Processes 19

2.6 Catalyst Deactivation and Regeneration 20

2.6.1 Catalyst Deactivation 20

2.6.2 Reforming side reactions mechanism 23

2.6.3 Purpose of Regeneration 28

2.6.4 Benefit of Regeneration 28

2.7 Catalyst Performance 28

2.7.1 Activity 28

2.7.2 Selectivity 29

2.7.3 Stability 29

2.8 KRPC Catalytic Reformer Unit (CRU) Background Information 30

2.8.1 Feed Stock Composition in a reforming unit 32

2.8.3 Operating Variables 35

2.9 Chemical Composition Analysis 38

2.9.1 Basic principles of XRD and XRF analysis 38

2.9.2 Basic Principles of SEM Analysis 39

2.9.3 Basic Principles of GC-MS Analysis 40

2.9.4 Basic Principles of FTIR Analysis 42

2.9.5 Surface area determination by Sear's method 42

CHAPTER 3 43

3.0 MATERIALS, EQUIPMENT AND METHODS 43

3.1 Materials 43

3.2 Apparatus 43

3.3 Equipment 44

3.4 Experimental Procedures 45

3.5 Parametric Study 46

3.6 Regeneration Processes 47

3.6.1 First stage combustion 49

3.6.2 Second stage combustion. 50

3.6.3 Proof burning (third stage combustion) 50

3.6.4 Oxychlorination 51

3.6.5 Calcination 51

3.6.6 Rinsing and Drying 52

3.6.7 Cooling 52

3.7 Catalysts' Reformation/Activity Performance Evaluations 52

3.8 Catalyst Performance Evaluation 53

3.9 Product Characterization 55

3.10 Limitations Encountered 56

CHAPTER FOUR 57

4.0 RESULTS AND DISCUSSION 57

4.1 Catalyst Characterization 57

4.1.1 FT-IR analysis of the catalysts 60

4.1.2 XRD pattern analysis 67

4.1.2. XRF Analysis 69

4.1.3 Carbon Composition of Catalyst 70

4.1.4 Morphology of Catalysts 72

4.1.5 Catalysts textural properties 83

4.2 Catalysts' Performance Evaluations 84

4.2.1 Component Identification Method 85

CHAPTER FIVE 89

5.0 CONCLUSIONS AND RECOMMENDATIONS 89

5.1 Conclusions 89

5.2 Recommendations 91

REFERENCES 92

APPENDICES 97

Appendix A 97

Appendix B 110

Appendix C 117

LIST OF FIGURES

Figure 2.1: Example of a processing scheme for refinery gasoline production with catalytic reforming 12

Figure 2.2: Schematic diagram of a typical semi-regenerative catalytic reformer unit in a petroleum refinery 13

Figure 2.3: Semiregenerative reformer 15

Figure 2.4: Cyclic regenerative reformer: Amoco's Ultraformer 17

Figure 2.5: UOP CCR Platformer (Reactor section). 19

Figure 2.6: Catalyst distribution in the reactors for feed and product in a reforming unit. 31

Figure 2.7: Catalyst distribution in the reactors in terms of temperature 31

Figure 3.1: Schematic Diagrams for the Laboratory Set-up for Parametric Study. 46

Figure 3.2: Schematic diagrams for the laboratory set-up for regeneration of deactivated catalysts. 48

Figure 3.3: Schematic diagram for the laboratory set-up for heavy naphtha reformation for catalyst performance 53

Figure 4.1: Catalyst weight loss in decoking presented in weight percentage at 15psi, 4hours and at various temperature range 57

Figure 4.2: Catalyst weight loss in decoking presented in weight percentage at optimum temperature, 4hrs and at various air flowrate. 58

Figure 4.3: Catalyst weight loss in decoking presented in weight percentage at optimum temperature and pressure and at various time range. 58

Figure 4.4: FTIR spectroscopy analysis of fresh, deactivated A and deactivated B catalyst before calcinations. 61

Figure 4.5: FTIR spectroscopy of fresh and deactivated A at 400^{o}C, 500^{o}C, 600^{o}C, 700^{o}C and 800^{o}C calcinations 63

Figure 4.6: FTIR spectroscopy of fresh and deactivated B at 400^{o}C, 500^{o}C, 600^{o}C and 700^{o}C and 800^{o}C calcinations 63

Figure 4.7: FTIR spectroscopy of fresh, deactivated A at 500^{o}C for 2, 4, 6 and 8hours calcinations 64

Figure 4.8: FTIR spectroscopy of fresh, deactivated B at 500^{o}C for 2, 4, 6 and 8hours calcinations 64

Figure 4.9: FTIR spectroscopy analysis of fresh, regenerated deactivated A and regenerated deactivated B catalyst 66

Figure 4.10: XRD patterns of the fresh, two deactivated catalysts and the regenerated catalysts. 67

Figure 4.11: Fresh catalyst pore-fibre length and surface area histogram 74

Figure 4.12: Deactivated A pore-fibre length and surface area histogram 76

Figure 4.13: Deactivated B pore-fibre length and surface area histogram 78

Figure 4.14: Regenerated deactivated A pore-fibre length and surface area histogram80

Figure 4.15: Regenerated deactivated B pore-fibre length and surface area histogram 82

Figure 4.16: A Mass Spectrum representing a sample composition of product from GCMS 85

Figure A.1: FTIR spectroscopy analysis of deactivated A on 400 ^{o}C calcinations. 99

Figure A.2: FTIR spectroscopy analysis of deactivated B on 400 ^{o}C calcinations 100

Figure A.3: FTIR spectroscopy of fresh, deactivated A and deactivated B catalyst at 400 ^{o}C calcinations 100

Figure A.4: FTIR spectroscopy of fresh, deactivated A and deactivated B catalyst at 500 ^{o}C calcinations. 101

Figure A.5: FTIR spectroscopy of fresh, deactivated Aand deactivated B catalyst at 600 ^{o}C calcinations 101

Figure A.6: FTIR spectroscopy of fresh, deactivated A and deactivated B catalyst at 700 ^{o}C calcinations 101

Figure A.7: FTIR spectroscopy of fresh, deactivated A and deactivated B catalyst at 800 ^{o}C calcinations 102

Figure A.8: FTIR spectroscopy of fresh and deactivated A at 400 ^{o}C, 500 ^{o}C, 600 ^{o}C,700 ^{o}C and 800 ^{o}C calcinations 102

Figure A.9: FTIR spectroscopy of fresh and deactivated B at 400 ^{o}C, 500 ^{o}C, 600 ^{o}C,700 ^{o}C and 800 ^{o}C calcinations 103

Figure A.10: FTIR spectroscopy of deactivated A at 500 ^{o}C for 2 hours calcinations 103

Figure A.11: FTIR spectroscopy of deactivated A at 500 ^{o}C for 4 hours calcinations 104

Figure A.12: FTIR spectroscopy of deactivated A at 500 ^{o}C for 6 hours calcinations 104

Figure A.13: FTIR spectroscopy of deactivated A at 500 ^{o}C for 8 hours calcinations 104

Figure A.14: FTIR spectroscopy of fresh, deactivated A at 500^{o}C for 2, 4, 6 and 8 hours calcinations 105

Figure A.15: FTIR spectroscopy of deactivated B at 500^{o}C for 2 hours calcinations 105

Figure A.16: FTIR spectroscopy of deactivated B at 500^{o}C for 4 hours calcinations 106

Figure A.17: FTIR spectroscopy of deactivated B at 500^{o}C for 6 hours calcinations 106

Figure A.18: FTIR spectroscopy of deactivated B at 500^{o}C for 8 hours calcinations 106

Figure A.19: FTIR spectroscopy of fresh, deactivated B at 500^{o}C for 2, 4, 6 and 8 hours calcinations 107

Figure A.20: FTIR spectroscopy analysis of regenerated deactivated A 107

Figure A.21: FTIR spectroscopy analysis of regenerated deactivated B. 108

Figure A.22: FTIR spectroscopy analysis of fresh, deactivated A and regenerated A catalyst 108

Figure A.23: FTIR spectroscopy analysis of fresh, deactivated B and regenerated B catalyst. 109

LIST OF TABLES

Table 2.1. Catalyst Quantities for fresh and old catalyst after regeneration. 32

Table 2.2: Design Feed (Naphtha) Stock Composition 33

Table 3.1: List of other equipment used in this work and their specifications 44

Table 4.1: Catalyst Weight loss in percentage of deactivated catalyst A and B after regeneration using the ranges of optimum conditions. 60

Table 4.2: XRF analysis of the catalysts 69

Table 4.3: Carbon Composition on Catalyst. 71

Table 4.4: EDX spots on the SEM image for the Fresh catalyst 74

Table 4.5: EDX spots on the SEM image for the deactivated A catalyst 76

Table 4.6: EDX spots on the SEM image for the deactivated B catalyst 78

Table 4.7 EDX spots on the SEM image for the regenerated A catalyst 80

Table 4.8: EDX spots on the SEM image for the regenerated B catalyst 82

Table 4.9: Surface Area Transition of Catalyst. 83

Table 4.10: Specific Surface Area of the catalysts. 84

Table 4.11: Summary of Catalysts Performance Evaluations 86

Table A.1: Catalyst Weight loss in decoking presented in weight percentage at 1bar, 4hrs and at various temperature range. 98

Table A.2: Catalyst Weight loss in decoking presented in weight percentage at optimum temperature 500 ^{o}C, 4hrs and at various air flowrate 98

Table A.3: Catalyst Weight loss in decoking presented in weight percentage at optimum temperature and pressure and at various time range. 99

Table B.1: Summarized GC-MS results for the feed (Treated heavy naphtha) 110

Table B.2: Summarized GC-MS results for reactor packed with Fresh Catalyst 111

Table B.3: Summarized GC-MS results for reactor packed with Deactivated A Catalyst 112

Table B.4: Summarized GC-MS results for reactor packed with Deactivated B Catalyst 113

Table B.5: Summarized GC-MS results for reactor packed with Regenerated Deactivated A Catalyst 114

Table B.6: Summarized GC-MS results for reactor packed with Regenerated Deactivated B Catalyst 115

Table C.1: Summarized GC-MS results for the reformates got from reactor packed with Fresh Catalyst 117

Table C.2: Summarized GC-MS results for the reformates got from reactor packed with Deactivated A Catalyst 118

Table C.3: Summarized GC-MS results for the reformates got from reactor packed with Deactivated B Catalyst 119

Table C.4: Summarized GC-MS results for the reformates got from reactor packed with Regenerated Deactivated A Catalyst 120

Table C.5: Summarized GC-MS results for the reformates got from reactor packed with Regenerated Deactivated B Catalyst 121

Table C.6: Typical product yields in a CCRU operation 122

LIST OF PLATES

Plate 2.8: Kaduna refining and Petrochemical Company 31

Plate 2.9: Catalytic Reforming Unit in Kaduna Refining and Petrochemical Company 32

Plate 3.2: HC/Oxygen gas tester for regeneration of deactivated catalysts. 48

Plate 4.1: SEM and EDX mappings images of fresh catalyst 72

Plate 4.2: SEM and EDX mappings images of deactivated A catalyst. 75

Plate 4.3: SEM and EDX mappings images of deactivated B catalyst. 77

Plate 4.4: SEM and EDX mappings images of regenerated deactivated A catalyst 79

Plate 4.5: SEM and EDX mappings images of regenerated deactivated B catalyst. 81

Plate A.24: Transducer with a thermocouple wire to check temperature difference. 118

LIST OF APPENDICES

Appendix A 97

Appendix B 110

Appendix C 117

LIST OF ABBREVIATIONS AND SYMBOLS

ABU	Ahmadu Bello University
….*et al*	….”and others”
API	American Petroleum Institute
BET	Brunauer-Emmett-Teller
CRU	Catalytic Reforming Unit
cm	centimeter
^{0}C	degree Celsius; (unit of temperature)
θ	Diffraction angle (^{0})
EDX	Energy Dispersive X-ray
FT-IR	Fourier Transform Infra-Red
GC-MS	Gas Chromatograph Mass Spectrometry
g	gram
in	inch
KRPC	Kaduna Refining and Petrochemical Company
kg	kilogram
m	metres
µm	micrometer
ml	milliliters
MLPD	million litres per day
Nm	nanometer
NARICT	National Research Institute for Chemical Technology, (Zaria)
NGRC	National Geoscience Research Centre, Kaduna
ppm	parts per million
SEM	Scanning Electron Microscopy

SSA	Specific surface area per unit mass
RIT	Reactor Inlet Temperature
RO1	First Reactor
RON	Research Octane Number
UOP	Universal oil products
wt %	weight percent
XRD	X-ray Diffraction.
XRF	X-ray Flourescence

CHAPTER ONE

1.0 INTRODUCTION

1.1 Background of study

A number of catalytic processes are employed in the petroleum industry for the purpose of converting crude petroleum to a variety of products having physical and chemical properties which make them suitable for use by consumers. Among the refining processes involving the use of catalysts are cracking, hydrocracking, hydrodesulfurization, hydrodenitrification and reforming. The catalytic reforming of naphtha converts low octane gasoline to high-octane gasoline, and produces benzene, toluene, and xylene (Aitani *et al*., 1995).

However, the catalyst is deactivated during these processes by formation of coke on its surface, which denotes the carbonaceous residues formed from secondary reactions within the catalyst. The catalyst is regenerated by burning off the coke with oxygen/nitrogen mixtures. Therefore, the interest in these catalysts lies not only in their high catalytic activity and selectivity, but also in the possibility of regenerating them several times so that their "lifetime'' is compatible with the cost of their production (Ren *et al*., 2002).

According to Ahmed *et al*. (2011) and Ren *et al*. (2007), coke deposits on platinum alumina catalyst are described in three forms when subjected to gravimetric method using thermo gravimetric analyzer (TGA). Ahmed and Rens work indicated weight loss in percentage (laid coke from 0-0.99 %, soft coke from 1.0-2.99 % and hard coke

from 3.0 % and above) at a lower heating range (10-15 ^{o}C/min) and rate of reaction in terms of individual weight loss for a certain temperature value.

Ordinarily, the plants in which such catalysts are employed have provision for regeneration of catalyst either in the reaction vessel itself or in an adjacent regenerator vessel to which the catalyst is transferred continuously. A number of catalysts are used for extended periods before they become deactivated. On-stream periods of months, or even years, are observed in some of the processes. In these cases, the refining units do not ordinarily include provision for catalyst regeneration and the refiner simply discards the catalyst when it has completely lost activity before replaces it with a fresh charge. On the other hand, the catalyst may be removed from the refining unit and regenerated in a regeneration unit which is neither attached nor related to the refining unit from which the catalyst is taken (Antos *et al*., 2004).

Theoretically, these catalysts can be regenerated by burning the carbonaceous deposits from the catalysts' surfaces and so restoring catalyst activity to a level of about 90 % of the activity of a fresh catalyst charge. Commonly, to regenerate these catalysts in fixed beds requires passing hot gas having very low oxygen content through the bed to burn the carbonaceous material from the catalyst. Hot spots commonly develop in the fixed beds with resultant sintering of the catalyst and formation of large catalyst clinkers. It has also been proposed to regenerate these catalysts by passing them through a rotating kiln similar to a cement kiln and in this method considerable attrition of the catalyst by breakage and poor contact of the regeneration gas with the catalyst surface leads to low catalyst recovery and to a rather poor level of reactivation (Williams *et al*., 1984).

The Kaduna refining and petrochemical company (KRPC) in Nigeria practices a semi regenerative type of reforming where the catalysts are left to deactivate up to 72 months before regeneration against 24 months globally practiced in advanced refineries. This is based on the assumption that the catalyst were not continually used properly and not operating at high severity (maximum throughput of 116 m^3/hr but operated at 50 % of the designed conditions). Most catalyst are dumped while the little ones left are blended with the fresh catalyst after separating by sieving the sintered ones out of the deactivated catalyst (Axien, 2002).

The typical average life span of catalytic reforming unit (CRU) catalyst compared to usage globally seven years depending on how active the catalyst remains and its feedstock composition. But most of local refineries in Nigeria uses the catalyst for upto ten years due to high cost of CRU catalyst as long as the desired gasoline blend has 88-90 % RON as compared to the stipulated 98 % global practice (Axien, 2002).

This work therefore focus on study of alternative regeneration strategy which is environmentally friendly that will ensure that the target of high RON which is a global standard is achieved in the local refineries.

1.2 Research Problem

The typical cost of reforming catalyst consumed in refinery like Kaduna Refining and Petrochemical Company (KRPC) is place at ₦192million per 25tonnes. The high cost of these catalysts necessitate the need for regeneration of these catalysts with a view of extending its activity life minimizing the refinery operating cost

Previous work on regeneration employing only chlorine as regeneration substrate, which can poison the catalyst and also resulting to more gas formation than require reformate during catalyst reforming high concentration of chlorine. Therefore the use of air, nitrogen and diluted chlorine together, was considered in this work.

There is scarcity of technical data on the use air, nitrogen and diluted chlorine together, hence the need to explore it so as to generate information to enhance the use of this process.

1.3 Research Scope

The research will cover:

- The characterization of the collected deactivated and regenerated catalysts and
- The removal of coke or other possible foulants from an onstream deactivated reforming catalyst.
- Analysis of decoking effect on the catalyst at specific operating conditions will be studied.

1.4 Research Aim and Objective

The aim of this research is to study the regeneration of catalytic reforming catalyst for the purpose of obtaining high grade octane gasoline.

The specific objectives include;

- To regenerate deactivated Platinum alumina base catalyst.
- To characterize the catalyst using FT-IR, XRD, XRF, SEM and GC-MS.
- To observe the variation of specific regenerating operation conditions and its effect on the catalyst.
- To evaluate the performance of the regenerated catalyst.

1.5 Research Justification

The research work will serve

- ❖ The act of regenerating/ characterizing platinum alumina base catalyst (deactivated catalyst) use in reforming unit will help to minimize pollution from off specification reformate and its products.
- ❖ Good regenerations can improve catalyst performance; improve yield, reduce operating costs, lower catalyst management costs because platinum alumina base catalyst are very expensive and also restores deactivated catalyst to its maximum potential.
- ❖ The use of air, nitrogen, and diluted chlorine combined together for regeneration produces more reformate than gas formation when only chlorine is used.

CHAPTER TWO

2.0 LITERATURE REVIEW

2.1 Introduction

Catalytic reforming technologies and processes have been the subject of numerous discussions and reviews over the past years, since the pioneering work of Vladimir Haensel and Universal Oil Product (UOP) on platinum on alumina catalyst and platforming in the 1940s (Sutton *et al.,* 1973). Catalytic reforming technology has evolved from semi-regenerative, fixed-bed processes to the more energy efficient, highly reliable, low operating cost, and continuous catalyst reforming units (Sivasanker and Ratnasamy, 1995).

Typical process objectives are the upgrading of low octane naphthas to high octane gasoline blending components, production of aromatics, chemical feedstock and hydrogen. Over the past decades, numerous advancements have been made with respect to key reforming processes and in the development of high-performance catalysts. Refiners will be relying on its catalytic reformers for reliable hydrogen supply for the various desulphurization processes required to achieve near-zero-sulfur gasoline and ultralow-sulfur diesel (World refining, 2001).

Reforming processes using platinum catalysts have become of major importance in petroleum refining during the past years. The processes help to increase the octane rating of naphtha and are more economical than any other refining process for the production of high octane gasoline.

2.2 Platinum/Alumina Base Catalyst.

2.2.1 Platinum

Platinum is a chemical element with the chemical symbol Pt and an atomic number of 78. It is a dense, malleable, ductile, precious, gray-white transition metal. Even though it has six naturally occurring isotopes, platinum is one of the rarest elements in the Earth's crust with an average abundance of approximately 5 µg/kg. It occurs in some nickel and copper ores along with some native deposits, mostly in South Africa, which accounts for 80 % of the world production. Platinum is in group 10 and Period 6 on the periodic tables of element. It is generally un-reactive. It exhibits a remarkable resistance to corrosion, even at high temperatures, and as such is considered a noble metal. The most common use of platinum is as a catalyst in chemical reactions. (Mel Schwartz, 2002).

In the petroleum industry, platinum is used as a catalyst in a number of separation processes, but especially in catalytic converter such as Reforming and isomerization processes where catalysts made by coating platinum onto an alumina substrate in the form of small pellets or beads. The platinum content of the catalyst is normally less than 0.6 % by weight. In most modern refineries platinum is combined with tin or rhenium for improved performance. Platinum is noted to have excellent catalysis effects in the oxidation of carbon monoxide and hydrocarbons to carbon dioxide. Also, it is used in manufacturing laboratory equipment, electrical contacts and electrodes, platinum resistance thermometers, dentistry equipment and jewelry (In Lide David, 2008).

2.2.2 Alumina

Alumina is a white or colourless oxide of aluminum. The common name for aluminium oxide (Al_2O_3) which is an amphoteric oxide. It is found in nature in the minerals such as corundum (Al_2O_3), diaspore ($Al_2O_3 \cdot H_2O$); gibbsite ($Al_2O_3 \cdot 3H_2O$) and most commonly in bauxite (an impure form of gibbsite). It is the only oxide formed by the metal aluminum. Largely, alumina is obtained from the mining and refining of the deposits of bauxite ore. Alumina is used in the manufacture of catalysts, abrasives, artificial rubies and sapphires (George, 2008).

Australia is the largest alumina refiner in the world, processing nearly one-third of the global total. Alumina, in its activated form, is used for a wide range of adsorbent and catalyst applications including the adsorption of catalysts in polyethylene production, in hydrogen peroxide production, as a selective adsorbent for many chemicals including arsenic, fluoride, in sulfur removal from gas streams.

2.2.3 Platinum/Alumina

Platinum/alumina catalyst is a monometallic catalyst in which Platinum catalyst uses an Alumina as a supporting material. The loading of the catalyst on the supporting base often ranges from 1 % to 5 %. Use of alumina support for platinum is a good choice because of its high surface area, attrition resistance, structural stability, favourable pore structure and adequate supply. Other supports in common use are silica, titanium dioxide, zeolite, or mixtures of these. A common method of catalyst preparation is by impregnation. During preparation, a high-surface-area porous support is contracted with a liquid solution of the active component. The active agent enters the porous support via capillary action, diffusion and adsorbed on the available surface sites.

Supported platinum catalysts are usually prepared by contacting hexachloroplatinic acid with either a dry or solvent-filled support. For example, in the preparation of platinum-on-alumina catalyst, platinum can be added to the calcined alumina particles by commingling this alumina with an aqueous solution of chloroplatinic acid. Supported platinum catalysts are widely used in many chemical processes, such as hydrogenation, oxidation, and reforming (Gary and handwerk, 1984).

2.3 Catalyst Reforming

Catalytic reforming, or hydroforming, is a well-established industrial process employed by the petroleum industry for improving the octane quality of naphtha or straight run gasoline. In reforming, a multi-functional catalyst is employed which contains a metal hydrogenation-dehydrogenation (hydrogen transfer) component, or components, substantially atomically dispersed upon the surface of a porous, inorganic oxide support, notably alumina. Noble metal catalysts, notably of the platinum type, are currently employed, reforming being defined as the total effect of the molecular changes, or hydrocarbon reactions, produced by dehydrogenation of cyclohexanes and dehydroisomerization of alkylcyclopentanes to yield aromatics; dehydrogenation of paraffins to yield olefins; dehydrocyclization of paraffins and olefins to yield aromatics; isomerization of n-paraffins; isomerization of alkylcyclo-paraffins to yield cyclohexanes; isomerization of substituted aromatics; and hydrocracking of paraffins which produces gas, and inevitably coke, the latter being deposited on the catalyst (William *et al*., 1984).

Platinum has been widely used commercially in recent years in the production of reforming catalysts, and platinum-on-alumina catalysts have been commercially

employed in refineries for the last few decades (In Lide David, 2008). In the last decade, polymetallic metal catalysts have been employed to provide, at reforming conditions, improved catalyst activity, selectivity and stability. Thus, additional metallic components have been added to platinum as promotors to further improve, particularly, the activity of selectivity, or both, of the basic platinum catalyst, e.g., iridium, rhenium, selenium, tin, and the like. Platinum-iridium catalysts, for example, possess superior activity for use in reforming operations as compared with platinum catalysts. Selenium has also been added to the platinum-iridium catalyst, the catalyst containing the triumvirate of metals possessing admirably higher selectivity in contrast with platinum catalysts, or platinum-iridium catalysts, respectively, selectivity being defined as the ability of the catalyst to produce high yields of C_5+ liquid products with concurrent low production of normally gaseous hydrocarbons, i.e., methane and other gaseous hydrocarbons, and coke (William *et al*., 1984).

In a typical process, a series of reactors constitute the heart of the reforming unit. Each reforming reactor is generally provided with fixed beds of the catalyst which receive up flow or down flow feed and each is provided with a preheater or interstage heater, because the reactions which take place are endothermic. A naphtha feed, with hydrogen, or recycle gas, is concurrently passed through a preheat furnace and reactor, and then in sequence through subsequent heaters and reactors of the series. The product from the last reactor is separated into a liquid fraction, i.e., a C_5+ or a C_5 /430° F. fraction, and a vapourous effluent. The latter is a gas rich in hydrogen, which usually contains small amounts of normally gaseous hydrocarbons, from which hydrogen is separated from the C_5+ liquid product and recycled to the process to minimize coke production. Hydrogen is produced as net yield (Antos *et al*., 2004).

The activity of the catalyst gradually declines due, at least in part, to the building-up of coke. Coke formation is believed to result from cracking and polymerization reactions; perhaps from the deposition of coke precursors such as anthracene, coronene, ovalene and other condensed ring aromatic molecules on the catalyst, these polymerizes to form coke. During operation, the temperature of the process is gradually raised to compensate for the activity loss caused by coke deposition. Eventually, however, economics dictates the necessity of reactivating the catalyst. Consequently, in all processes of this type the catalyst must necessarily be periodically regenerated by removal of the coke from the catalyst. Typically, in the regeneration, the coke is burned from the catalyst at controlled conditions. In a regeneration of this type, the catalyst is contacted with oxygen at flame front temperatures ranging about 426 °C to about 565 °C., this being generally followed by a secondary burn with increased oxygen concentrations as coke is depleted from the catalyst. Coke has also been removed from catalysts by contact with hydrogen at elevated temperature (Beltramini, 1995).

There are many chemical reactions that occur in the catalytic reforming process, all of which occur in the presence of a catalyst and a high partial pressure of hydrogen. Depending upon the type or version of catalytic reforming used as well as the desired reaction severity, the reaction conditions range from temperatures of about 495 to 525 °C and from pressures of about 5 to 45 bar. The commonly used catalytic reforming catalysts contain noble metals such as platinum and/or rhenium, which are very susceptible to poisoning by sulfur and nitrogen compounds. Therefore, the naphtha feedstock to a catalytic reformer is always pre-processed in a hydrodesulfurization unit which removes both the sulfur and the nitrogen compounds (Antos *et al*., 2004).

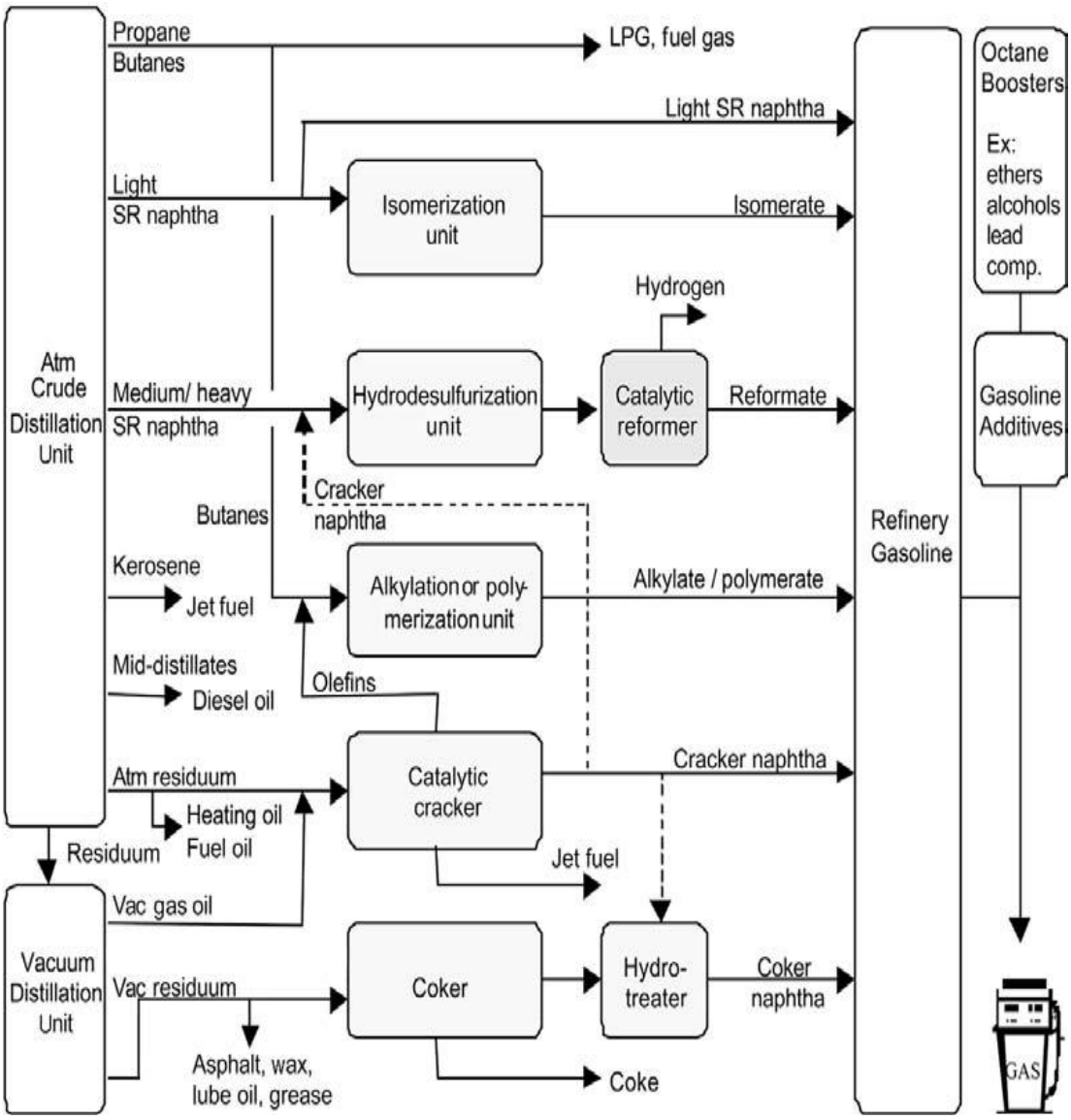


Figure 2.1. Example of a processing scheme for refinery gasoline production with catalytic reforming (Doolin *et al*., 1995)

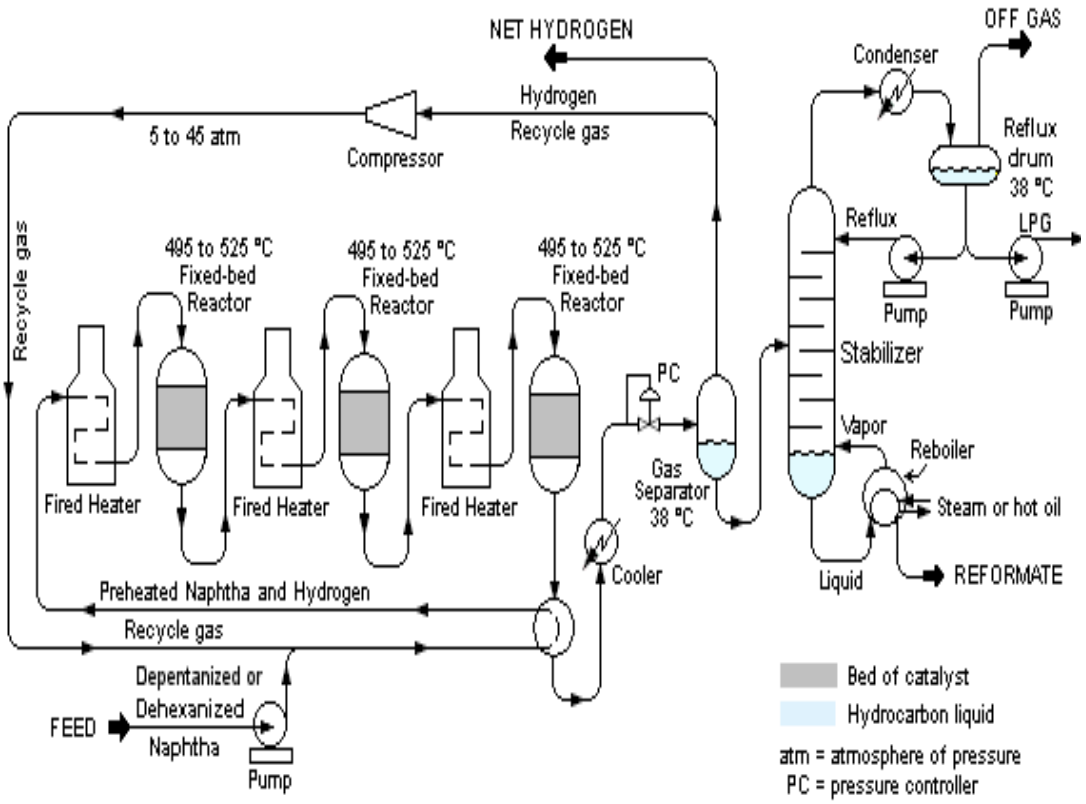


Figure 2.2: Schematic diagram of a typical semi-regenerative catalytic reformer unit in a petroleum refinery (Gary and Handwerk, 1984).

2.4 Catalytic Reforming Processes (Regenerative Methods)

The reforming process is generally classified into three types of regenerative methods:

1. Semi-regenerative.

2. Cyclic (fully regenerative).

3. Continuous regenerative (moving bed).

This classification is based on the frequency and mode of regeneration. The semi-regenerative scheme dominates the reforming capacity at about 57 % of the total capacity followed by continuous regenerative at 27 % and cyclic at 11 % (Clause *et al*., 1998). Most grassroots reformers are designed for continuous catalyst regeneration

(CCR). In addition, many units that were originally built as semi-regenerative units have been revamped to continuous regeneration units. The semi-regenerative type requires unit shutdown for catalyst regeneration, whereas the cyclic process utilizes a swing reactor for regeneration in addition to regular reactors. The continuous process permits catalyst replacement during normal operation (Aitani, 1995).

2.4.1 Semi-regenerative Process

The semi-regenerative process is characterized by continuous operation over long periods, with decreasing catalyst activity. Eventually, the reformers are shut down periodically as a result of coke deposition to regenerate the catalyst in situ. Regeneration is carried out at low pressure (approximately 8 kg/cm^2) with air as the source of oxygen. The development of bimetallic and multimetallic reforming catalysts with the ability to tolerate high coke levels has allowed the semi-regenerative units to operate at 14–17 kg/cm^2 with similar cycle lengths obtained at higher pressures. It is believed that all reforming licensors have semi-regenerative process design options. The semi-regenerative process is a conventional reforming process that operates continuously over a period of up to 1 year. As the catalytic activity decreases, the yield of aromatics and the purity of the by-product hydrogen drop because of increased hydro cracking (Antos *et al*., 2004).

Semi-regenerative reformers are generally built with three to four catalyst beds in series. The fourth reactor is usually added to some units to allow an increase in either severity or throughput while maintaining the same cycle length. The longer the required cycle length, the greater the required amount of catalyst. Conversion is maintained more or less constant by raising the reactor temperatures as catalyst activity declines.

Sometimes, when the capacity of a semi regenerative reformer is expanded, two existing reactors are placed in parallel, and a new, usually smaller, reactor is added (Aitani, 1995)

Frequently, the parallel reactors are placed in the terminal position. When evaluating unit performance, these reactors are treated as though they are a single reactor of equivalent volume. The research octane number (RON) that can be achieved in this process is usually in the range of 85– 100, depending on an optimization between feedstock quality, gasoline qualities and quantities required, as well as the operating conditions required to achieve a certain planned cycle length (6 months to 1 year). The catalyst can be regenerated in situ at the end of an operating cycle. Often the catalyst inventory can be regenerated 5 to 10 times before its activity falls below the economic minimum, whereupon it is removed and replaced (Doolin *et al*., 1995).

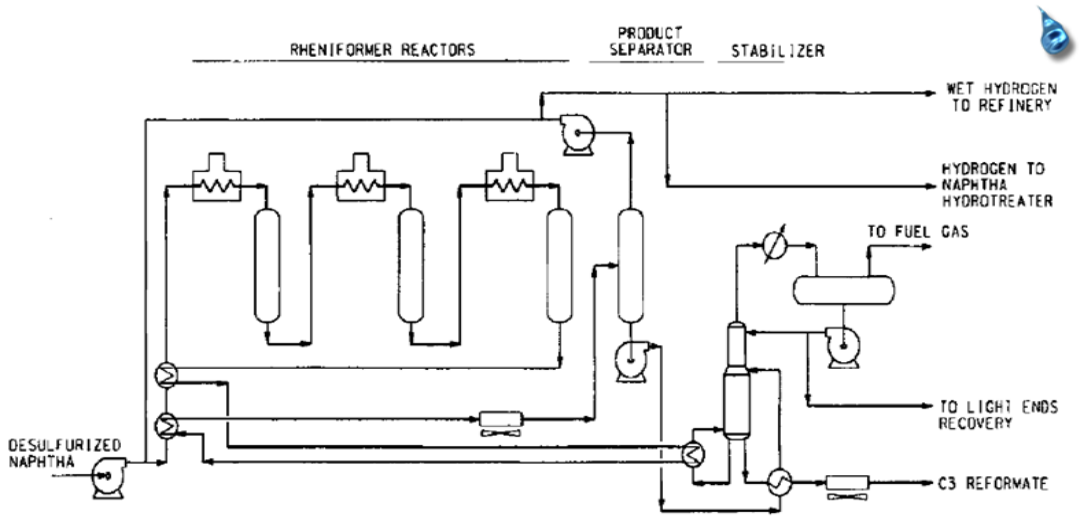


Figure 2.3: Semi-regenerative reformer (Doolin *et al*., 1995).

2.4.2 Cyclic (Fully Regenerative) Process

The cyclic process typically uses five fixed catalyst beds, similar to the semi regenerative process, with one additional swing reactor, which is a spare reactor. It can substitute any of the regular reactors in a train while the regular reactor is being regenerated. In this way, only one reactor at a time has to be taken out of operation for regeneration, while the process continues in operation. Usually, all the reactors are of the same size. In this case, the catalyst in the early stages is less utilized; therefore, it will be regenerated at much longer intervals than in the later stages. The cyclic process may be operated at a low pressure, a wide boiling range naphtha feed, and low hydrogen to- naphtha ratio. Coke lay-down rates at these low pressures and high octane severity (RON of 100–104 range) is so high that the catalyst in individual reactors becomes exhausted in time intervals of less than 1 week to 1 month. The process design of the cyclic process takes advantage of low unit pressures to gain a higher C_{5+} reformate yield and hydrogen production. The overall catalyst activity, conversions and hydrogen purity vary much less with time than in the semi-regenerative process.

However, a drawback of this process is that all reactors alternate frequently between reducing atmospheres during normal operation and an oxidizing atmosphere during regeneration. This switching policy needs a complex process layout with high safety precautions and requires that all the reactors be of the same maximum size to lake switches between them possible (Antos *et al*., 2004).

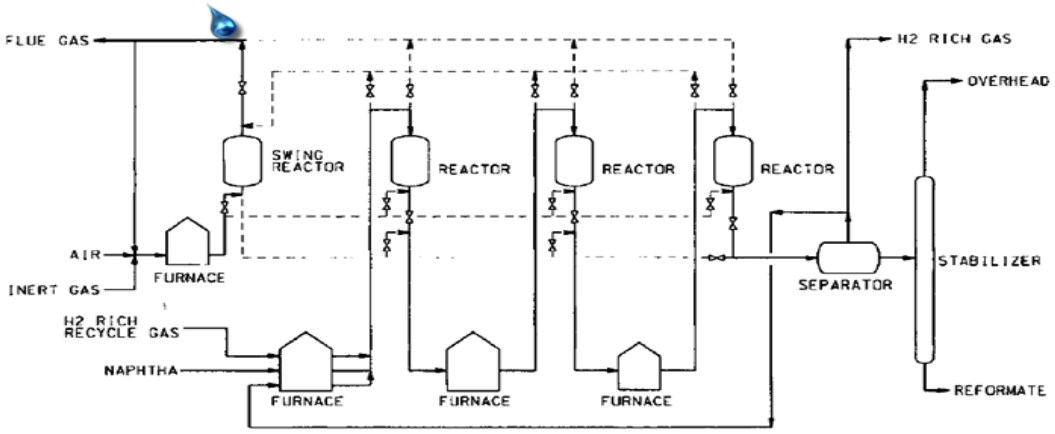


Figure 2.4: Cyclic regenerative reformer: Amoco's Ultraformer (Doolin *et al*., 1995)

2.4.3 Continuous Regenerative Process

The Continuous Regenerative Process (CCR) process is characterized by high catalyst activity with reduced catalyst requirements, more uniform reformate of higher aromatic content, and high hydrogen purity. The process can achieve and surpass reforming severities as applied in the cyclic process but avoids the drawbacks of the cyclic process. The continuous process represents a step change in reforming technology compared to the semi regenerative and cyclic processes. Since its introduction in the early 1970s, it has gained wide acceptance in refining and petrochemical industries worldwide. In this process, small quantities of catalyst are continuously withdrawn from an operating reactor, transported to a regeneration unit, regenerated, and returned to the reactor system. In the most common moving-bed design, all the reactors are stacked on top of one another. The fourth (last) reactor may be set beside the other stacked reactors. The reactor system has a common catalyst bed that moves as a column of particles from top to bottom of the reactor section. Coked catalyst is withdrawn from the last reactor and sent to the regeneration reactor, where the catalyst is regenerated on a continuous basis (Antos *et al*., 2004).

However, the final step of the regeneration, i.e., reduction of the oxidized platinum and second metal, takes place in the top of the first reactor or at the bottom of the regeneration train. Fresh or regenerated catalyst is added to the top of the first reactor to maintain a constant quantity of catalyst. Catalyst transport through the reactors and the regenerator is by gravity flow, whereas that from the last reactor to the top of the regenerator and back to the first reactor is by the gas-lift method. Catalyst circulation rate is controlled to prevent any decline in reformate yield or hydrogen production over time on stream. In another design, the individual reactors are placed separately, as in the semi-regenerative process, with modifications for moving the catalyst from the bottom of one reactor to the top of the next reactor in line. The regenerated catalyst is added to the first reactor, and the deactivated catalyst is withdrawn from the last reactor and transported back to the regenerator. The continuous reforming process is capable of operation at low pressures and high severity by managing the rapid coke deposition on the catalyst at an acceptable level. Additional benefits include elimination of downtime for catalyst regeneration and steady production of hydrogen of constant purity (93 % compared to 80 % in the semi-regenerative process). Operating pressures are in the 3.5–17 kg/cm^2 range and design research octane number is in the 95–108 range (Antos *et al*., 2004).

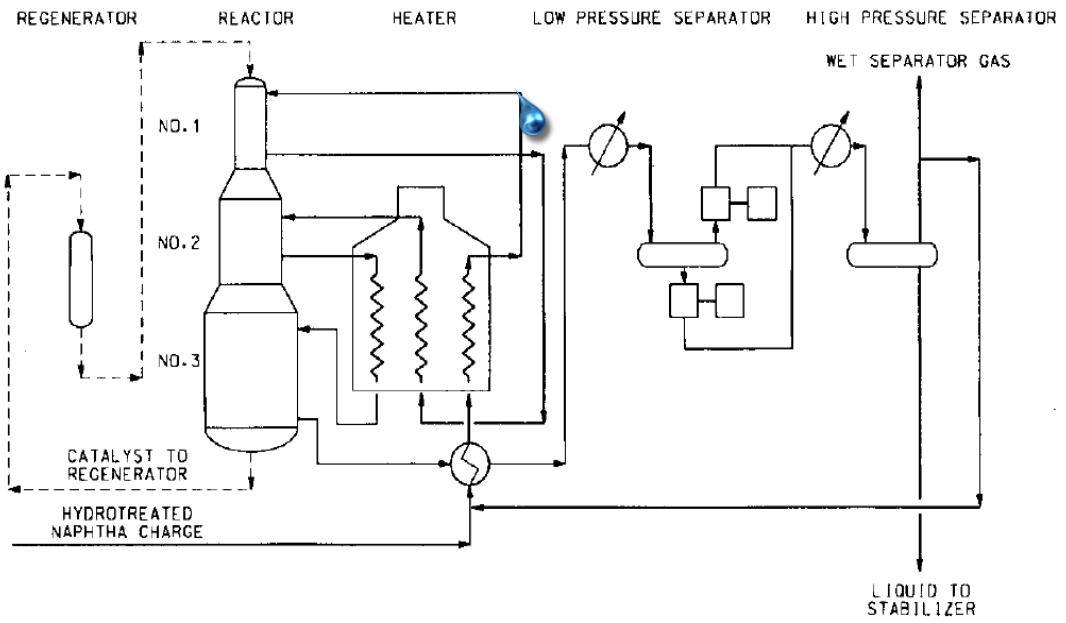


Figure 2.5: UOP CCR Platformer (Reactor section) (Doolin *et al*, 1995).

2.5 Commercial Reforming Processes

Several commercial reforming processes are available for license worldwide, dominated by Universal Oil Product (UOP), Axens and Chiyoda Technologies for semi-regenerative and continuous reforming. Other licensors included Houdry Division, Chevron, Engelhard, Exxon Mobil, and Amoco, but none of them is currently actively licensing. The processes differ in the type of operation (semi-regenerative or CCR), catalyst type, catalyst regeneration procedure and process engineering design. All licensors agree on the necessity of hydrotreating the feed to lower the level of poisons for the platinum based reforming catalyst. Temporary poisons are sulfur and nitrogen, while Arsenic (As), Lead (Pb) and other metals are permanent poisons. Proper conditions of hydrogen, pressure, temperature, and space velocities are able to reduce these poisons to the acceptably low levels of modern catalysts. Numerous process design modifications and catalyst improvements have been made in recent years (Doolin *et al*., 1995).

2.6 Catalyst Deactivation and Regeneration

2.6.1 Catalyst Deactivation

Performance of the catalyst decreases with respect to time due to deactivation. Deactivation can occur by a number of different mechanisms, both chemical and physical in nature. These are commonly divided into classes, namely coke formation or fouling, poisoning, sintering contamination on active sites and agglomeration. Other mechanisms of deactivation include masking and loss of the active elements via volatilization, erosion and attrition (Bartholomew and Sorensen, 1983)

2.6.1.1 Coking

For catalytic reactions involving hydrocarbons (or even carbon oxides) side reactions occur on the catalyst surface leading to the formation of carbonaceous residues (usually referred to as coke or carbon) which tend to physically cover the active surface. Coke deposits may amount to 15 % or even 20 % (w/w) of the catalyst and accordingly they may deactivate the catalyst either by covering of the active sites, and by pore blocking. Sometimes a distinction is made between coke and carbon. The difference is however somewhat arbitrary: usually carbon is considered the product of CO disproportionation ($2CO \rightarrow C+CO_2$), whereas coke is referred to the material originated by decomposition (cracking) or condensation of hydrocarbons (Gate *et al*., 1988).

The chemical nature of the carbonaceous deposits depends very much on how they are formed, the conditions of temperature and pressure, the age of the catalyst, the chemical nature of the feed and products formed. Several authors pointed out a direct relationship between the amount of coke deposited and the aromatic and polynuclear aromatic

content of the feed. Also, it has been reported that coke formation occurs more rapidly when a hydrogen acceptor, such as an olefin, is present, in line with the hypothesis of a carbonium ion chemistry for coke formation (Bartholomew, 1994).

In practice, the coke deposition may be controlled to a certain extent by using an optimal catalyst composition and an appropriate combination of process conditions. During the reaction an equilibrium is reached between the rate of coke production and the rate of coke removal by gasifying agents (e.g. H_2, H_2O and O_2 that remove coke as CH_4, CO and COx, respectively) so that steady-state conditions, corresponding to a certain level of coke present on the catalyst surface, are eventually reached. Otherwise, if the rate of coke deposition is higher than that of coke removal, a suitable regeneration procedure must be applied (Forzatti and Lietti, 1999).

2.6.1.2 Poisoning

Poisoning is the loss of activity due to the strong chemisorption on the active sites of impurities present in the feed stream or as a result of products from desired reaction. Chemisorptions of compounds that modify, block or restructure the catalyst surface morphology. The adsorption of a basic compound onto an acid catalyst (e.g. isomerization catalyst) is an example of poisoning. A poison may act simply by blocking an active site (geometric effect), or may alter the adsorptivity of other species essentially by an electronic effect. Poisons can also modify the chemical nature of the active sites or result in the formation of new compounds (reconstruction) so that the catalyst performance is definitively altered (Bartholomew, 2001).

Poisons can be classified as ``reversible" or ``irreversible". In the first case, the poison is not too strongly adsorbed and accordingly regeneration of the catalyst usually occurs simply by poison removal from the feed. This is the case, for example, of oxygen containing compounds (e.g. H_2O and CO_x) for the ammonia synthesis catalysts. These species hinder nitrogen adsorption, thus limiting the catalyst activity, but elimination of these compounds from the feed and reduction with hydrogen removes the adsorbed oxygen to leave the iron surface as it was before. However, gross oxidation with oxygen leads to bulk changes which are not readily reversed: in this case the poisoning is ``irreversible", and irreversible damages are produced. Upon poisoning, the overall catalyst activity may be decreased without affecting the selectivity, but often the selectivity is affected, since some of the active sites are deactivated while others are practically unaffected. This is the case of ``multifunctional" catalysts, which have active sites of different nature that promote, simultaneously, different chemical transformations. The Pt/Al_2O_3 reforming catalysts are typical examples: the metal participates in the hydrogenation - dehydrogenation reactions whereas alumina acts both as support and as acid catalyst for the isomerization and cracking reactions. Hence basic nitrogen compounds adsorb on the alumina acid sites and reduce isomerization and cracking activity, but they have little effect on dehydrogenation activity (Forzatti and Lietti, 1999).

Poisoned catalyst can hardly be regenerated, and therefore the best method to reduce poisoning is to decrease to acceptable levels the poison content of the feed. Another approach to prevent poisoning is to choose proper catalyst formulations and design (Bartholomew and Sorensen, 1983).

2.6.1.3 Sintering

Sintering usually refers to the loss of active surface via structural modification of the catalyst. This is generally a thermally activated process and is physical in nature. Sintering occurs both in supported metal catalysts and unsupported catalysts. In the former case, reduction of the active surface area is provoked via agglomeration and coalescence of small metal crystallites into larger ones with lower surface-to-volume ratios. Two different but quite general pictures have been proposed for sintering of supported metal catalysts, i.e. the atomic migration and the crystallite migration models. In the first case, sintering occurs via escape of metal atoms from a crystallite, transport of these atoms across the surface of the support (or in the gas phase), and subsequent capture of the migrating atoms on collision with another metal crystallite. Since larger crystallites are more stable (the metal-metal bond energies are often greater than the metal-support interaction), small crystallites diminish in size and the larger ones increase (Bartholomew, 1994).

2.6.2 Reforming side reactions mechanism

Reforming side reactions mechanism or adverse reactions leading to deposit on catalyst.

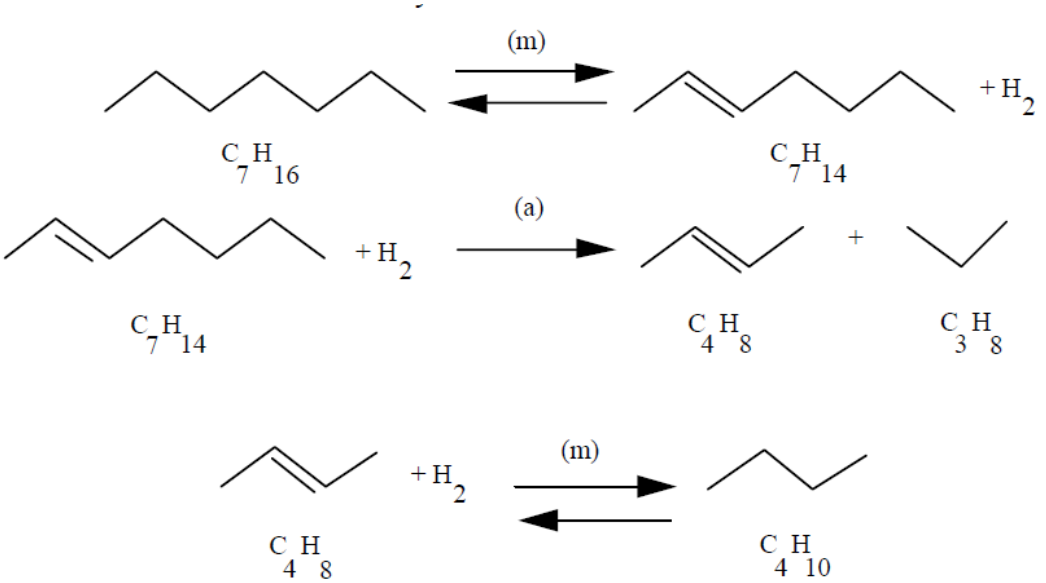
2.6.2.1 Cracking

Cracking reactions include hydrocracking and hydrogenolysis reactions.

Hydrocracking affects either paraffins (normal or iso) or olefins: It involves both the acid and metallic function of the catalyst. It is to some extent, a parallel reaction to paraffin dehydrocyclization (Beltramini, 1995).

It can be represented schematically by a first step of dehydrogenation which involves the metallic function of the catalyst, followed by a cleavage of the resulting olefin and

the hydrogenation of the subsequent short chain olefin. The second reaction is promoted by the acidic function of the catalyst.



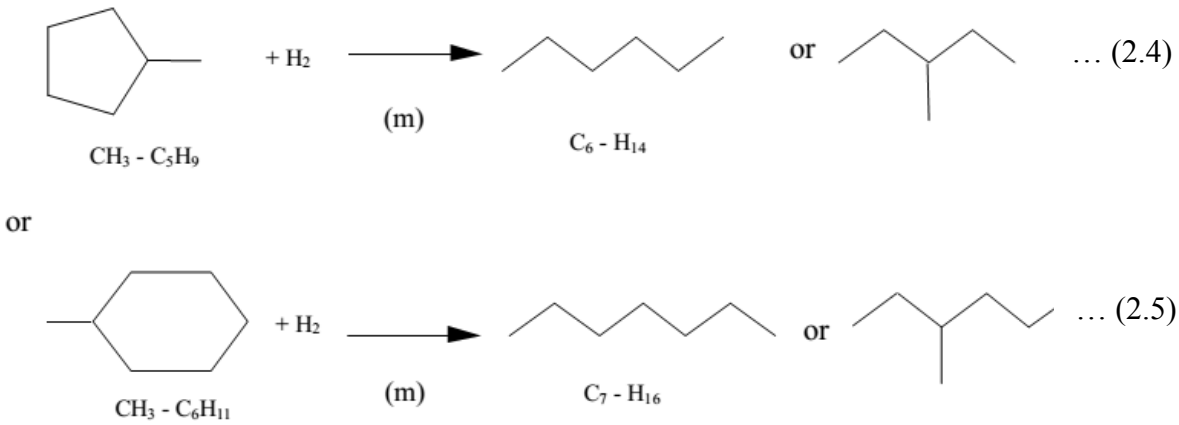
… (2.1)

… (2.2)

… (2.3)

The first reaction involves the same reactants as the dehydrocyclization and is likewise catalysed by the metallic function.

Hydrocracking also affects the naphthenes, the overall reaction can be summarized as follows:



… (2.4)

… (2.5)

At the selected operating conditions, hydrocracking reaction could be almost complete. Fortunately, it is somewhat limited by its kinetics. Compared to its desirable concurrent reaction (dehydrocyclization), hydrocracking becomes significant as the temperature increases. It is also favoured by high pressure. The main effects of hydrocracking are

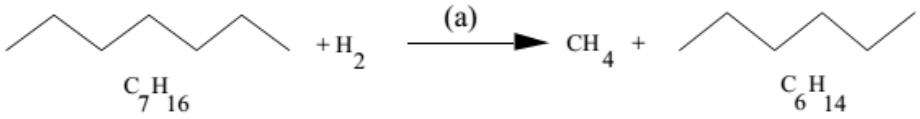
A decrease of paraffins in the reformate which results in an increase of the aromatics percentage (i.e. an increase in octane) and a loss of reformate.

A decrease in hydrogen production.

An increase of production (Mohammad *et al*., 2013)

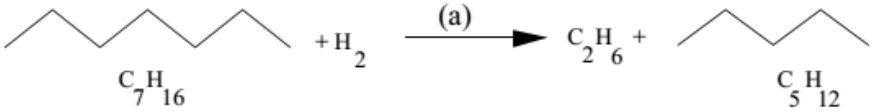
2.6.2.2 Hydrogenolysis

This undesirable reaction has some similarity with hydrocracking since it involves hydrogen consumption and cleavage of bonds. But it is promoted by the metallic function of the catalyst and leads to lighter hydrocarbon C1 + C2 - even less valuable than LPG (C3 + C4). It can be represented schematically as follows:



… (2.6)

or

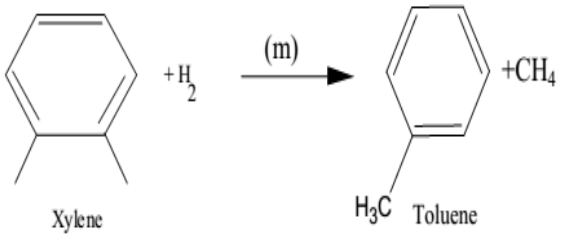


… (2.7)

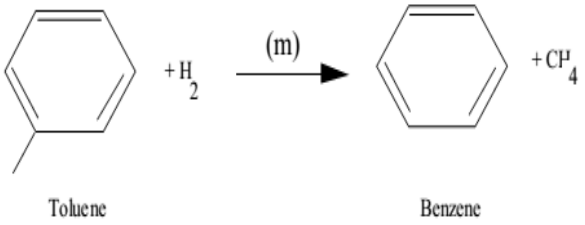
Like hydrocracking it is exothermic and favoured by high pressure and high temperature.

2.6.2.3 Hydrodealkylation

Hydrodealkylation is the breakage (or cleavage) of the branched radical (-CH_3 or -C_2H_5) of an aromatic ring. Xylene (two radical groups) can be dealkylated into toluene (one radical group) which in turn can be dealkylated to benzene. The standard representation is:



… (2.8)

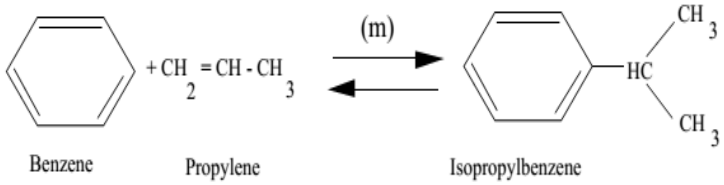


… (2.9)

Hydrodealkylation consumes hydrogen and produces methane. It is favoured by high temperature and high pressure and promoted by the metallic function of the catalyst (Mohammed *et al*., 2013).

2.6.2.4 Alkylation

Alkylation is a condensation reaction which adds an olefin molecule on an aromatic ring. It results in an aromatic with an increased molecular weight. The reaction proceeds as follows:

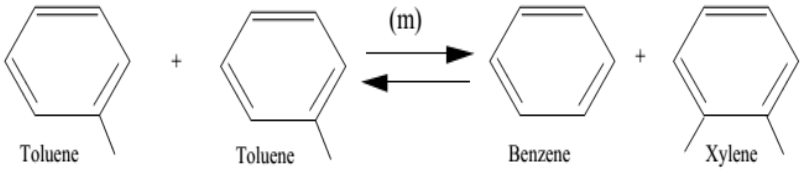


… (2.10)

This reaction, promoted by the catalyst metallic function, is not hydrogen consuming. But it leads to heavier molecules which may increase the end point of the product. In addition the high molecular weight hydrocarbons also have a high tendency to form coke. This reaction must be avoided (Mohammed *et al*., 2013).

2.6.2.5 Transalkylation (alkyl disproportionation)

Two toluene rings (one branched CH_3 radical) can disproportionate to produce one benzene ring (no branched radical) and one xylene ring (two branched radicals), as shown:



… (2.11)

This reaction, promoted by the catalyst metallic function, occurs mainly in very severe conditions of temperature and pressure.

2.6.2.6 Coking

Coke formation on the catalyst results from a very complex group of chemical reactions, the detailed mechanism of which is not yet fully known. Coke formation is linked to heavy unsaturated products such as polynuclear aromatics (or polycyclics which can be dehydrogenated) resulting either from the feed or from the polymerization of aromatics involved in some of the reforming reactions (dehydrocyclization, disproportionation). Traces of heavy olefins or diolefins may also result from the reforming reactions (dehydrocyclization, alkylation, for instance) and promote coke formation. A high end boiling point of the feed means greater amount of polyaromatics and then a higher coking tendency. Since condensation is promoted by high temperature, poor distribution in a reactor favours local high temperatures and coke build up. Coke deposit on the catalyst reduces the active surface area and greatly reduces catalyst activity (Mohammad *et al*., 2013).

2.6.3 Purpose of Regeneration

The objectives of the regeneration include:

- Surface area should be high.
- Metal Pt should be highly dispersed.
- Acidity must be at a proper level.
- Regeneration changes by the severity of the operating conditions.
- Coke formation can be offset for a time by increasing reaction temperatures (Ren et al., 2002).

2.6.4 Benefits of Regeneration.

Poor catalyst regeneration will lead to low product yields and increased operating expense, so good regenerations can improve catalyst performance, reduce operating costs, and lower catalyst management costs (Ren et al., 2002).

2.7 Catalyst Performance

Performance of a catalyst may be described in terms of activity, selectivity and stability.

2.7.1 Activity

Catalytic activity is the augmentation of the rate and energy of a chemical reaction by a catalyst. Activity is any change-increase or decrease in the reaction's rate. A more

active catalyst is able to achieve the same product yield or severity at a lower reaction temperature relative to a less-active catalyst (Oloworishe, 2014).

2.7.2 Selectivity

The selectivity of the catalyst refers to the relative yield of desired product compared to another catalyst operating with the same severity target (RON) under similar process parameters (pressure, H_2/HC). As with most reaction systems, high selectivity is desired as long as the performance can be maintained (Oloworishe, 2014).

2.7.3 Stability

Stability is a measure of how long a desired performance can be maintained and it usually reflects the coking tendency of the catalyst as it affects both activity and selectivity. Higher stability in a fixed-bed catalyst translates into a longer cycle length while meeting process severity targets-i.e, more profitable on-stream time. For reforming units equipped with continuous catalyst regeneration (CCR), higher stability means lower coking tendencies and slower regeneration cycles, thereby adding operational flexibility. Such operating flexibility provides opportunities to process more demanding feed, such as higher end point feed or an increased catalyst life resulting from a reduced regeneration frequency. Higher catalyst stability can also allow reducing the recycle gas requirement, thus lowering operating costs (Le Goff *et al*, 2012).

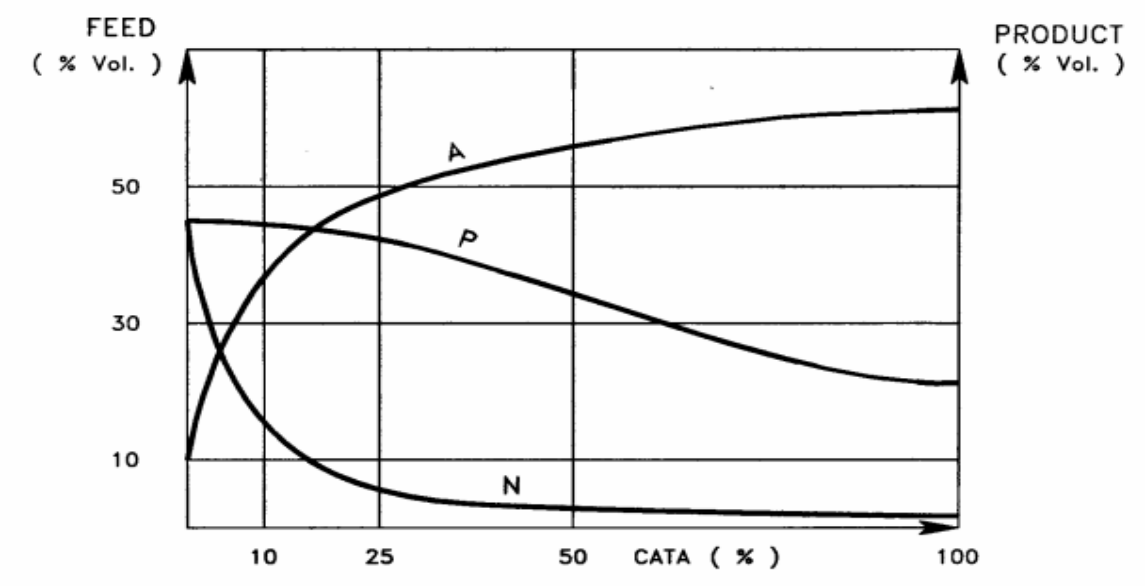
2.8 KRPC Catalytic Reformer Unit (CRU) Background Information

About April 2010, KRPC noticed a shift in the reactor temperature profile indicating a reduced reaction in first reactor. During this period, a catalyst sample sent to Axens for analyses revealed about 2600 ppm Iron (Fe) contamination. Axens considers contamination of 1000 ppm on the catalyst as a maximum limit. KRPC CRU catalyst contamination level was about 2.6 times the maximum limit in the first reactor. This contamination affects the metal function of the catalyst and hence the noticed shift in reaction profile. At about the same time, there was a breakdown of the chloride injection and thus no chloride was injected into the process. With the reduced catalyst chloride levels, the catalyst activity declined to a point where from a technical perspective there were no more significant reactions to move the naphtha components towards aromatics. This showed in the decline in octane to about 76 RON with 493 ^{o}C reactor inlet temperature (RIT) and about 92 % Hydrogen purity. This situation led KRPC to stop operation and execute a total turn around maintained and catalyst regeneration.

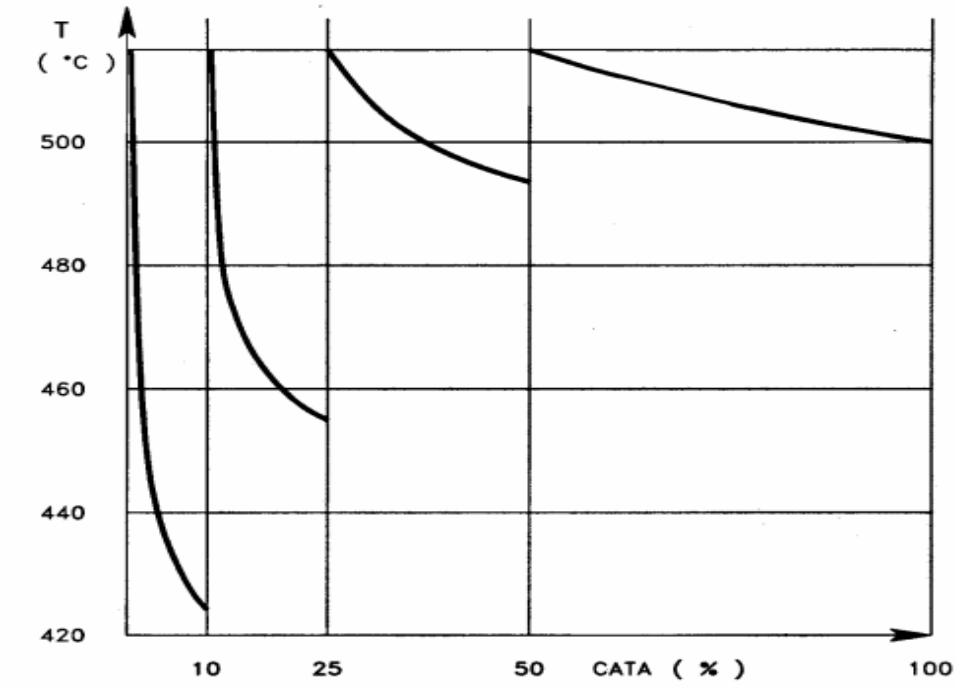
Figure 2.6 shows for a given feed (paraffins: 45 %, naphthenes 45 %, aromatics 10 %) the profile of the amount of paraffin, naphthene and aromatic (P.N.A) along the catalyst volume. In this case there is no need for more than 10 % of the catalyst in the first reactor because the naphthenes dehydrogenation results in a temperature too low to sustain the reaction any longer. The reactor effluent is reheated to allow for the naphthenes dehydrogenation to continue and the paraffin dehydrocyclization to start. Over the next 15 % of catalyst, distributed in the 2nd 6 reactor, temperature drops again to a level where reheating is required to enable the paraffin dehydrocyclization to proceed.

The catalyst typical distribution in this case is: R1 = 10 %; R2 = 15 %; R3 = 25 % and R4 = 50 %

Each specific case, obviously, requires a specific catalyst distribution.



Figures 2.6: Catalyst distribution in the reactors for feed and product in a reforming unit (Axen, 2009).



Figures 2.7: Catalyst distribution in the reactors in terms of temperature (Axen, 2009).

After catalyst regeneration in KRPC, the quantity of fresh and old catalyst that are blended together for reforming process unit are shown in Table 2.1

Table 2.1: Quantities of Catalyst for fresh and old catalyst after regeneration in KRPC

Reactor No.	R01	R02	R03	R04
Fresh catalyst, kg	7511.00	9916.00	1995.00	0.00
Old Catalyst, kg	0.00	0.00	13556.40	22970.20
Toatl catalyst,kg	7511.00	9916.00	15551.40	22970.20
Distribution in reactors %	13.42	17.72	27.80	41.06
Loading Density, kg/m^3	603.48	607.68	777.07	639.31

2.8.1 Feed Stock Composition in a reforming unit.

Naphtha feedstocks to reformers typically contain paraffins, naphthenes, and aromatics with 6–12 carbon atoms. Most feed have to be hydrotreated to remove metals, olefins, sulfur, and nitrogen, prior to being fed to a reforming unit. A typical straight run naphtha from crude distillation may have a boiling range of 150–400^{0}F (65–200^{0}C) Carl (2013).

In addition to naphthas from crude distillation, naphthas can be derived from a variety of other processes that crack heavier hydrocarbons to hydrocarbons in the naphtha range. Cracked feedstocks may be derived from catalytic cracking, hydrocracking, cokers, thermal cracking, as well as visbreaking, fluid catalytic cracking, and synthetic naphthas obtained, for example, from a Fischer–Tropsch process.

In the work of George et al (2005) it was confirmed that light paraffinic naphthas are more difficult to reform than heavier naphthenic hydrocarbons. The distillation values for the initial boiling point, the mid-point at which 50% of the naphtha is distilled over, and the end point are often used to characterize a naphtha. Feed hydrotreating is used to reduce feedstock contaminants to acceptable levels. Common poisons for reforming catalysts that are found in naphtha are sulfur, nitrogen, and oxygen compounds. Removing these requires breaking of a carbon-sulfur, -nitrogen or -oxygen bond and formation of hydrogen sulfide, ammonia, or water, respectively. Hydrotreaters will also remove olefins and metal contaminants.

Table 2.2: Design Feed (Naphtha) Stock Composition (Chiyoda, 1980).

Properties	Values
Specific gravity	0.745
Top Boiling Point Cut (^{o} C)	70-175
Paraffins (Volume %)	51.9
Naphthenes (Volume %)	35.3
Aromatics (Volume %)	12.8
Sulphur content	1 ppm wt maximum
Water content	5 ppm wt maximum
Nitrogen content	1 ppm wt maximum
C_{5+} content: light naphtha	not more than 1 wt %
Maximum butane content of light naphtha	shall be 2 % wt.



Plate 2.8: Kaduna Refining and Petrochemical Company



Plate 2.9: Catalytic Reforming Unit in Kaduna Refining and Petrochemical Company.

Chemical composition**:** The detailed chemical composition of the feed is determined by gas chromatography analysis. As a rough approximation, knowledge of the repartition

of the different hydrocarbon families, allows to define the main properties of the feed. This repartition mainly P = Paraffins, O = Olefins, N =Naphthenes, A =Aromatics (PONA), defines the feed and helps in designing the severity of the reformer conditions. The value of N + 2A is a useful way of characterizing the feed but which cannot be substituted to its detailed analysis. The value is related to the actual and potential aromatics content of the feed. The higher this value, the lower the severity of the reformer conditions to meet the same specifications. As a matter of fact the lower the paraffin content is, the higher the temperature of the reactors inlet would have as the dehydrocyclization is the more endothermic reaction. In case of feed coming from visbreaking, coke faction units, and containing olefins, it is obvious that a previous dehydrogenation is compulsory (Chiyoda, 1980).

2.8.3 Operating Variables

2.8.3.1. *Pressure*

On a thermodynamics point of view, all the reactions to promote, except the isomerization one, are enhanced by a low pressure as it involved hydrogen production. The side reactions are favoured either by a high pressure (cracking) or by a low pressure (coking). The design pressure is the result of economics computation relating to the life of the catalyst and thus duty of the recycle compressor.

2.8.3.2. *Temperature*

The temperature at the reactor inlet is related to the catalyst activity at the corresponding period of its cycle. As a matter of fact, to maintain the octane number in case of gasoline production, it is necessary to increase the operating temperatures, all other operating condition being steady, to compensate the activity lowering of the catalyst. Thus, the yields will decrease as well as the purity of the recycle gas. The reactions of cracking are most favoured by a temperature increase, as they have the higher activation energy. The reactors inlet temperatures are generally the same. Due to the main reactions taking place in each of them, different temperature drops are observed. As the average temperature is the highest into the third reactor, the coke formation will be more important on its catalyst.

2.8.3.3 Space velocity

The weight space velocity is defined as the ratio of the feed flow rate (kg/hour) to Overall catalyst quantity (kilogrammes). It is a kinetic characteristics corresponding to the average residence time of the feed on the catalyst. If for any reason the space velocity has to be changed, regarding to the design one, the reactor inlet temperature have also to be changed to hold the same severity of the catalyst, and to meet the same octane number and yields. Nevertheless, to avoid hydro-cracking and to protect the catalyst against coke formation, for these changes the following rules apply

To increase the space velocity: Increase the feed flow rate.

To decrease the space velocity: Decrease the feed flow rate.

2.8.3.4 Hydrogen to hydrocarbon ratio

It is defined as the ratio of recycled pure hydrogen (kmol/hour) to feed flowrate (kmol/hour). High hydrogen to hydrocarbon ratio corresponds both to high hydrogen purity and to a high compressor capacity. Furthermore, improving the thermal exchanges on the catalyst, high hydrogen to hydrocarbon ratio allows lower reactors inlet temperatures, the reactors getting more isotherm than with low hydrogen to hydrocarbon ratio. However, high hydrogen to hydrocarbon ratio increases the hydrogen partial pressure, protecting the catalyst against coke formation and improving the cycle duration. The influence of the hydrogen to hydrocarbon ratio on the octane number and on the yields is rather small. On the economic point of view, increasing the hydrogen to hydrocarbon ratio results in the over - sizing of the furnaces and of the compressor. Thus the chosen hydrogen to hydrocarbon ratio is a balance between economical and technical duties.

2.8.3.5 Quality of feed

The characteristics of the feed being able to influence the unit performances are related to its physical properties and to the impurities it could contain.

Distillation range**:** Light fractions (below 80^{o}C) have poor naphthenic and aromatic hydrocarbons content, it is thus, not advantageous to feed the reactor with them. Heavy cuts (above 180^{o}C) have a high naphthenic and aromatic hydrocarbons content, thus, they need a lower severity to get good yields; nevertheless these cuts contain unstable compounds leading to coke formation on the catalyst, deactivating it. Impurities in the feed: The catalyst can be inhibited, either temporary or definitely by poisons contained

in the feed. The impurities in the feed will always be limited to the following values, their detection being performed according to the methods required.

As < 5 ppb, Pb < 5 ppb, Cu < 5 ppb, Fe < 5 ppb, Ni < 5 ppb, Halogens (F, Cl) < 1 ppm all detected by atomic absorption.

Organic Nitrogen < 1ppm detected by Kjeldahl method.

Water and Oxygenated products < 4 ppm detected by Karl Fisher method.

Sulfur < 1ppm detected by Wick bolt combustion

2.9 Chemical Composition Analysis

2.9.1 Basic Principles of XRD and XRF Analysis

X-ray fluorescence in which x-rays are used to stimulate secondary characteristic x-radiation may be used for the quantitative analyses of major and minor elements with an atomic number greater than that of sodium. Characteristic x-rays are diffracted by an analyzing crystal, and the diffraction angle and intensity provide information about the element and its concentration. This technique is accurate and fast for routine analyses (Bawa, 2012).

The underlying physics of XRF entail the ionization of component atoms of materials when they are exposed to short-wavelength X-rays or to gamma rays. Ionization consists of the ejection of one or more electrons from the atom, and may occur if the atom, and may occur if the atom is exposed to radiation with an energy greater than its

ionization potential. X-rays and gamma rays can be energetic enough to expel tightly held electrons from the inner orbits of the atom. The removal of an electron in this way renders the electronic structure of the atom unstable, and electrons in higher orbitals fall into the lower orbital to fill the hole left behind. In falling, energy is released in the form of a photon, the energy of which is equal to the energy difference of the two orbitals involved. Thus, the material emits radiation, which has energy characteristic of the atoms present. The term fluorescence is applied to phenomena in which the absorption of radiation of a specific energy results in the re-emission of radiation of different energy. Each of these transition yields a fluorescence photon with a characteristic energy equals to the difference in energy of the initial and final orbital. The wavelength of this fluorescence radiation can be calculated from Planck's law:

$$\lambda = hc/E \qquad \ldots (2.12)$$

The intensity of each characteristic radiation is directly related to the amount of each element in the material. This is the basis of a powerful technique in analytical chemistry. Chemical analysis of a sample is carried out by employing a primary X-ray beam to excite fluorescence radiation from the sample (Bawa, 2012).

2.9.2 Basic Principles of SEM Analysis

The extent of dispersion of an active ingredient (platinum metal) on a support (γ-alumina) can be determined by Scanning electron microscopy (SEM) technique. SEM analyzes the surface of materials. It also measures and evaluates surface pitting, failure analysis, characterization of dust, deposits, contaminants, particles, filter residues, and other applications (Goldstein, 2003).

SEM uses a focused beam of high-energy electrons to generate a variety of signals at the surface of the solid specimens. The signals derived from such electron-sample interactions reveal information about the sample including external morphology (texture), chemical composition, and crystalline structure and orientation of materials making up the sample. In most applications, data are collected over a selected area of the surface of the sample, and a 2-dimensional image is generated that displays spatial variations in these properties. Areas ranging from approximately 1 cm to 5 microns in width can be imaged in a scanning mode using conventional SEM techniques (magnification ranging from 20 X to approximately 30,000 X, spatial resolution of 50 to 100 nm) (Goldstein, 2003).

Although, in recent time, the use of electron probe microanalysis (EPMA) is rapidly becoming standard practice for measure of metal dispersion. This gives us a relatively rapid and unambiguous method for investigating the location, not only of active materials but also potential catalyst poisons. Other known techniques for measuring metal dispersion are electron microscopy, and gas adsorption (Cody *et al*, 1994).

2.9.3 Basic Principles of GC-MS Analysis

The gas chromatograph/mass spectrometry (GC/MS) instrument separates chemical mixtures (the GC component) and identifies the components at a molecular level (the MS component). It is one of the most accurate tools for analyzing environmental samples. It is considered a powerful and widely used technique for analysis of hydrocarbons in naphthas. GC works on the principle that a mixture will separate into

individual substances when heated. The heated gases are carried through a capillary column with an inert gas (such as helium). The flow of the gases through the dedicated column allows transport of the different molecules at different rates thus leading to separation. As the separated substances emerge from the column opening, they flow into the MS. Mass spectrometry identifies compounds by the mass of the analyte molecule. A flame ionization detector creates and detects a signal proportional to the concentration of each hydrocarbon as the components exit the column. It operates by collecting (by an electrode) the ions of the flame produced during combustion of the hydrocarbon. The detector response is approximately proportional to the weight of carbon present which greatly simplifies quantitative analysis (Oloworishe, 2014).

The rate of hydrocarbon transport through the column is dependent on the carrier gas velocity, which may be adjusted based on the injector pressure and the oven temperature. The lightest hydrocarbons (methane and ethane) are transported very quickly through the column and separation requires low/ambient temperature (George *et al*, 2005).

Mass spectrometry is considered the only definitive analytical detector. It has a library of known mass spectra, covering several thousand compounds, which are stored on a computer. It is important to note that a limitation of GC-MS could be time consumption, but with the newly developed portable GC-MS model, this challenge may be offset (Oloworishe, 2014).

2.9.4 Basic Principles of FT-IR Analysis

Fourier Transform Infrared spectroscopy (FT-IR): the structure of adsorbed molecules and carbon deposits on supported metal catalysts is determined by using FT-IR technique. The soft coke is determined by SHIMADZU FT-IR 8400S instrument under controlled atmospheric conditions. 50 mg catalyst sample was ground in an agate mortar and mixed well with KBr (potassium bromide) power. The product was pressed into a self supporting disc at 6205 kpa. The prepared sample disc was then placed in the centre of the reaction chamber, fixed in between a folded tungsten grid. Then the spectra are recorded by SHIMADZU FT-IR spectrometer.

2.9.5 Surface Area Determination by Sear's Method

The surface area of the products was determined from Sear's Method.

The procedure is as follows:

1. 1.5g of materials were acidified with dilute HCl using burette drop wise until pH is 3-3.5
2. 30g of NaCl was added to the solution with stirring and then made up to 150ml.
3. The solution was then titrated with 0.1M of NaOH till pH of 9 was reached.
4. The specific surface area is given by

   $S\ (m^2/g) = 32V-25$

Where V is the volume of NaOH needed to raise the pH of the solution from 4-9.

CHAPTER 3

3.0 MATERIALS, EQUIPMENT AND METHODS

3.1 Materials

The materials used in this work are:

1. Fresh and deactivated reforming catalyst (Pt/Al_2O_3) from Kaduna Refining and Petrochemical Company (KRPC).
2. Sodium Bicarbonate
3. Dichloropropane (DCP)
4. Treated Heavy Naphtha
5. Compressed Air
6. Nitrogen (BOC Gas Ltd)
7. Distilled water

3.2 Apparatus

The apparatus used in the course of this work are:

1. Measuring cylinders (1000 ml, 500 ml, 10 ml), Pyrex
2. Crucibles
3. Laboratory mortar and pestle
4. Tyler mesh Sieve (70 µm)
5. Spatula and Plastic spoons
6. Conical flasks (500 ml), Pyrex
7. Beakers (1000 ml and 500 ml)Pyrex
8. Sinta glass filter funnel (Quickfit TM)
9. Sample containers (plastic)

10. Plastic bucket
11. Empty drip container (500 ml)
12. Buchnel flask (1 litre)
13. Thermometer (-10 ^{o}C to 360 ^{o}C)
14. Glass rod
15. Ceramic pot
16. Desiccators (Dry seal type, Jencons)
17. Sample bottles (glass and plastic)

3.3 Equipment

List of the equipment used for both synthesis and characterization.

Table 3.1: List of other equipment used in this work and their specifications

S/N	Name	Model	Manufacturer
1	Weighing Scale (0-180 g)	1455T 18	WEDA,Holland
2	Oven	M OV-420 (0-260 ^{o}C)	Gallenkamp England
3	Analytical Balance	AB 204 (0 – 180 g)	MettlerToledo Switzer land
4	Distilled water machine	A4000	Aquatron Chem. Eng, ABU
5	pH meter	Bibby Scientific Ltd. Jenway 3510 Model	England.
6	X-ray Fluorescence Machine	Minipal 4	PANalytical, Netherlands

7	X-ray Diffractometer	Empyreal	PANalytical, Netherlands
8	Scanning Electron Microscope	Pro X	Phenom- World Co., Holland
9	Tube Furnace		Naberthem, Germany
10	Exposed Element Furnace	TIKIR 11/12	Heraeus, Holland
11	GC-MS Machine	QP2010 PLUS	Shimadzu, Japan
12	HC/ Oxygen Gas tester	ALCAIR	KRPC, Kaduna
13	Air Compressor	JIALILE	ZHE Jiang, Japan

3.4 Experimental Procedures

The procedures followed were adopted from literature (Axen, 2009). The catalyst chosen for this experiment were fresh and two deactivated A and B Pt/Al_2O_3 naphtha reforming catalysts from Catalytic Reforming Unit (CRU) of KRPC. The deactivated catalysts A and B were collected online after 14000 hours and 10000 hours cycle of reforming operation process. It was that the predominant deactivation mechanism of the collected catalyst was theoretical mechanism include sintering before it was separated into the needed particle size through sieving process.

1.0 g each of the fresh and collected deactivated catalyst A and B were crushed using laboratory mortar and pestle to powdered form and XRD, XRF, SEM, and FT-IR analyses were done on them and recorded.

3.5 Parametric Study

The various portions of the two deactivated A and B catalysts to be used were initially weighed and recorded. Each of the various parametric study operations were boosted with nitrogen to clear any form of hydrocarbon left on the deactivated catalyst and other impurities, making it inert. And the nitrogen flow kept constant at 2 kg/cm^2. The setup is as shown in Figure 3.1. The two deactivated catalyst sourced were calcined at different temperatures (400 ^{O}C, 500^{O}C, 600 ^{O}C, 700 ^{O}C, 800 ^{O}C), at constant air flow rate of 1 kg/cm^2 for a reaction time of 4 hours each to obtain the optimum temperature. The deactivated catalyst was also calcined at optimum temperature and reaction time of 4 hrs while the flow rate was varied at 0.7 kg/cm^2, 1 kg/cm^2, 1.4 kg/cm^2, 1.8 kg/cm^2 and 2.1 kg/cm^2. Then the deactivated catalyst calcined at optimum temperature and flow rate while the reaction time was varied at 2 hours, 4 hours, 6 hours and 8 hours. This was to study the effect of temperature, time and flow rate on the nature or pattern of regeneration i.e. amount of coke burnt off.

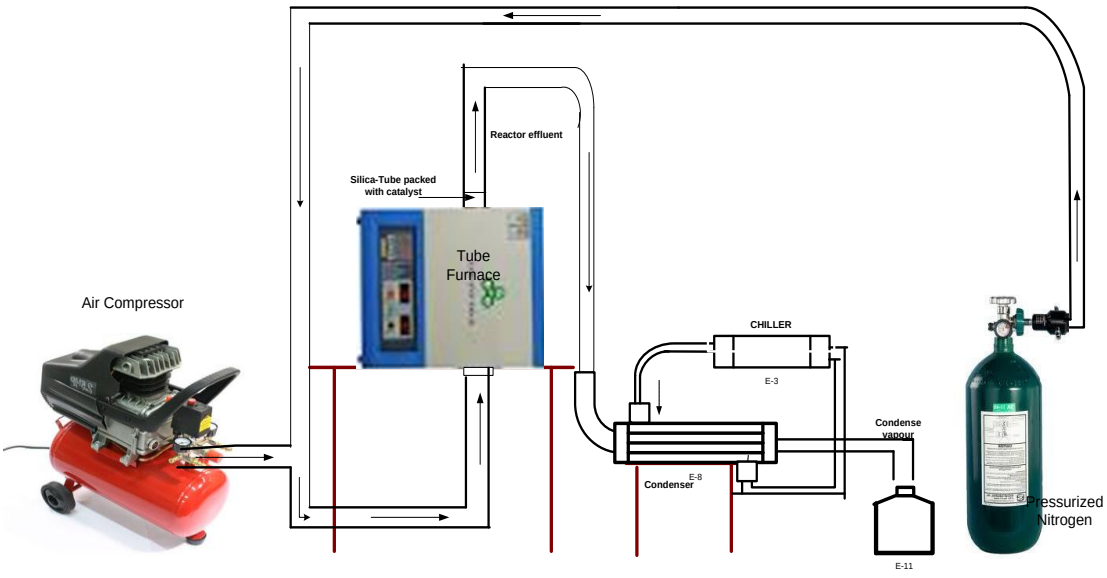


Figure 3.1 Schematic Diagram for the Laboratory Set-up for Parametric Study.

3.6 Regeneration Processes

The regeneration consists of three phases or stages, i.e., carefully controlled combustion of coke with air under nitrogen circulation (combustion), chloride injection under oxygen partial pressure (oxychlorination), and calcinations. The regeneration (combustion of coke) was done in three stages in other to have good control of the combustion process (coke combustion) and not to exceed the required temperature of 520 ^{o}C of which when exceeded damages the mechanical structure of the catalyst. Also, as to make sure the coke deposit are completely burnt off because using only a stage combustion and starting at high elevated high temperature will quickly give a significant drop in reactor outlet temperature and not all coke deposit on the catalyst will be burnt off. The burning will be so rapid to the extent the mimic reactor can melt or if it's of good quality, it will affect the catalyst (losing all its activity). So the gradual increase in reactor inlet temperature (400 ^{o}C - 480 ^{o}C) was just a control to avoid catalyst damage and protecting reactor internals.

Two grams of $NaHCO_3$ salt was dissolved in 100 ml of distilled water and the mixture was well stirred to give an aqueous solution with pH within 8 and 9. Also the dichloropropane (DCP) solution was also diluted in water of ratio 1:20 (see appendix A-1 for the calculations). Each deactivated catalyst undergoes same operating conditions. And the regeneration process starts with the reactor containing 2 g of deactivated catalyst first purged with nitrogen until hydrocarbon content was below 0.2 vol % using HC/ Oxygen Gas tester (Plate 3.1)**.** The compressor was started at low speed to contain less than 0.5 vol %. oxygen entering the reactor and the reactor effluent cooler (chiller) commissioned at -20 ^{o}C. The regeneration diagrammatic setup is as shown in Figure 3.2



.

Plate 3.1: Hydrocarbon/ Oxygen Gas tester for Regeneration of Deactivated catalysts.

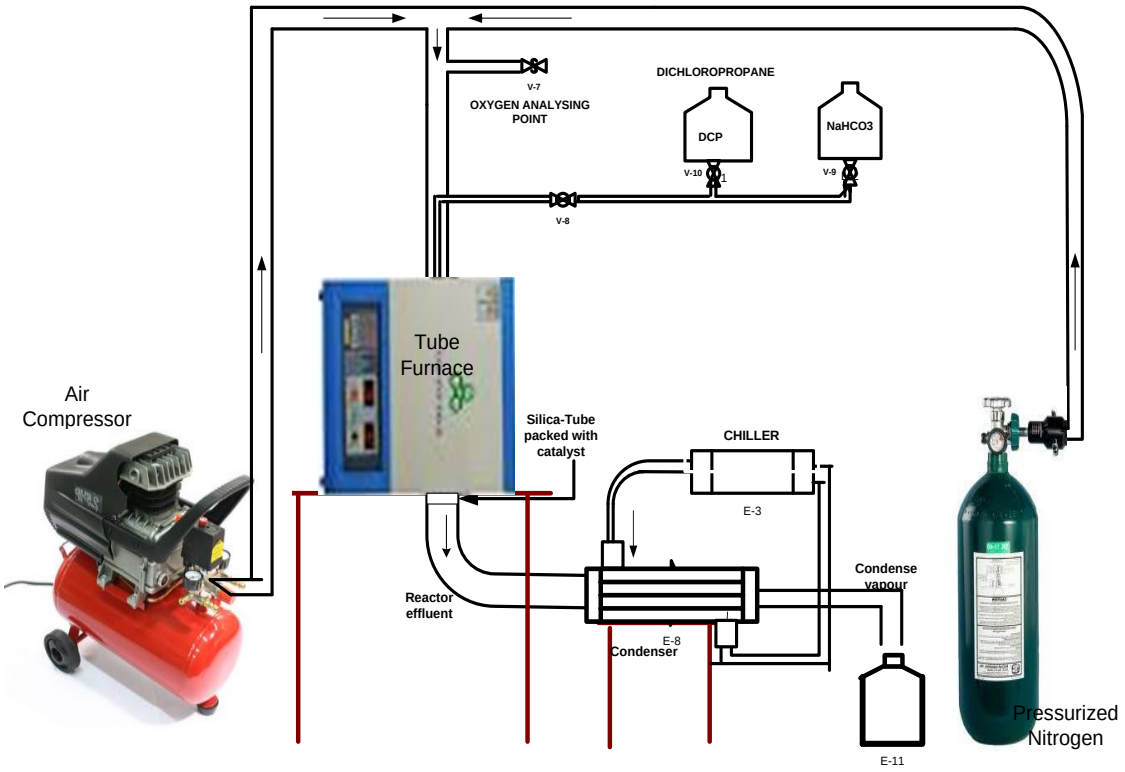


Figure 3.2: Schematic diagrams for the laboratory set-up for regeneration of deactivated catalysts.

3.6.1 First stage combustion

The tube furnace (heater) was commissioned and the inlet temperature raised to 400^{o}C in the presence of nitrogen only. The $NaHCO_3$ circulation commenced while the inlet temperature was stabilized at 400 ^{o}C. At 350 °C the chloride injection resumed (20/1 H_2O/Cl molar ratio). i.e. the DCP was continuously injected (started at low rate initially and rate increased to a specific level, watching closely ΔTs closely) at a rate to maintain the chloride on catalyst. The compressor was commissioned and regeneration air flowrate was controlled in such a way that the temperature increase through the catalyst bed does not exceed 40 °C, (outlet Rx temperature - inlet Rx temperature).

It was ensured that the temperature of the combustion zone was not higher than 450°C and this was checked through bed thermocouple. This was achieved by decreasing the air flowrate (the injection of air can be eventually stopped) in order to maintain a temperature at reactor outlet not exceeding 440 °C. In order to monitor the temperature increase, the oxygen concentration at reactor inlet was controlled in the range of 0.5 volume % and under no circumstances was it allowed to exceed 0.8 volume %. The burning generally started with an oxygen concentration of 0.1 volume % in the gas entering the reactor. As long as combustion takes place, the air flowrate must be adjusted in order to limit the temperature increase through the catalyst bed at 40°C or to maintain the reactor outlet temperature at 440 °C maximum.

The pH analysis of the circulating sodium bicarbonate solution was conducted at 2 to 5 minutes interval with litmus paper and pH meter targeting pH 8-9 so as to neutralize the acid which leaches from the catalyst. The air injection was stopped immediately there

was significant drop in outlet temperature and oxygen level start increasing in regeneration gas, which is an indication of the end of the first combustion phase.

3.6.2 Second stage combustion

When the first combustion was completed and the reactor temperature stabled back at 400°C, the inlet temperature was then progressively increased to 440 °C under nitrogen circulation then oxygen concentration was then increased from 0.5 to 1 volume % while DCP and $NaHCO_3$ were still in circulation. The reactor temperature difference (ΔT) was maintained at 40 °C, oxygen content of regeneration gas increased to 0.6 vol % after which air injection was adjusted if there is significant drop in outlet temperature on the catalyst bed and oxygen level start increasing in regeneration gas and outlet temperature not exceeding 480 °C. Air injection rate was decreased as soon as secondary combustion occurs, then oxygen content adjusted to 0.5vol % thereafter air injection stopped to maintain reactor inlet temperature at 440 °C (Axen, 2009).

3.6.3 Proof burning (third stage combustion)

The reactor inlet temperature was slowly increased from 440 °C to 480 °C over a period of 10 mins. Oxygen content was increased from 0.5 vol to 2 vol % in steps of 0.8 vol %, 1.2 vol %, 1.6 vol % and 2.0 vol % maintaining each step of O_2 concentration for 20 mins as soon as reactor inlet temperature of 480 °C was attained. Residual coke burning was observed for as indicated by a decrease in the O_2 concentration of the circulating gas. Air rate was adjusted when combustion was

observed and average reactor outlet temperature was monitored not exceeding 510°C (Axen, 2009).

If reactor temperature difference (ΔT) was 0 °C or negative, reactor cooling commences but if still positive, chloride adjustment (oxychlorination) continues, so air injection was stopped and regeneration gas circulated for 10 mins at 480 °C and when the oxygen concentration at reactor outlet equals the oxygen concentration of 2.0 vol % at reactor inlet, the combustion phase was considered complete with reactor outlet temperature not exceeding 520 °C.

3.6.4 Oxychlorination

At 520 °C stable average bed temperature, the oxygen concentration in the gas was increased to 5 vol % in 10 mins by adjusting the air injection rate while observing dichloropropane (DCP) circulation carefully for any restart of the combustion. The bed temperature at 520 °C and 5 vol % O_2 was maintained for 1hr within which calcination commenced.

3.6.5 Calcination

After the 30 mins hold at 520 °C and 5 vol % O_2, the O_2 concentration was increased to 14 vol % in another 1hr (Axen, 2009). Bed temperature was maintained at 510°C and 14 vol % O_2 for 2hrs without exceeding an outlet reactor temperature of 520°C.

3.6.6 Rinsing and Drying

At the end of the calcination phase at Bed temperature of 520 °C, while the chlorine injection still in service, caustic solution was stopped and rinsed with distilled water for 10 mins, maintaining oxygen concentration higher than 3 vol % before the chlorine dichloropropane (DCP) injection was also stopped and drained. The drying period was carried out in about 30 mins and not more than 1 hour.

3.6.7 Cooling

While maintaining oxygen concentration in the regeneration gas higher than 3 vol. %, the reactor inlet temperature was decreased to 350°C. The heater and compressor were shut down to allow the catalyst cool down far below 180°C before it was poured into desiccators for activity performance test.

3.7 Catalysts' Reformation

In a typical run, about 2.0 g of the catalyst sample was packed (loaded) halfway within a tubular reaction vessel, a 56 cm long by 1.0 cm internal diameter stainless 'silica tube'. The diagrammatic set-up is as shown in Figure 3.3. Glass-fibres were placed before and after the catalyst bed to homogenize the reactant mixture and temperature. Prior to any reaction, the reactor's temperature was steadily increased to the desired reaction temperature (465 °C) and maintained at that temperature (Oloworishe, 2014)

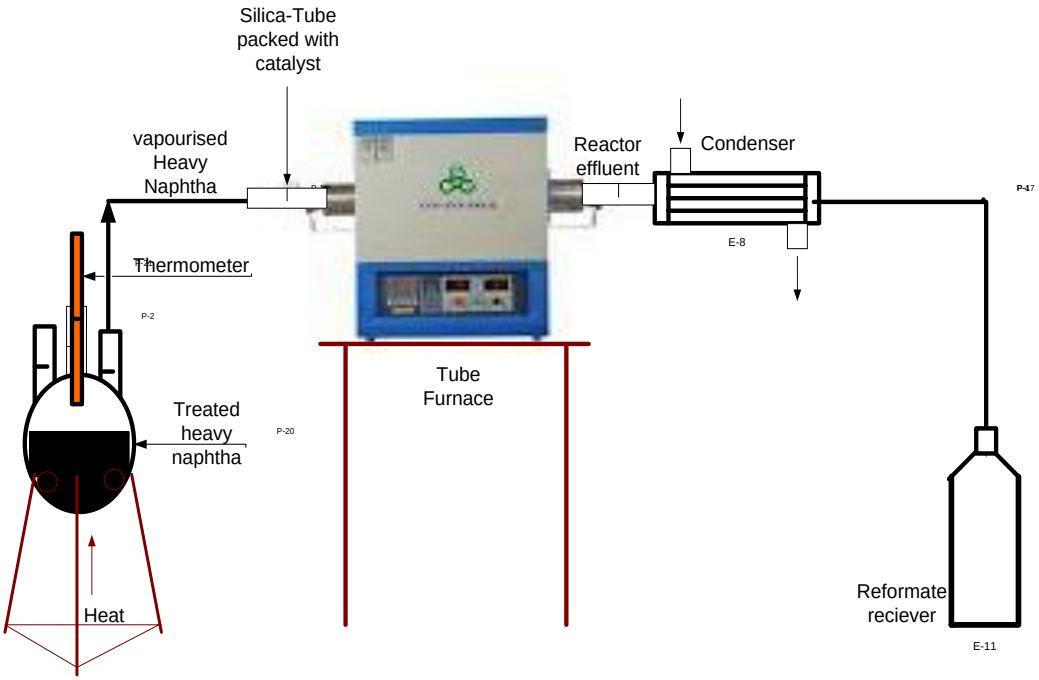


Figure 3.3: Schematic diagram for the laboratory set-up for heavy naphtha reformation for catalyst performance.

Treated heavy naphtha in a flask was heated (to vapourize) and the vapour was channelled downstream into the reactor. The vapour outlet (reformate) from the reaction zone was condensed as it passed through the condenser. The condensed reformate was collected as product. The procedure was done for fresh and the two deactivated catalyst at the same reaction temperature of 465 ^{0}C. The constituents and compositions of reformate obtained in each case were determined with the aid of a QP2010 PLUS GC-MS machine at national research institute for chemical technology, (NARICT), Zaria.

3.8 Catalysts' Performance Evaluations

The catalyst performance evaluation was examined on the basis of catalyst's ability to enhance the yield of reformate from treated heavy naphtha. The treated heavy naphtha

feed was not pure (see Appendix B, Table B.1). The assumed composition of the byproducts (i.e the dry gases) in the entire products was cited from the work of Kalra (2009). The operating reaction temperature used for the reforming was 465 ^{0}C for the various catalysts packed.

Treated heavy naphtha feeds (F) $\xrightarrow{\text{(reforming)}}$ Products

Product = Sample collected + byproducts

Byproducts = (H_2 + off-gases + LPGs) = X

Sample collected = Unconverted feed (N) + reformate (R)

Hence, from the chromatogram of each sample analyzed, the area assigned to the unconverted treated heavy naphtha was taken as N, while the total area assigned to all reformates was taken as R.

Recall, X = 14.50 wt % of the entire product (Kalra, 2009).

Let

Feed (treated heavy naphtha) = F

Such that

Products = $R + N + X$

Feed consumed: $f = F - N = X + R$

Thus, the percentage yield (Y_R) of reformates for each run/sample is

$$Y_R = \frac{R}{\text{Treated heavy naphtha } \textit{consumed}} \times 100\,\% = \left(\frac{R}{X+R}\right) \times 100\,\%$$

Where

R = wt % of reformate

N = wt % of unconverted feed

X = wt % of the byproducts.

Theoretically, the area under a peak is proportional to the amount of analyte present in the chromatogram. The area of the peak is proportional to the concentration of an analyte in the original sample. Concentration was obtained using a calibration curve created by finding the response for a series of concentrations of analyte, or by determining the relative response factor of an analyte. The relative response factor is the expected ratio of an analyte to an internal standard (or external standard) and was calculated by finding the response of a known amount of analyte and a constant amount of internal standard.

3.9 Product Characterization.

The elemental composition (in oxide form) of product obtained was determined using the energy dispersive X-Ray florescence (ED-XRF) machine (Minipal 4), and the X-ray diffraction (XRD) patterns were obtained using Empyreal, PANalytical diffractometer employing Cu Kα radiation (λ = 0.154nm) at the National Geoscience Research Laboratories (NGRL), Kaduna. Scanning electron microscopy (SEM) imaging and Surface area using sear's method were conducted at the Department of Chemical Engineering, ABU, Zaria. Fourier Transform Infrared spectroscopy (FT-IR) and Gas Chromatograph/Mass Spectrometry (GC-MS) were obtained using SHIMADZU FT-IR spectrometer and QP2010 PLUS GC-MS at the National Research Institute for Chemical Technology (NARICT), Zaria. at the National Research Institute for Chemical Technology (NARICT), Zaria.

3.10 Constraint Encountered

Certain limitations were encountered during the course of this work.

(1) The setup cannot allow knowing the actual composition and quantity of feed converted, how much naphtha has been vapourised or product that has been condensed and cannot measure exactly the composition of the feed remaining in the container and composition after condensation.

(2) Inability to capture some of the by-products of cracking of reforming reactions, which includes: LPGs and off-gases, thus, making the catalyst performance evaluation to be examined only on the basis of the catalysts' ability to enhance reformate yield from the feed. Thus, the yield is taken as the ratio of the desired product (reformate) to the total products. The weight proportion of the by-products was assumed to have a fixed value of 14.50 wt % of the entire products, as earlier confirmed by Karla (2009). See Table C6 (Appendice C) for details.

CHAPTER FOUR

4.0 RESULTS AND DISCUSSION

The results of all the investigations carried out in this work are presented and discussed in this chapter.

4.1 Catalyst Characterization

The fresh, deactivated catalyst (Deactivated A and B) and the regenerated catalysts were all analyzed using XRD, XRF, FT-IR and SEM and the results are discussed as follows:

The modified method used in determining the optimum conditions for regeneration were initially based on gravimetric method (weight loss) by coke burning in air at various temperatures, air flow rate and time.

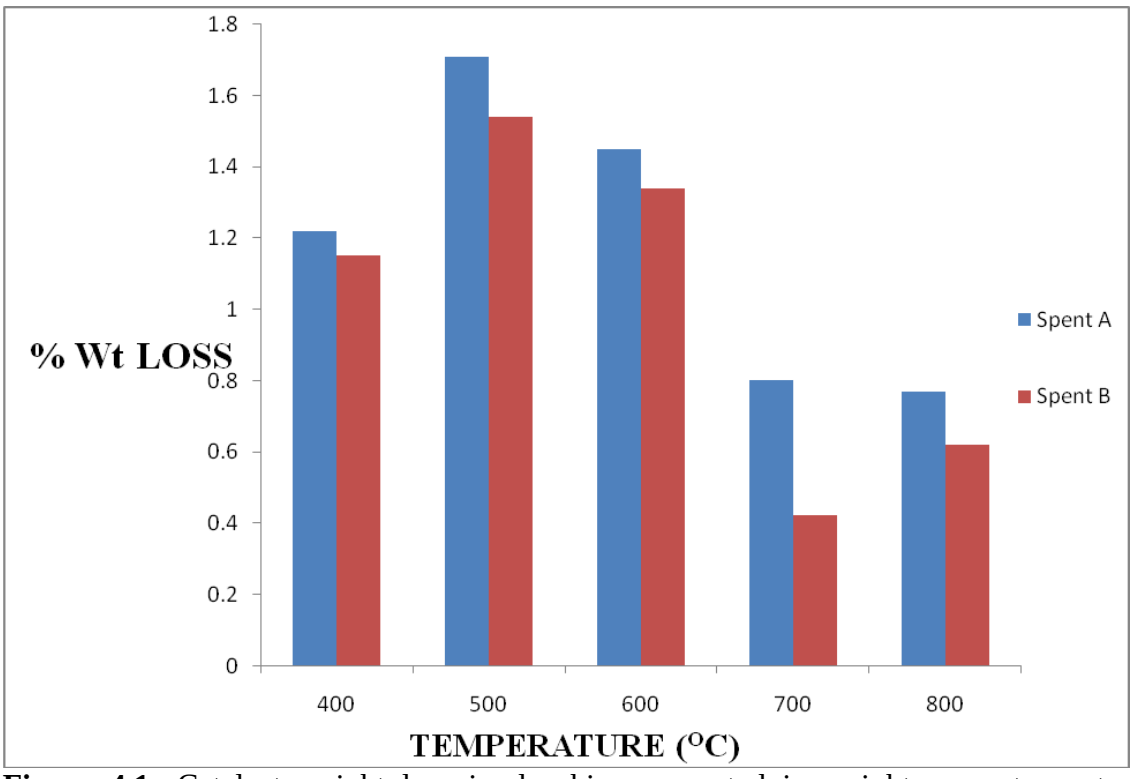


Figure 4.1: Catalyst weight loss in decoking presented in weight percentage at 1kg/cm^2, 4 hours and at various temperature ranges.

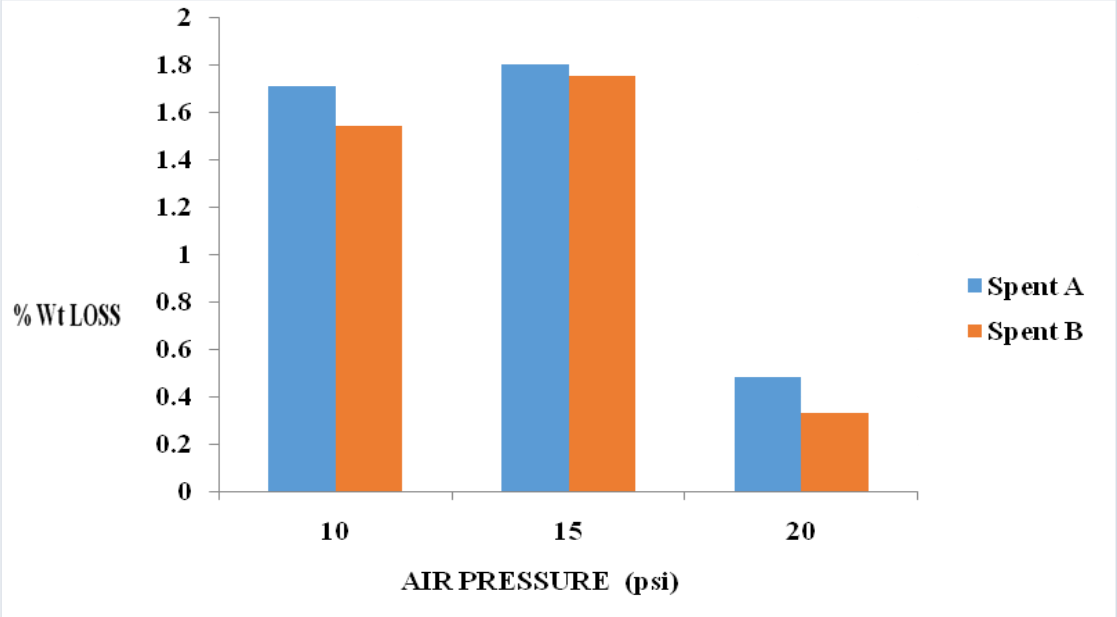


Figure 4.2: Catalyst weight loss in decoking presented in weight percentage at optimum temperature, 4 hours and at various air flowrate.

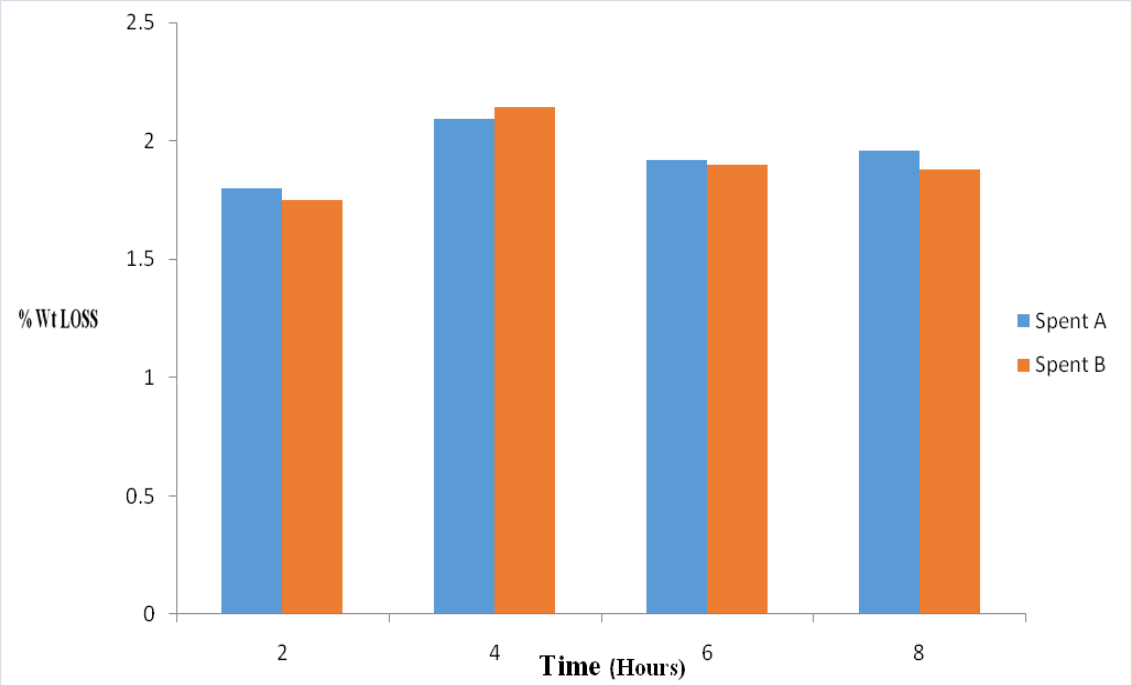


Figure 4.3: Catalyst weight loss in decoking presented in weight percentage at optimum temperature and pressure and at various time range.

Also, the deactivated catalyst weight loss (%) were recorded and plotted as shown in Figures 4.1 - 4.3 to observe the weight loss after varying each operating parameters

and the best calcinations as the temperature increased from 400 to 800 ^{0}C and that of air pressure (0.7 – 1.8 kg/cm^2) and time variation from 2 hours to 8 hours.

From Figure 4.1, the flow of air pressure was maintained at 1 kg/cm^2 with constant nitrogen flow at 2 kg/cm^2 over a temperature range of 400^{o}C to 800 ^{o}C for the two deactivated catalyst. The observed weight loss during this period is due to decoking process and two sets of losses were observed. The rate of weight loss between temperature 400^{o}C and 600 ^{o}C is higher than weight loss at higher temperatures (700 ^{o}C and 800 ^{o}C). These may be due to the nature of coke. As the temperature increases from 400 ^{o}C to 600 ^{o}C there were rapid weight loss far above 1 % observed, showing presence of soft coke weight loss on catalyst while at higher temperature (700 ^{o}C and 800 ^{o}C) they were found to be below 1 % as all shown on Figure 4.1. But the weight loss was more pronounced at 500^{o}C (1.72 % for deactivated A and 1.54 % for deactivated B), so it was on this basis that it was used as the optimum temperature for the variation of air pressure flow at 4 hours calcination period. Figures 4.2 and Table A.2 show that more coke were burnt off at moderately low air pressure because 0.7 and 1 kg/cm^2 gave also a soft coke presence with most percentage weight loss for both deactivated A and B, while higher air flow pressure had lesser weight loss. This is because air pressure with the nitrogen gas pressure of 2 kg/cm^2 (2.1 kg/cm^2) with the 1 kg/cm^2 was considerable enough to give higher yield of reformate for a given octane number which was the reason for minimizing pressure drop and operating at lower practical pressure. But 1 kg/cm^2 was chosen as the optimum operating pressure because it had more coke burnt off with 1.80 % and 1.75 % for deactivated A and deactivated B, respectively. Figure 4.3 for catalyst weight loss in decoking presented in weight percentage at optimum operating temperature and pressure and at various time

range were found to all have soft coke presence irrespective of time variation. It was however obsereved that after 4 hours of calcination was there no increase in weight loss of coke deposit instead a slight decrease was observed as the calcination time increases.

From Table 4.1, it can be seen that after regeneration of the deactivated deactivated catalyst A and B. 2.49 % and 2.63 % was the weight loss of carbonaceous deposit on the on Pt/Al_2O_3 which shows presence of soft coke on the two deactivated catalyst as compared to when there was total shut down of a reforming plant for regeneration given approximately 3.0 - 3.3 % weight loss on catalyst depicting hard coke deposit.

Table 4.1: Catalyst weight loss in percentage of deactivated catalyst A and B after regeneration using the ranges of optimum conditions.

Catalyst	Weight Of Catalyst (g)		Catalyst Weight loss (%)
	Before Regeneration	After Regeneration	
Deactivated A	2.009	1.959	2.49
Deactivated B	2.056	2.002	2.63

4.1.1 FT-IR Analysis of the Catalysts.

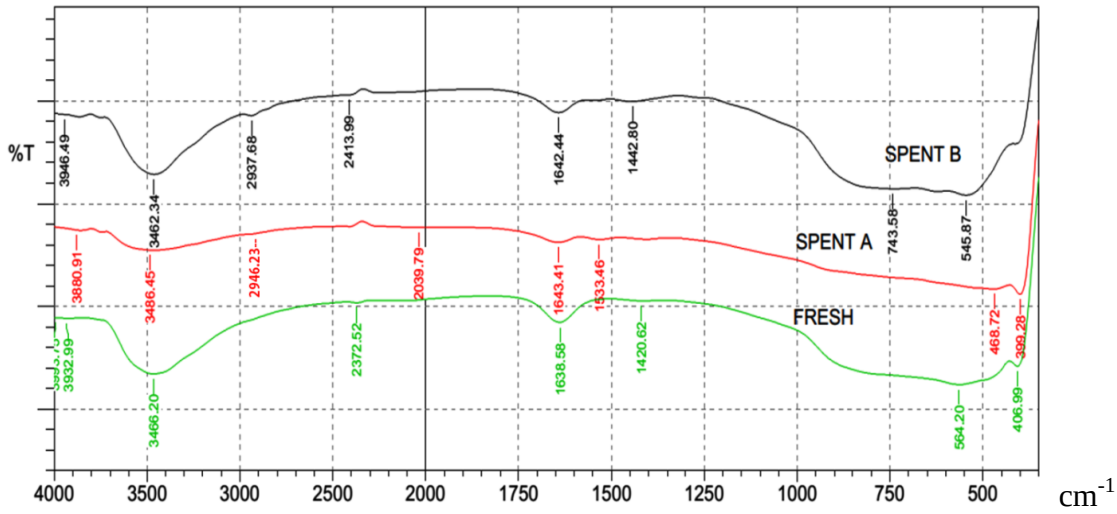


Figure 4.4: FT-IR spectroscopy analysis of fresh, deactivated A and deactivated B catalyst before calcinations.

The absorption bands of 3466.20, 3486.45 and 3462.34 cm^{-1} in the Figure 4.4 of fresh, deactivated A and deactivated B respectively still affirmed NH stretching vibrations of NH_2 in aromatic amines and amides group. The absorption band between 3000 and 2800cm^{-1} are assigned to aromatic and aliphatic rings which were probably produced by polycyclic aromatics like chrysene. The absorption bands at 2946.23 cm^{-1} and 2937.68 cm^{-1} (deactivated A and deactivated B) corresponded to CH antisym and sym stretching of $–CH_3$ and $–CH_2$- in aliphatic compound which agree with symmetric and asymmetric flexion vibration of the C-H bonds associated with CH_3 (Ruixia et al., 2003). The results obtained can be attributed to presence of commercial coke which is a manifestation of the presence of heavy unsaturated product from hydrocracking reaction during reforming such as poly-aromatics. Deactivated A with a band of 2039.79 cm^{-1} confirms the presence of structure of aromatic compounds from the pattern of the weak overtone and combination tone bands. Also absorption band at

1643.41 cm^{-1} (deactivated A) and 1642.44 cm^{-1} (deactivated B) also confirmed C=C stretching of C=C in alkenes i.e showing traces of heavy olefins and di-olefines not saturated to form paraffins which are later converted to aromatics during reforming process also promote coking from the hydrocracking reaction effect on the catalyst. 1533.46 cm^{-1} absorption band on deactivated A shows the presence of aromatic ring. Likewise, the band 1442.80 cm^{-1} on deactivated B corresponded to CH_3 antisym deformation of CH_3 in aliphatic compounds as also seen on fresh catalyst.

The entire absorption band below 900 cm^{-1} confirms C-H out of plane bending, i.e. 743.5 cm^{-1} of deactivated B shows phenyl ring substitution bands as reported by Manos *et al*, (2007).

The deactivated (deactivated) catalysts were calcined at varying temperature, time and air pressure (oxygen level) using unifactorial method to know the range of operating conditions to be used for proper regeneration of the deactivated catalyst. The various results were characterized using FT-IR and the spectra for each operating conditions can be seen cascaded in Figures 4.5 to 4.8.

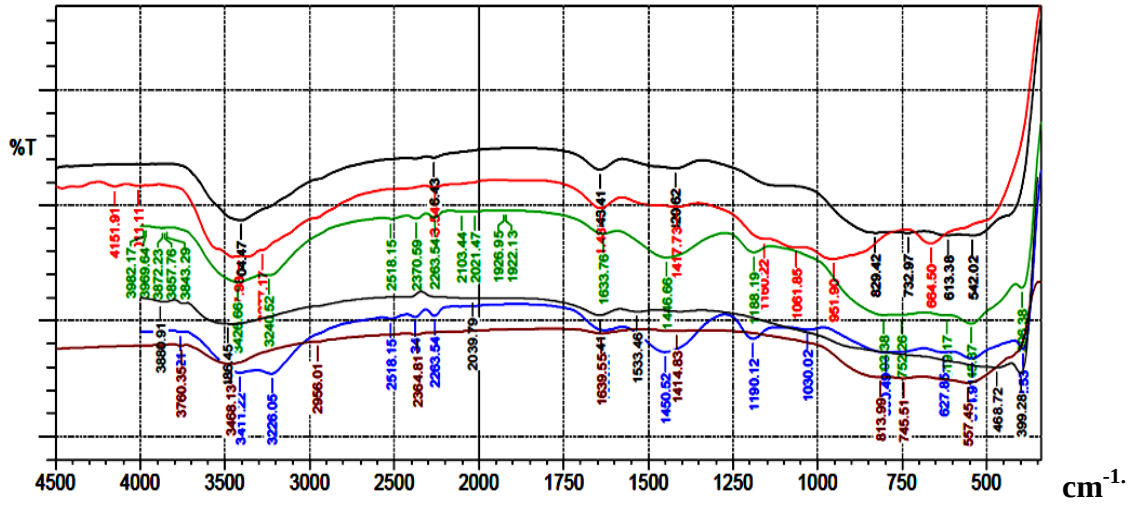


Figure 4.5: FT-IR spectroscopy of fresh and deactivated A catalyst at 400^{o}C, 500^{o}C, 600^{o}C, 700^{o}C and 80 ^{o}C calcinations

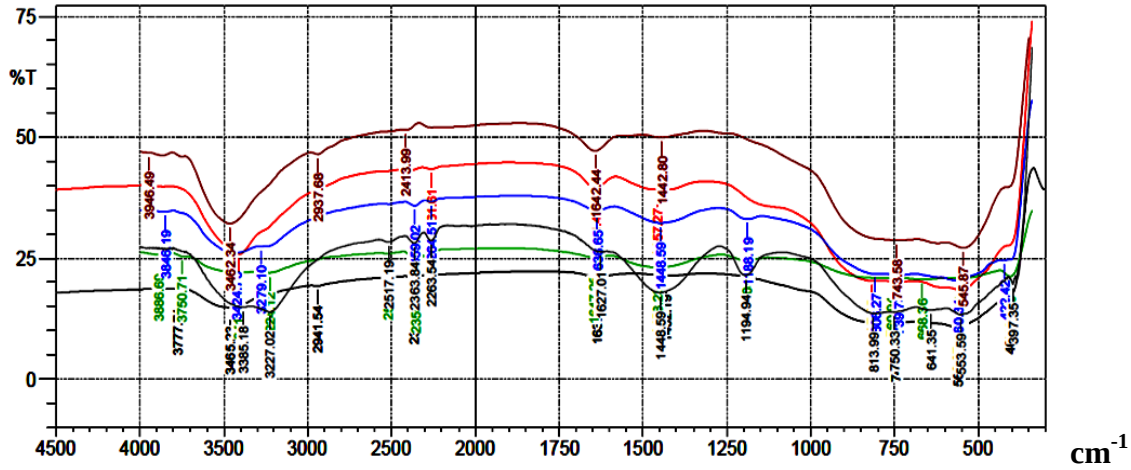


Figure 4.6: FT-IR spectroscopy of fresh and deactivated B at 400^{o}C, 500^{o}C, 600^{o}C and 700^{o}C and 800^{o}C calcinations

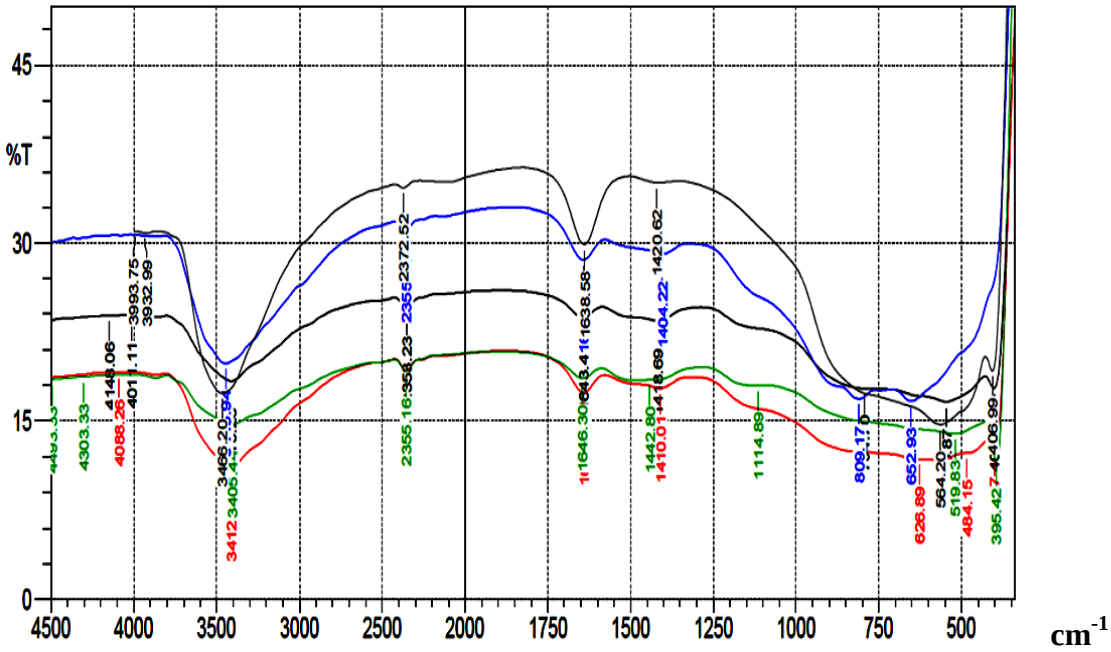


Figure 4.7: FT-IR spectroscopy of fresh, deactivated A at 500°C for 2, 4, 6 and 8 hour calcinations

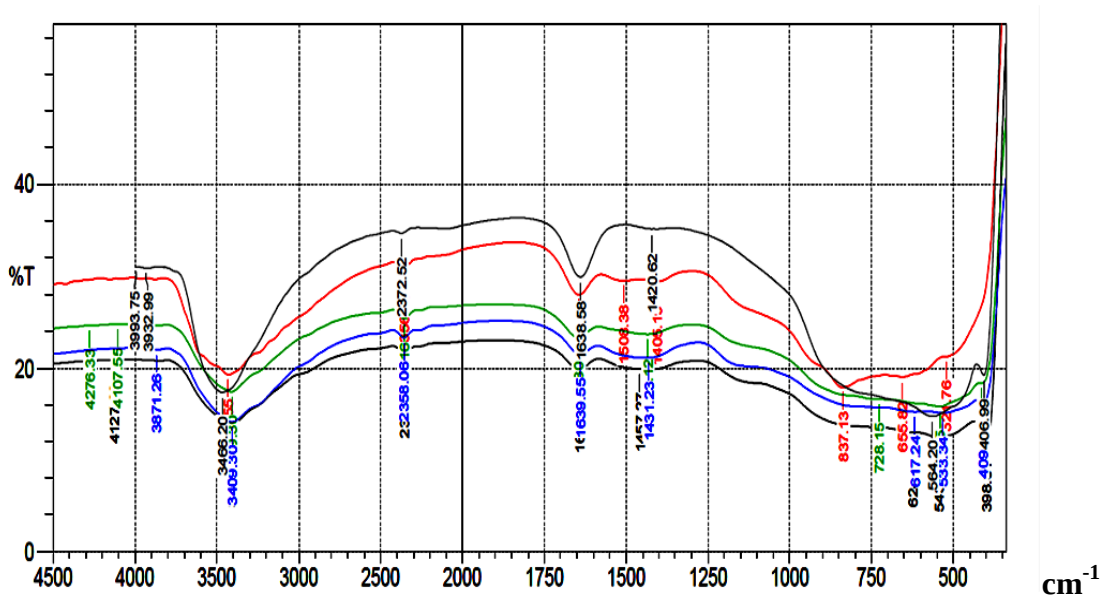


Figure 4.8: FT-IR spectroscopy of fresh, deactivated B at 500°C for 2, 4, 6 and 8 hour calcinations

Figures 4.5 and 4.6 present the spectra of calcined deactivated A and B at different temperatures. From the results, it can be seen that the absorption band (2937.68cm^{-1} deactivated A and 2946.23cm^{-1} deactivated B) that the initially presence of coked catalyst on Figure 4.4 was found to disappeared after the catalyst was calcined at 400^{o}C, 500^{o}C and 600^{o}C under nitrogen gas as deposited on Figure 4.5 and 4.6, which revealed that coke precursors can be eliminated at such temperatures**.** However at higher calcination temperatures of 700 ^{o}C and 800 ^{o}C the presence of coke is still observe as shown in Figure 4.5 (2948.62 and 2956.01 cm^{-1} on deactivated A) and Figure 4.6 (2941.54 and 2937.60 cm^{-1} on deactivated B). The results also shows that the process of sintering also occur at these temperature.

From these observations, it can be deduced that calcination at 700^{o}C and above, the occluded substrate in the catalyst were subjected to thermal cracking and carbon is deposited. It is also apparent that the materials (coke) that would have been given off as volatile gases were cracked resulting into carbon. It is however not recommended to carryout regeneration at high level (elevated temperature) otherwise secondary reactions (hydrocracking, hydrodealkylation and other undesired reactions) will be promoted.

Considering time variation with optimum temperature (500 ^{o}C) and a lower air pressure (1 kg/cm^2) chosen as a result of conditions with highest percentage weight loss of deposit on the two deactivated catalyst. Figures 4.7 and 4.8 showing cascaded time variation for deactivated A and B respectively. The results shows that there is little or no variation in peaks i.e. showing all functional group that can be seen in the fresh catalyst but in terms of percentage weight loss (Figure 4.3) for 2, 6 and 8 hrs are lower

compare to that of 4 hours. The increase in time results into higher severity which results in increased octane during reforming, lower reformate yield and higher coke deposit.

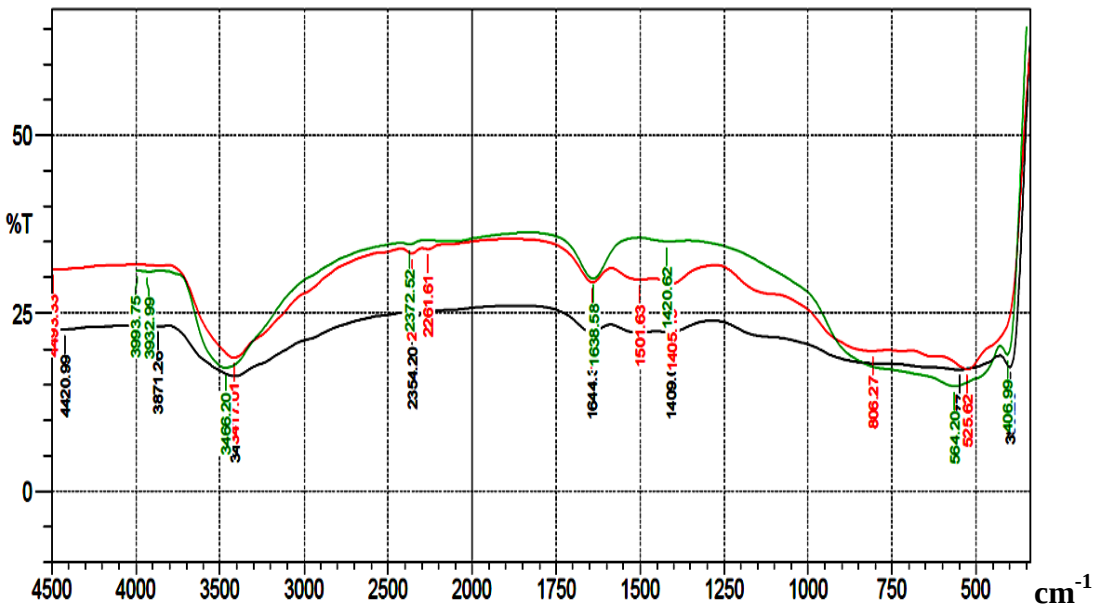


Figure 4.9: FT-IR spectroscopy analysis of fresh, regenerated deactivated A and regenerated deactivated B catalyst.

The main absorption bands in Figure 4.9 at 3417.01 cm^{-1}(deactivated A) and 3410.26 cm^{-1} (deactivated B) corresponded to OH stretching vibrations (due to OH-Pt bond) i.e. hydrogen bonded in alcohols and phenols. The absorption bands at 2359.02, 2354.20 and 2261.61 cm^{-1} has no significant effective functional group because of its weak intensity while absorption band at 1644.37 and 1641.48 cm^{-1} corresponded C=C stretching of C=C in alkenes were due to the adsorption of olefin and aromatics on the catalyst metal surface (Ruixia et al., 2003). This may indicate that the coke species found near the active metal are soft coke and it is mainly made up of unsaturated hydrocarbon and heavy aromatics. The results also confirmed that, the industrial or

commercial coke catalyst represented between bands 3000 and 2800 cm^{-1} (2937.68 and 2946.23 cm^{-1}) are missing after regeneration. This result revealed that the coke precursors were eliminated after treatment under nitrogen gas in the presence of controlled air and dichloropropane (chlorine).

4.1.2 XRD pattern analysis.

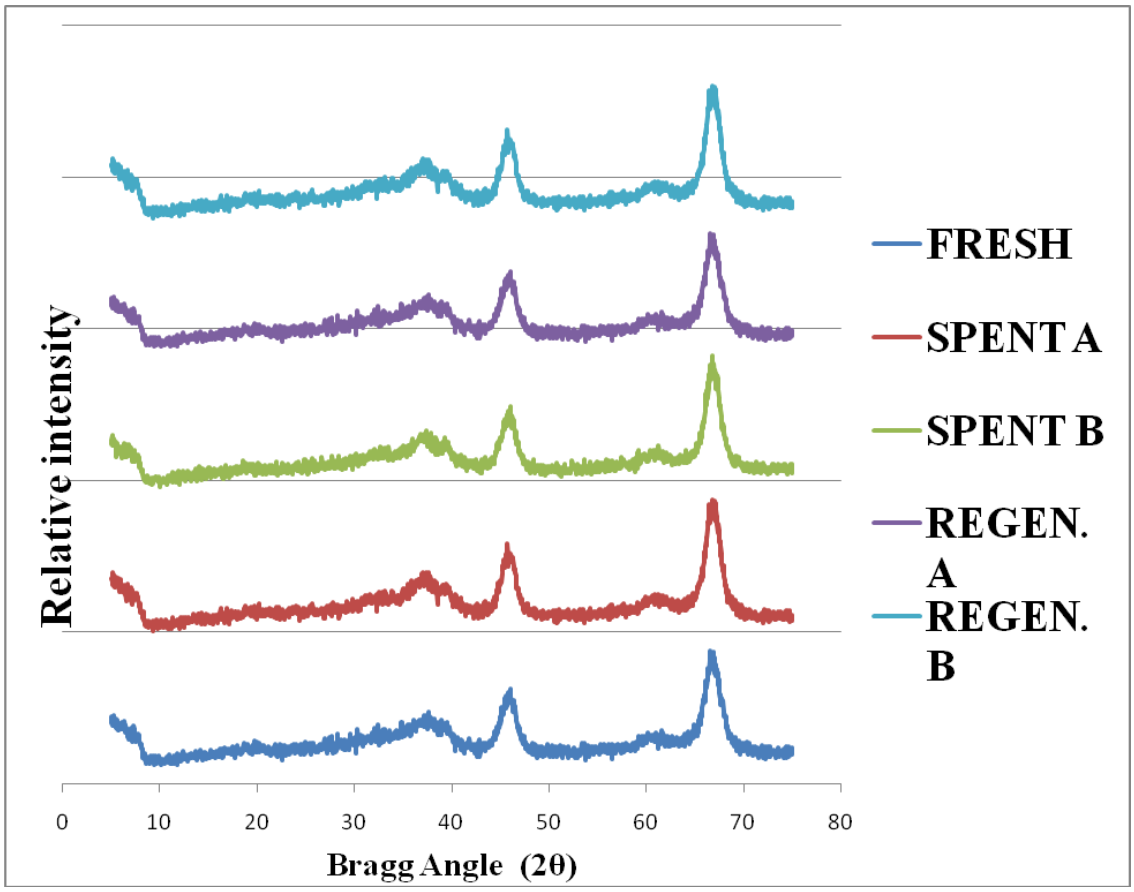


Figure 4.10: XRD patterns of the fresh, two deactivated catalysts and the regenerated catalysts.

The XRD diffractograms obtained from Empyreal PANalytical Diffractometer for the catalysts (fresh, deactivated A and B) are as shown in Figure 4.10 above. The low intensity counts and the broad peaks that characterized the diffractographs of the

support (γ-Al_2O_3) averred to the fact that the gamma-alumina is amorphous. The platinum catalysts have closely related bragg angles (2θs) with those of the support (alumina), but little or no significant difference with their intensity counts. The XRD diffraction peaks and bragg angles for platinum exist at 40^0, 47^0, 68^0 (Figure 4.9) for all the catalyst which appears to coincide with the support (gamma-alumina) which exist at 37^0, 39^0, 46^0, 60^0, 67^0 except that platinum shows a distinct peak at 47^0 and 68^0. These interpretations agree with the works of Hosseini *et al* (2011) and Bawa (2012). The works of Yasuharu *et al* (2005) also corroborated the fact of XRD pattern of platinum has bragg angles of 17^0, 40^0, 46^0, 67^0. Likewise, Gobara *et al* (2014) affirmed that Pt/Al_2O_3 catalyst have Bragg angles of 39.8^0, 46.5^0 and 67.8^0 which are attributes of Pt metallic phase in accordance with the ICDD database: JCPDS 01-1190. Despite the heat effect on regeneration of the catalysts it shows that thermally the structure was not destroyed and carbon has no much significance on the structure of the catalysts

4.1.2. XRF Analysis.

Table 4.2: XRF of the catalysts result of analysis (oxide %)

	Fresh	Deactivated A	Deactivated B	Regenerated Deactivated A	Regenerated Deactivated B
SiO_2	1.03	_	0.59	0.32	0.78
Al_2O_3	89.9	92.23	92.2	91.89	91.08
K_2O	0.01	_	0.03	_	_
Na_2O	<0.01	<0.01	<0.01	<0.01	<0.01
MgO	0.02	_	0.04	_	0.04
P_2O_5	0.78	0.64	0.48	0.68	0.59
Cl	2.95	_	_	0.98	1.08
CaO	0.278	0.322	0.269	0.301	0.265
TiO_2	0.20	0.410	0.408	0.382	0.26
V_2O_5	0.18	0.275	0.15	0.242	0.17
Cr_2O_3	0.14	_	0.13	0.09	0.13
MnO	_	_	0.025	_	0.014
Fe_2O_3	0.032	1.02	2.51	0.84	1.02
NiO	_	0.022	0.013	0.014	0.010
CuO	0.042	0.030	0.034	0.032	0.034
ZnO	0.02	0.082	0.051	0.04	0.031
ZrO_2	0.4	_	0.4	0.12	0.4
Ag_2O	0.03	0.89	0.01	0.67	0.43
BaO	0.74	0.56	0.33	0.64	0.42
ReO_7	0.1	_	_	_	_
PtO_2	2.47	2.38	2.13	2.39	2.26
IrO_2	_	0.42	_	_	_
TOTAL	99.332	99.291	99.81	96.641	99.024

Table 4.2 shows the percentage oxide form of elemental composition using XRF. The alumina (Al_2O_3) and the platinum were more dominant. From table 4.2, it could be seen that there was a proportional increase in the support (alumina) after reforming has taken place on the deactivated catalyst compared to fresh catalyst (89.9 % to 92.23 % deactivated A 89.9 % to 92.2 % deactivated B). While little decrease in platinum (2.47 % to 2.38 % deactivated A and 2.47 % to 2.13 deactivated B) and loss of chlorine which was completely used up during reforming process.

Majorly, the fluctuation of the oxide was as a result of the loss of chlorine which was completely used up spreading across some of the other oxides for example alumina material increased probably as a result of chlorine loss and decrease of masses of other oxides. The effect of regeneration or removal of some carbonaceous material, chlorine which was earlier used up resurfaced on the catalyst after the activity was boosted with dichloropropane and the alumina (support) decreases while other oxides too regained almost their original compositions. The SiO_2 reappearing in the regenerated deactivated catalyst was probably due of machine error during analysis which could affect the total oxides if removed and no much material to re-run same analysis.

4.1.3 Carbon Composition of Catalyst.

The organic carbon content composition was carried out in the Laboratory of Soil Science Department, Faculty of Agriculture, Ahmadu Bello University, Zaria) using the Walkley black method. The percentage carbon on each catalyst was tabulated in Table 4.3.

Table 4.3: Carbon composition on catalyst.

Catalyst	Carbon Composition (%)
Fresh	0.012
Deactivated A	0.317
Deactivated B	3.705
Regenerated Deactivated A	0.189
Regenerated Deactivated B	0.317

The composition in Table 4.3 shows considerable deposition of carbon on the catalyst during reforming at the 140000 and 10000 hours life cycle of the deactivated catalyst A and B. It was observed that there was much deposit of carbon on the first collected catalyst (deactivated B) possibly due to the presence of more hydrocracking reaction taking place. The high carbon deposits found on the deactivated catalyst decreased after regeneration due to the burning off the coke (carbon) deposited on the catalyst. The presence of carbon on the fresh catalyst could be as a result of catalyst adsorbing atmospheric deposit when exposed.

4.1.4 Morphology of Catalysts.

The extent of dispersion of an active ingredient (platinum metal) on a support (γ-alumina) was determined by Scanning electron microscopy (SEM) technique. And Energy dispersion xray showing the elemental composition present while SEM analyzes the surface of materials.

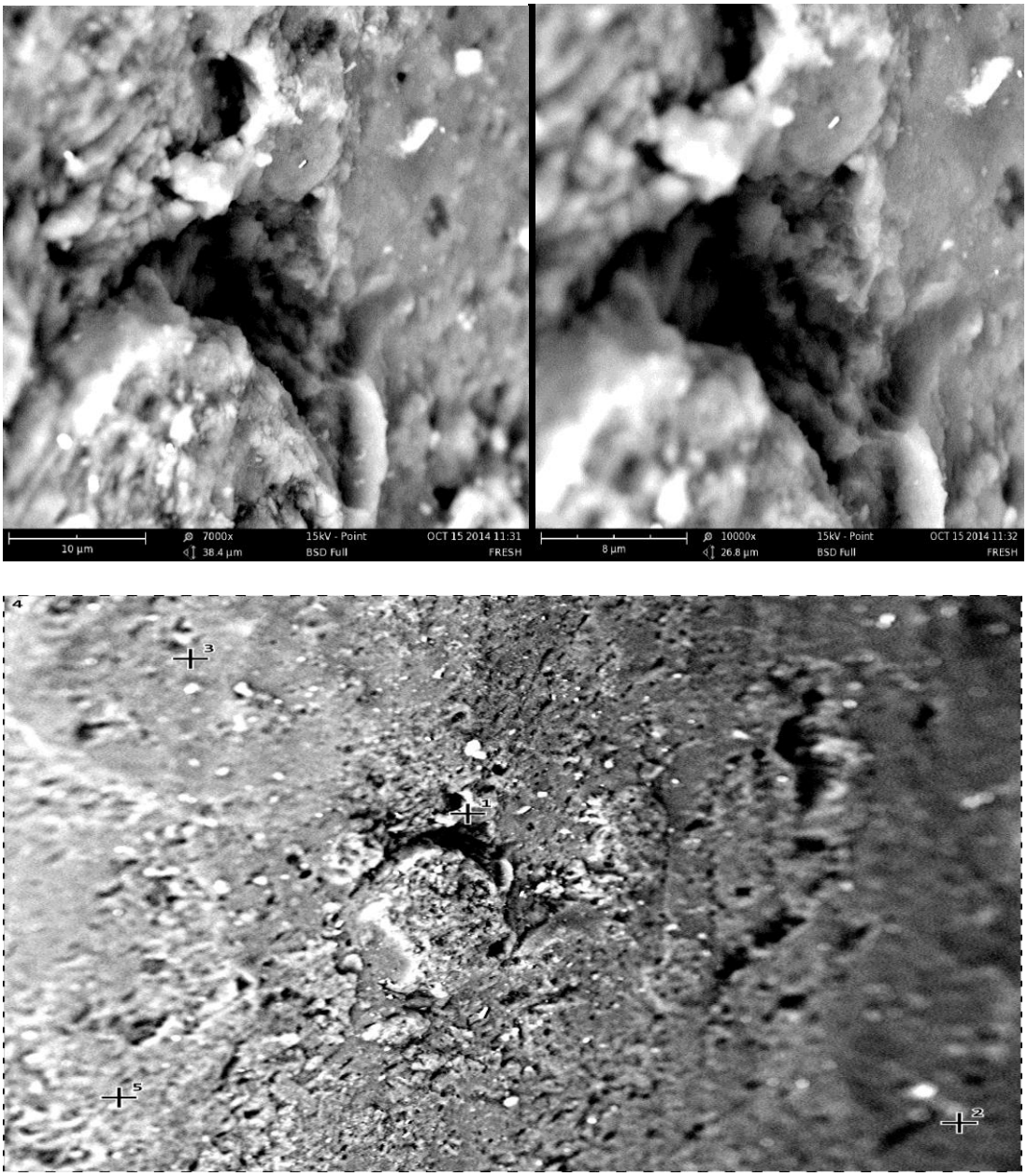


Plate 4.1: SEM and EDX mappings images of Fresh catalyst

Plates 4.1 to 4.5 show the SEM images obtained for each of the catalysts sample. Plate 4.1 shows the image of fresh catalyst, and from these results a uniformity in the crystal size (cluster) of metal and geometric distribution of the amorphous nature of the support for 8 µm and 10 µm magnification with open pore size was observed. The characteristic favours the penetration of feed thereby enhancing the desired reactions. Plates 4.2 and 4.3 of deactivated catalyst A and B shows the presence of heavy mass of organic compounds deposited due to temperature effect. This has made the support more disperse all over, given rise to little deposit of black spots of carbon amidst the catalyst, blockage of some pores and little signs of sintering. But after regeneration (Plates 4.4 and 4.5), the carbon deposit are reduced, more opened pores and clusters were observed.

The spots on each micrograph were used to show two major elemental concentration of carbon and aluminium (support) by EDX as seen from Plates 4.1 to 4.5. The result revealed that the carbon deposit on the catalyst increases for various spot as the catalyst get deactivated. This reduces after regeneration respectively as shown in Tables 4.4 to 4.8. While on the other hand the support on the catalyst represented by aluminium decreases when the catalyst gets deactivated and increases after regeneration. These shows that the pore that were initially blocked had been opened up after thermal treatment of deactivated catalysts.

Table 4.4: EDX spots on the SEM image for the fresh catalyst.

SPOT	Carbon Concentration (%)	Aluminium Concentration (%)
1	0	34.7
2	0	32.3
3	1.2	30.1
4	0	30.8
5	0	32.1

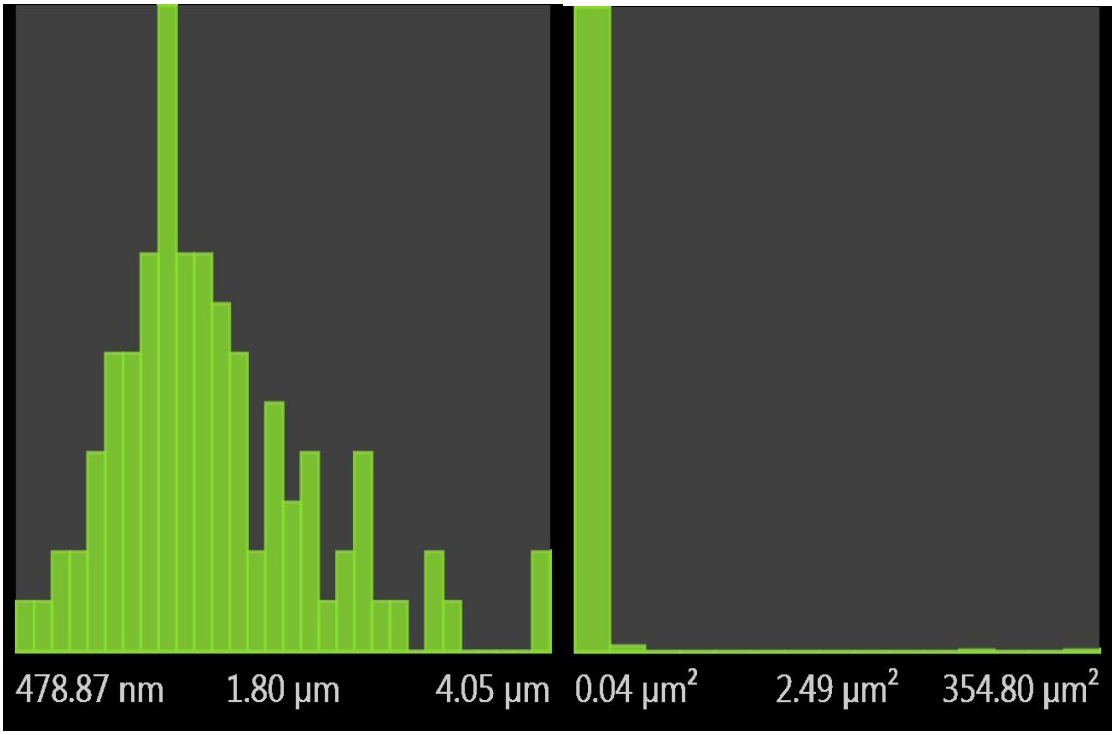


Figure 4.11: Fresh catalyst Pore-fibre length Histogram and Fresh catalyst Pore-Surface area histogram

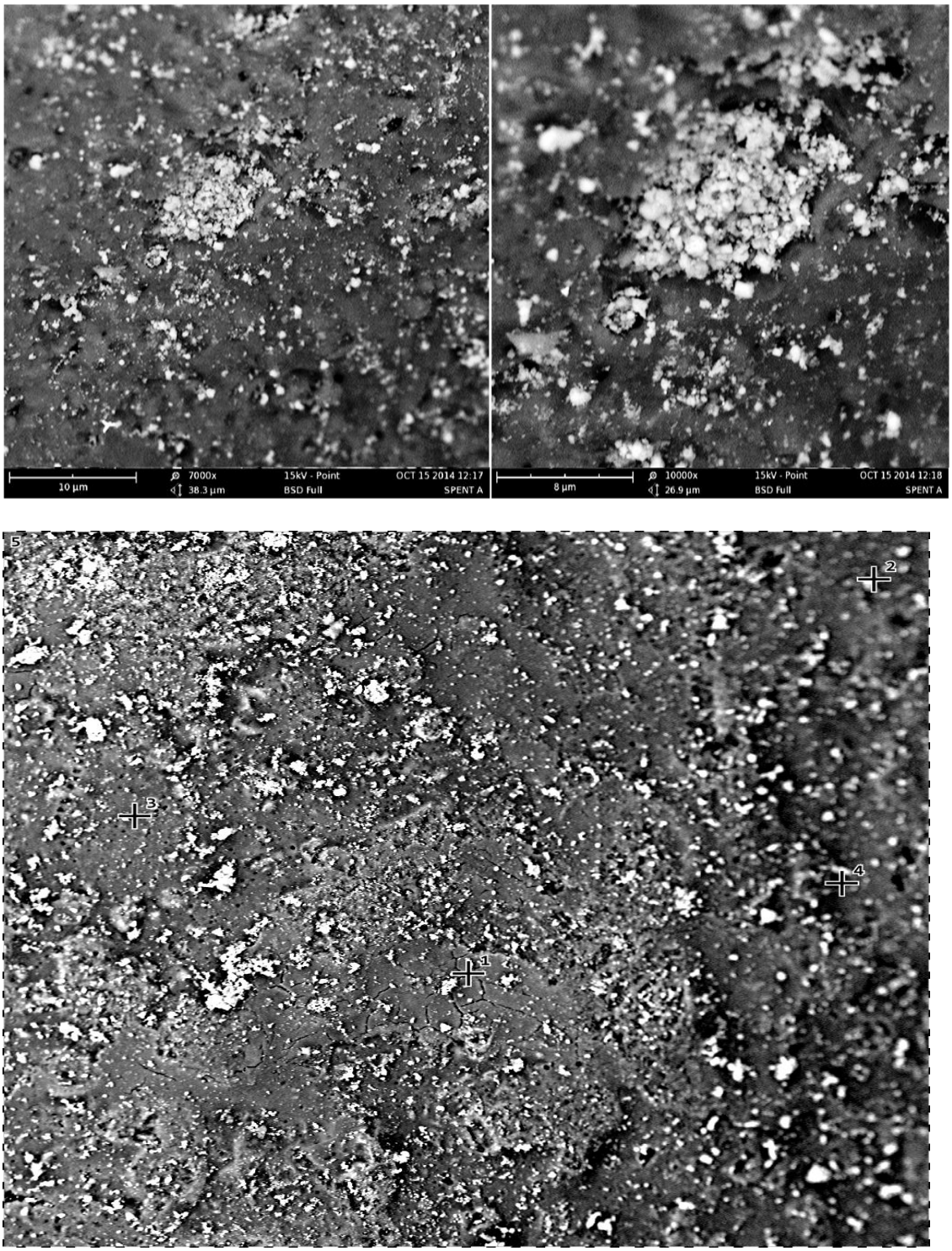


Plate 4.2: SEM and EDX mapping images of deactivated A catalyst.

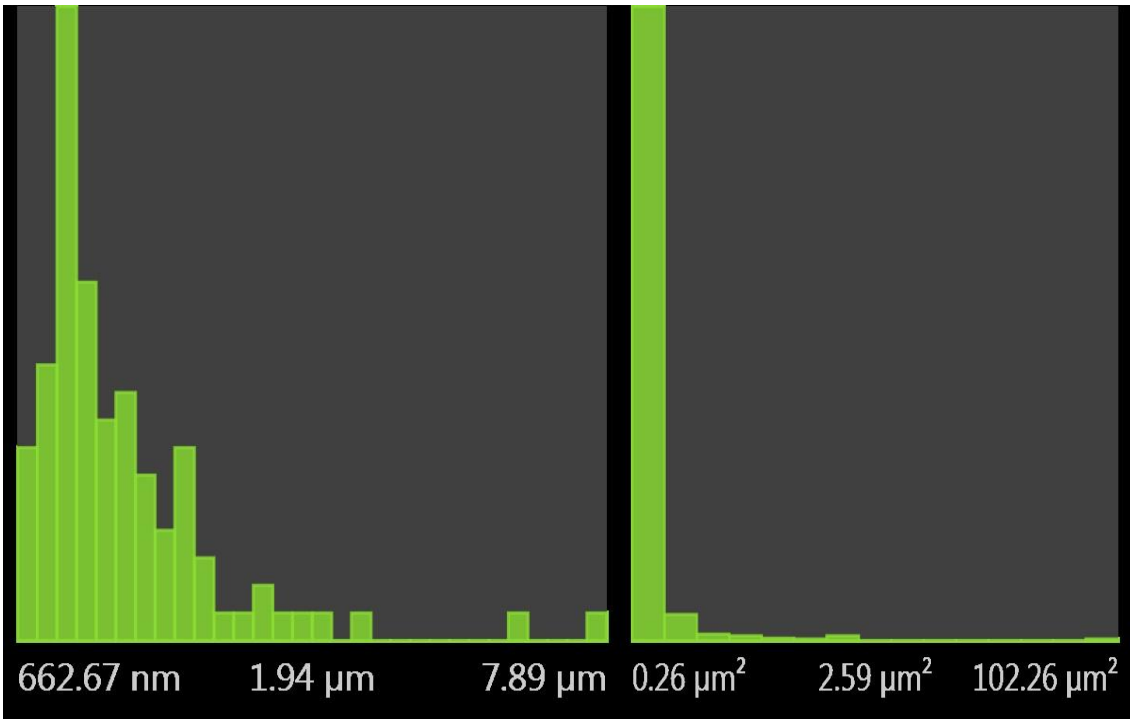
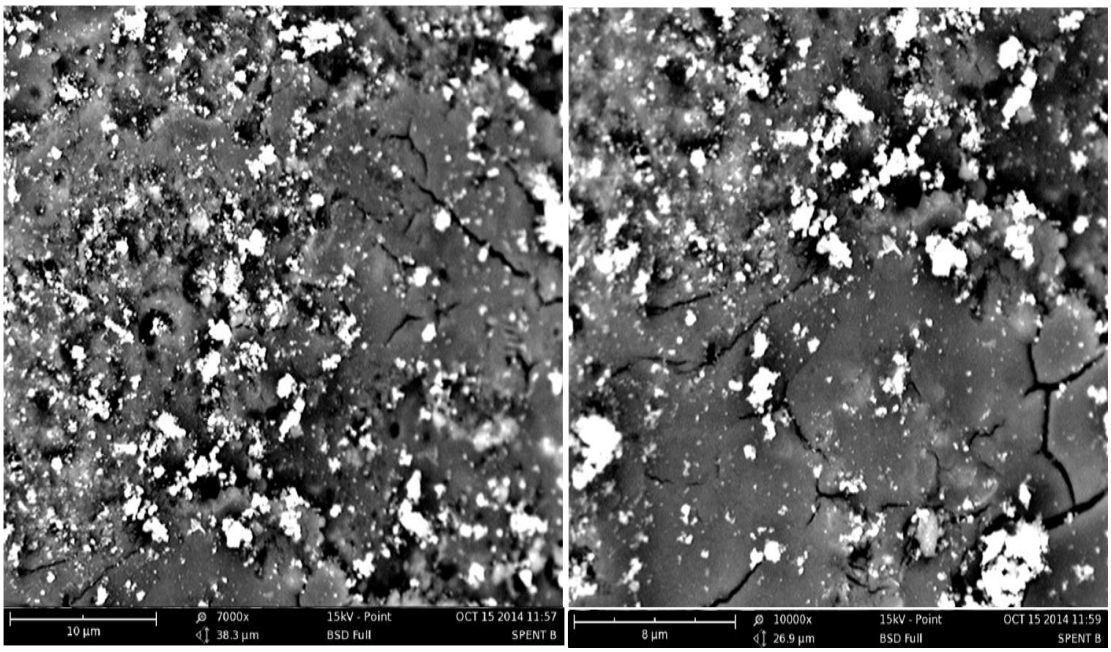


Figure 4.12: Deactivated A pore-fibre length histogram and deactivated A pore-surface area histogram.

Table 4.5: EDX spots on the SEM image for the deactivated A catalyst.

SPOT	Carbon Concentration (%)	Aluminium Concentration (%)
1	12.9	12.1
2	10.1	17.3
3	17.0	19.9
4	37.1	13.8
5	37.8	21.1



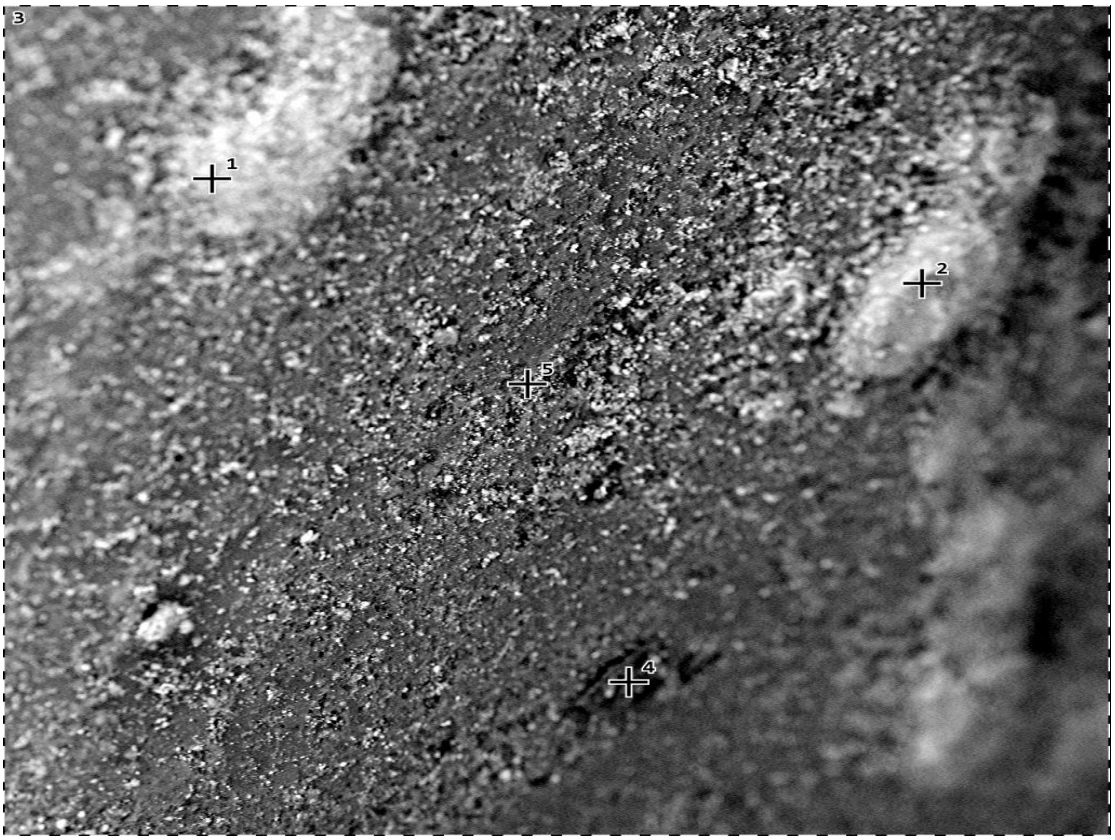


Plate 4.3: SEM and EDX mapping images of deactivated B catalyst.

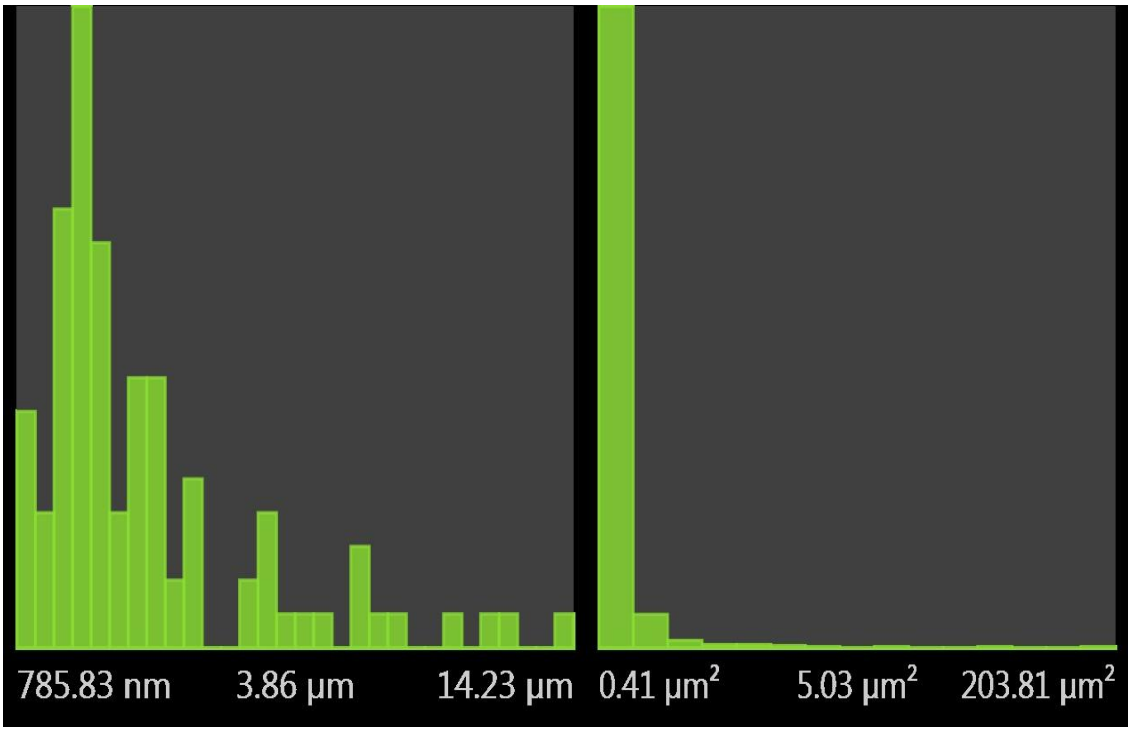


Figure 4.13: Deactivated B pore-fibre length histogram and deactivated B pore-surface area histogram

Table 4.6: EDX spots on the SEM image for the Deactivated B catalyst.

SPOT	Carbon Concentration (%)	Aluminium Concentration (%)
1	3.7	31.3
2	1.5	26.1
3	0	31.5
4	0	29.0
5	1.4	29.4

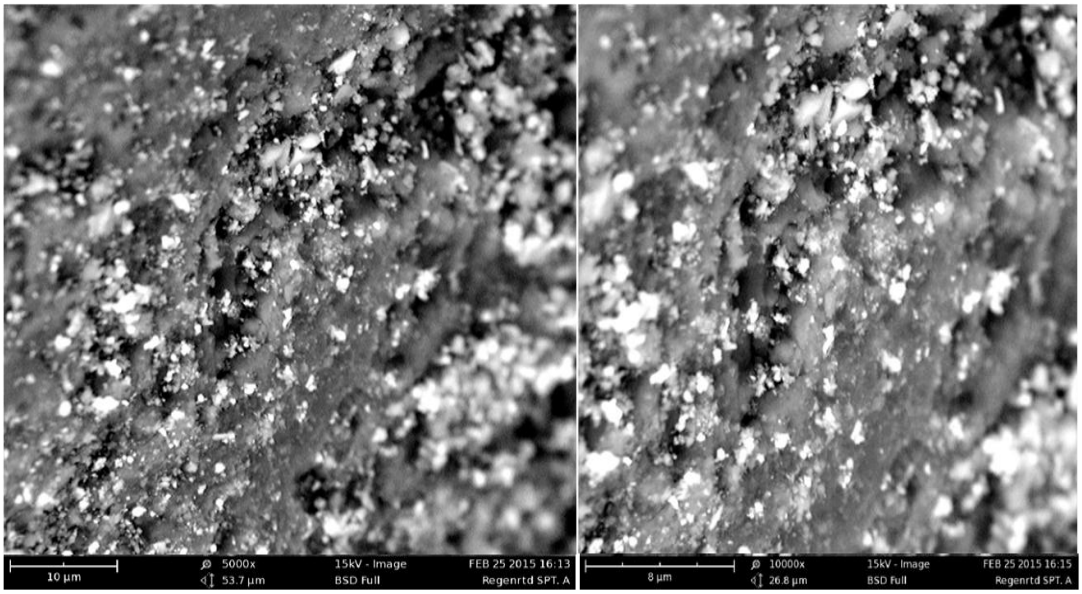




Plate 4.4: SEM and EDX mapping images of regenerated deactivated A catalyst.

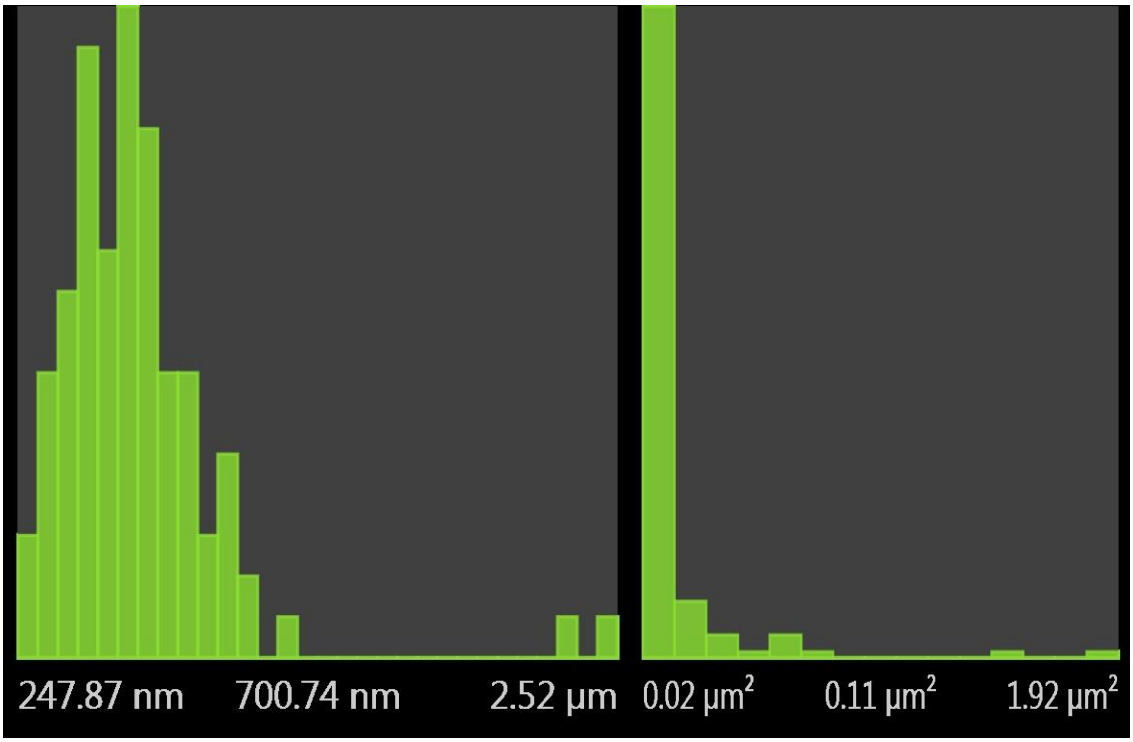


Figure 4.14: Regenerated deactivated A pore-fibre length and regenerated deactivated A pore-surface area histogram

Table 4.7: EDX spots on the SEM image for the regenerated deactivated A catalyst.

SPOT	Carbon Concentration (%)	Aluminium Concentration (%)
1	5.1	28.2
2	3.4	24.7
3	11.2	30.1
4	15.8	28.9
5	12.6	29.8

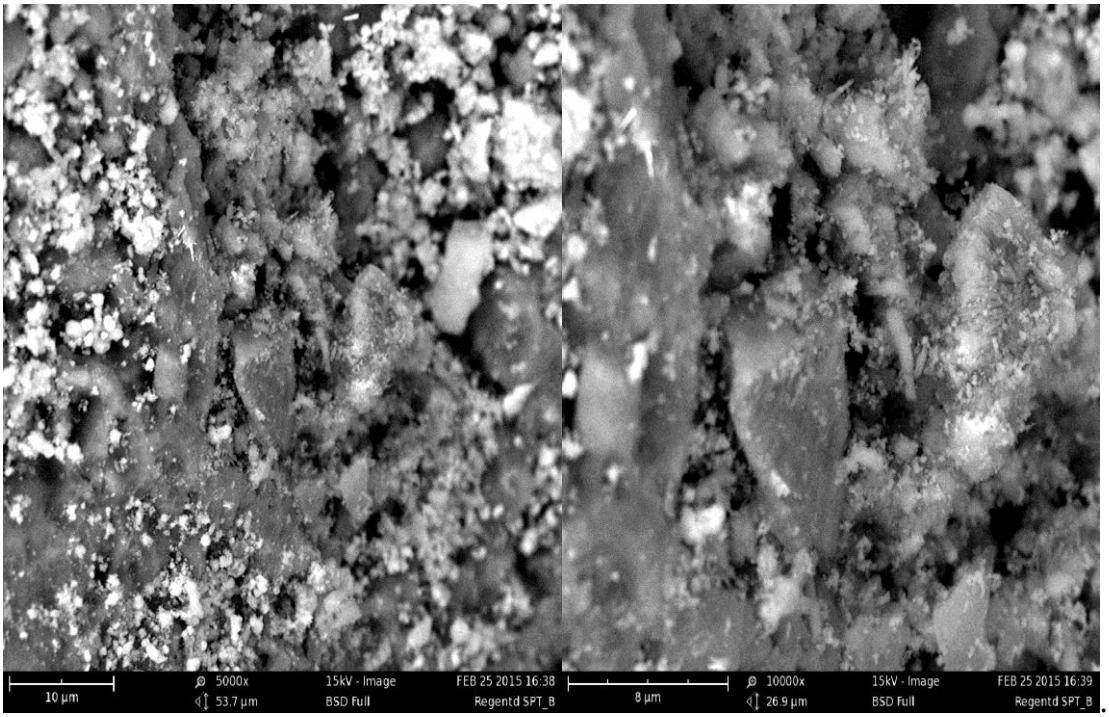




Plate 4.5: SEM and EDX mapping images of regenerated deactivated B catalyst

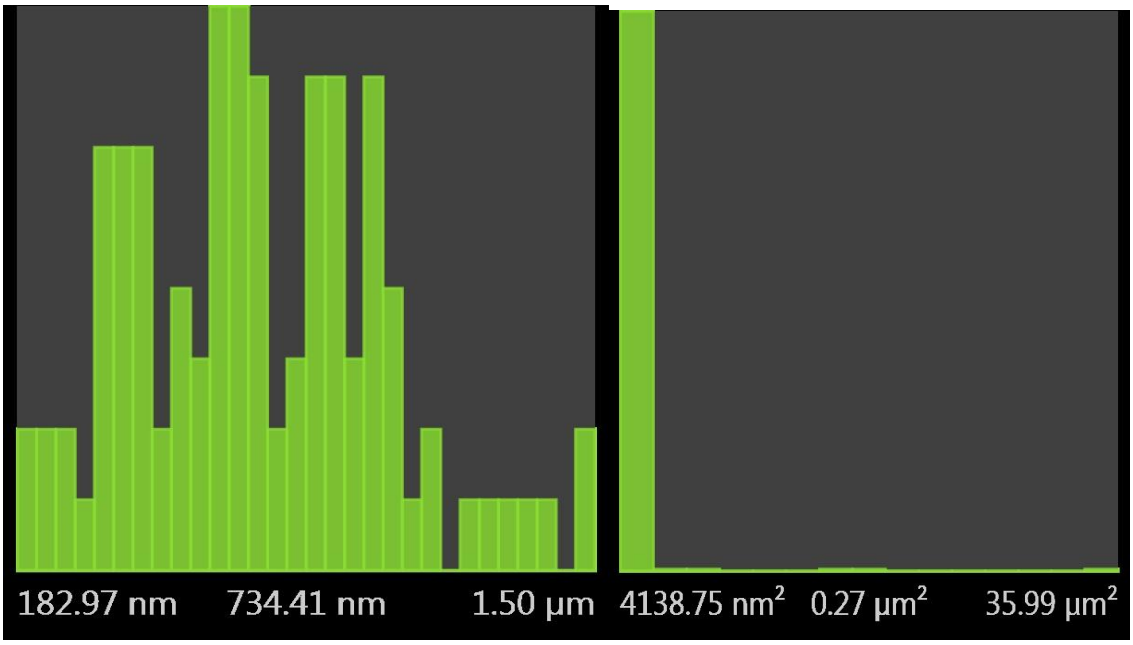


Figure 4.15: Regenerated deactivated B pore-fibre length and regenerated deactivated B pore-surface area histogram

Table 4.8: EDX spots on the SEM image for the regenerated deactivated B catalyst.

SPOT	Carbon Concentration (%)	Aluminium Concentration (%)
1	1.1	32.4
2	0.8	29.6
3	0	31.9
4	0	30.1
5	0.3	29.8

Figures 4.11 to 4.15 that the SEM image surface area is divided into micro, meso and macro pore group. The surface area became more opened on regeneration of the catalyst for both deactivated A and B after chemical and thermal treatment burnt off some of the carbonaceous material deposited on the catalyst. This was clearly shown in the increment in the small, average and large surface area group as shown in the summary given in Table 4.9.

4.1.5 Catalysts textural properties.

Table 4.9: Surface Area Transition of Catalyst (SEM).

Catalyst	Surface Area		
	Small (Micro)	Average (Meso)	Large (Macro)
Fresh	0.04μm^2	2.49μm^2	354.80 μm^2
Deactivated A	0.02 μm^2	0.11 μm^2	1.92 μm^2
Deactivated B	4138.75nm^2	0.27 μm^2	35.99μm^2
Regenerated A	0.26μm^2	2.59 μm^2	102.26 μm^2
Regenerated B	0.41 μm^2	5.03 μm^2	203.81 μm^2

Table 4.10: Specific Surface Area of the catalysts (Sear's method).

Catalyst		Specific Surface Area (SSA) (m^2/g)
FRESH		365.4
DEACTIVATED	A	147.8
	B	183.0
REGENERATED	A	208.6
	B	215.0

The specific surface area was determined using Sear's method and presented in Table 4.10. There were signicant increases in the regenerated catalyst compared to the deactivated catalyst (deactivated A and B). SSA for of deactivated A increased by 41 % while deactivated B increased by 17 %. The large percentage increase was as a result of the method used to obtain the surface area, but increase in surface area results to slight improvement in the surface morphology.

All deactivated catalysts have smaller specific surface area than the fresh catalyst. Comparatively the deactivated A deactivated catalyst has the least specific surface area, these was because organic compounds with higher boiling points were covering the catalyst surface more than that of deactivated B which results in the decrease of the specific surface area compared to fresh catalyst.

a. Catalysts' Performance Evaluations

The main calculations for the reformate yield extracted from GS-MS result for all the catalysts can be seen in appendix A.

4.2.1 Component Identification Method

Qualitatively, chromatographic data is presented as a graph of detector response (y-axis) against retention time (x-axis), which is called a chromatogram. This provides a spectrum of peaks for a sample representing the analytes present in a sample eluting from the column at differ2ent times. Retention time was used to identify analytes under identical conditions. Also, the pattern of peaks (which was constant for a sample under constant conditions) was used to identify complex mixtures of analytes. The GC was incorporated to a mass spectrometer (i.e. GC-MS), such that the MS identified the analytes represented by the peaks. (Oloworishe., 2014).

Quantitative, the GC-MS system used have computer software used to draw and integrate peaks, and thus match the obtained MS spectra to library spectra. Thus, an analytes present in a sample eluting from the column was named by match-making, and the most likely analyte's names were given (in order of probability; SI) in each spectrum. For instance, the spectrum (connoted by the GC-MS machine as Hit# 1) shown in Figure 4.11 is "Benzene"- which is the compound name with its isomers (each placed within the two double-dollar-sign) (Oloworishe., 2014).

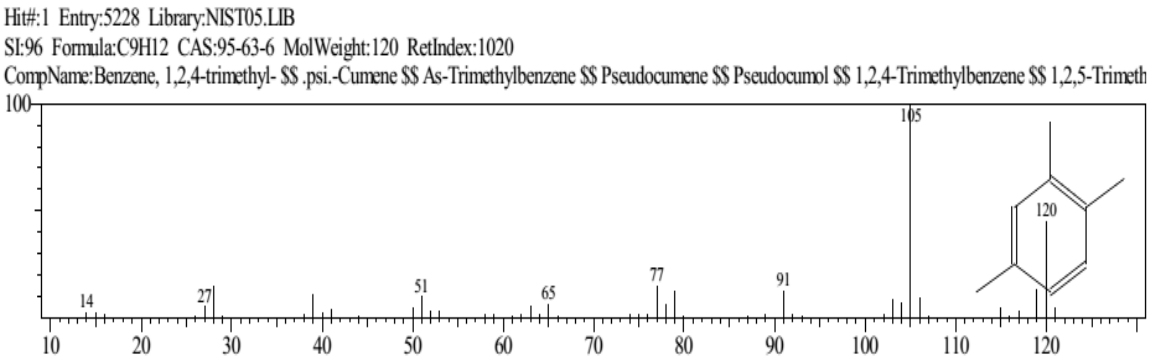


Figure 4.16: A Mass Spectrum representing a sample composition of product from GC-MS

Table 4.11: Summary of catalysts performance evaluations

Catalyst	Iso-paraffin (%)	Aromatic (%)	Max Yield attained (%)	Selectivity Iso-paraffin (%)	Selectivity Aromatic (%)
Fresh	71.67	5.81	84.24	77.92	6.32
Deactivated A	19.20	2.98	60.47	52.34	8.12
Deactivated B	44.52	6.11	77.74	68.36	9.38
Regenerated A	42.75	4.86	76.65	68.83	7.82
Regenerated B	67.64	7.70	83.86	75.29	8.57
Reforming Sample	34.06	34.03	82.44	41.21	41.20

Table 4.11 was deduced from Appendix C. It can be seen that the reformate produce from fresh catalyst has the highest yield of reformate (84.24 %) produced while reformate sample collected from KRPC after its regeneration has 82.44 % yield. The deactivated catalysts dropped to 60.47 % and 77.74 % due to the presence of carbonaceous material deposited on it and after regeneration the percentage reformate yield increased to 76.65 % and 83.86 % of regenerated deactivated catalyst A and B, respectively.

At reaction temperature of 465 ^{0}C, the reformate yield for the deactivated to regenerated catalyst increased from 60.47 % to 76.65 % for deactivated A and 77.74 % to 83.86 % for deactivated B respectively**,** but the aromatics produced were all below 20 % which does not attain the minimum of 70 % aromatics required of a standard

reformate as specified by API (1994). Even the reformate sampled from KRPC has its aromatics below required 70 %. These confirmed that the support (alumina) on the catalyst has low selectivity for aromatics at the reaction temperature of 465 ^{0}C used for the reforming, but good selectivity for iso-paraffins. See Appendix B. Thus, reformate obtained, resulted mainly from the isomerization of treated heavy naphtha (paraffinic feed), and possible cracking products. But the reformate produced was far more than the gas formation as compared to the work of Zharkov *et al*.,(2001) that regenerated only with chlorine and more gas formation was observed instead of the required reformate.

In terms of selectivity of all the catalysts, the improved experimental set up shows the reforming reactions only favoured more of isomerization but little dehydrocyclization because the chlorinated support on the platinum catalyst on Table 4.4. Table 4.4 has the potential to catalyze isomerization and cyclization reactions wherein iso-paraffins are majorly produced even after regeneration, whereas aromatics are mainly produced by dehydrocyclization reactions, which are largely promoted by an active metal.

The selectivity of all the catalysts for iso-paraffin was quite impressive; ranging from 52.34 %, 68.36 %, 68.83 %, 75.29 % and 77.92 % of deactivated A and B, regenerated A and B and fresh respectively. While the selectivity of all the catalysts for aromatics were relatively low; ranging from 6.32 %,8.12 %, 9.38 %, 7.28 % and 8.57 % of fresh, deactivated A and B and regenerated A and B which favours more for gasoline blending than being used as petrochemical feedstock in the production of linear alkyl benzene. But comparing with sampled reformate from KRPC shows the findings favors both isomerisation and dehydrocyclization i.e. iso-paraffin and aromatic selectivity

almost in the same proportion probably as a result of product from a more concise industrial setup.

CHAPTER FIVE

CONCLUSIONS AND RECOMMENDATIONS

5.1 Conclusions

The following conclusions were made from the research carried out:

1. The optimum regeneration condition of temperature, air pressure (with regeneration gas) and time obtained were $500^{O}C$, 1 kg/cm^2 (plus 2 kg/cm^2 regeneration gas) and 4 hours respectively.
2. The decoking effect done and regeneration of the deactivated catalyst A and B showed presence of soft coke (1.0 -2.9 % weight loss) as compared to when the plant is after the normal shut down cycle of 72 months which gave approximately 3.0 - 3.3 % weight loss on catalyst depicting hard coke deposit.
3. The wave band length from FT-IR that showed presence of deposit of coke (2800-3000 cm^{-1}) disappeared, showing some high level of regeneration of the deactivated catalyst.
4. There was no observable difference in the XRD pattern for the fresh, deactivated and regenerated catalyst because the bragg angle of the platinum and alumina (support) for all the catalyst both coincide and exist at, 39^0, 46^0 and 68^0. Also, active metal and the support were intact during and after the regeneration process.
5. XRF analyses indicated the presence of several oxides in the fresh and likewise after regenerating the deactivated catalyst, such as Alumina (Al_2O_3), Cl and PtO_2 which help maintain good activity for a longer period of time.

6. The morphology of the surface shown by micrograph depict that the area became more open after regeneration showing increase in porosity due to efficient thermal treatment and even dispersion of the metal on the support.
7. The change in the Specific Surface Area (SSA) and the fibre length of the regenerated catalyst through Sear's or SEM method increases (41 % for deactivated A and 17 % for deactivated B) after successful regeneration. And the increases are similar to the pattern reported in literatures.
8. The catalyst performance test conducted on the fresh, deactivated and regenerated catalyst using treated heavy naphtha as substrate revealed that regenerated catalyst A has reformate yield value of 83.86% which was relatively higher than the literature value of 82.44% reported for sample obtained by Axen IFP group in KRPC after a turnaround maintenance session. Furthermore, with reaction temperature of 465^{o}C, all the catalyst favoured isomerisation and cracking reactions that produces more isoparaffin and less aromatics.
9. The aromatic level of the reformate product from regenerated catalyst was more suitable for gasoline blending but less as petrochemical feedstocks, these could be as a result of constrains that were in experimental rig.
10. The regenerated deactivated catalyst B favours isomerisation reaction more than regenerated deactivated catalyst A, hence yield of more iso-paraffin by deactivated catalyst B took place during reforming.

5.2 Recommendations

1. It is recommended that a direct on-line analyzer like GC-MS machine (to capture uncondensable and volatile gases e.g. LPG, CO, CO_2) and draegler tube (to monitor the chlorine concentration) be incorporated to the rig (the laboratory set-up). This will make it possible for precise and proper accountability of all the products of reforming and regeneration system.

2. Verification of metal dispersion may be made more explicit if TEM technique is adopted instead of the SEM technique used herein. Also BET should be widely available locally instead of sending samples abroad.

3. Beside treated heavy naphtha used in this work for performance test, normal paraffin such as n-C_6, n-C_7, n-C_8 should be used so as to avoid unconverted paraffin in the product

REFERENCES

Ahmed, R; Sinnathambi, C.M; Subbarao, D; (2011). Kinetic of de-coking of spent reforming catalyst. Journal of Applied Sciences, II: 1225-1230.

Aitani, A.M. Catalytic reforming processes (1995); In Catalytic Naphtha Reforming; Antos, G.J., Aitani, A.M., Parera, J.M., Eds.; Marcel Dekker: New York; P. 409.

Antos, G.; Moser, M.; Lapinski, M, (2004); .The new generation of commercial catalytic naphtha reforming catalysts. In: Prentice, Antos, G., Aitani, A., (Eds.); Marcel Dekker: Catalytic Naphtha Reforming New York P.335.

API-American Petroleum Institute (1994). Research Project 65, Sixteenth Annual Report

Axens Process Brochures for Octanizing and Aromizing Processes (2002); Axens IFP Group Technologies, Rueil-Malmaison, Paris, France.

Axens Catalyst Handbook for regeneration of reforming catalyst (2009). Axens IFP Group Technologies, Rueil-Malmaison, Paris, France.

Barthelomew, C.H ; (2001). Mechanism of catalyst deactivation. Applied Catalysis A, 212: 17-60.

Barthelomew, C.H ; (2001). Catalyst deactivation (1994). Studies in Surface Science and Catalysis, vol 88, Elsevier, Amsterdam; P.1.

Bawa G. S. (2012). Development of gamma-alumina from Kankara Kaolin for potential application as catalysts support. M.Sc Research Project. Chem. Eng. Dept, Ahmadu Bello University, Zaria.

Beltramini, J.N. (1995); Regeneration of reforming catalyst. In Catalytic Naphtha Reforming; Antos, G.J., Aitani, A.M., Parera, J.M., Eds.; Marcel Dekker: New York; P.365.

Carl B. (2013); Catalytic reforming of C_5 to C_{12} naphtha modeled through the kinetic modeling toolkit: A B.Eng thesis submitted to the Engineering Faculty of the University of Delaware.

Chiyoda Chemical Engineering and Construction CO.LTD (1980). Nigerian National Petrolueum Corporation. Kaduna Refinery Project Operating Manual for process Units CRU VOL. IV Yukohama, Japan , IV, 1-8,

Ciapetta, F.G.; Wallace, D.M. (1971); Catalytic naphtha reforming. Catal.Rev., 5, 67.

Clause, O.Dupraz, C. and Frank, J. (1998). Continuing innovation in catalytic reforming, presented at the NPRA Annual Meeting, San Antonio. March

Cody I. A., Dumfries D. H., Neal A. H., and Riley K. L., (1994). High porosity, high surface area isomerization catalyst and its uses (U.S. Patent 5290426). http://googleads.g.doubleclick.net/pa

Doolin, P.K; David, J; Soni O. Oyekan (1995); Catalyst Regeneration and Continous Reforming Issues. In Catalytic Naphtha Reforming; Antos, G.J., Aitani, A.M., Parera, J.M., Eds.; Marcel Dekker: New York; P.433.

Edgar, M.D. (1983). Catalytic reforming of naphtha in petroleum refineries. In Applied Industrial Catalysis; Leach, B.E., Ed.; Academic Press: New York,; Vol. 1, P.123.

Forzatti Pio; Luca Lietti (1999). Catalyst deactivation. Catalysis 165, Elsevier, Milan; P.1.

Gary, J.H. and Handwerk, G.E. (1984). Petroleum Refining Technology and Economics (2nd Edition ed.). Marcel Dekker, Inc. ISBN 0-8247-7150-8.

Gates, B.C.; Katzer, J.R.; Schuit, (1979) G.C.A. Reforming. In Chemistry of Catalytic Processes; McGraw-Hill: New York,; P. 184.

George J. A. and Abdullahi M. Aitani (2005). Catalytic Naphtha Reforming, 2nd Edition, Marcel Dekker Inc., New York, NY 10016, U.S.A

George, M. W. (2008). "Platinum-group metals". U.S. Geological Survey Mineral Commodity Summaries (USGS Mineral Resources Program). http://minerals.usgs.gov/minerals/pubs/commodity/platinum/mcs-2008-plati.pdf.

Goldstein, J. (2003) Scanning electron microscopy and x-ray microanalysis. Kluwer Adacemic/Plenum Pulbishers, P. 689.

Hosseini S. A, Aligholi N., and Dariush S. (2011). Production of γ-Al_2O_3 from Kaolin; Open Journal of Physical Chem., Vol 1, Pg 23-27, Dept of Applied Chem., University of Tabriz, Tabriz, Iran, Published August 2011 (accessed via http://www.SciRP.org/journal/ojpc)

In Lide David R. CRC Contribution (2007-2008). "Platinum''. CRC Handbook of Chemistry and Physics 4. New York: CRC press. P. 26.

Kalra S. K. (2009). Essentials of Refinery Processes; Indian Oil Corporation Ltd Panipat Refinery. (Cited online at petrofed.winwinhosting.net on June 25, (2014) by 11:00AM).

Le Goff P., Ross J., and Lopez J. (2012). Redefining reforming catalyst performance: High Selectivity and stability. cited online at www. hydrocarbonprocessing.com

Little, D.M. 1985. Catalytic Reforming; Pennwell Books: Tulsa, OK.

Manos ,G.; Wang, B. (2007). A novel thermogravimetric method for coke precussor characterization. J. Catalysis, 250 : 121-127.

Meeting the challenges of cleaner fuels, June (2001), World Refining; Chemical Week Associates Production; P. 12

Oloworishe F. J. (2014). Development of Pt-Zn/Al_20_3 catalyst for n-octane. M.Sc Research Project. Chem. Eng. Dept, Ahmadu Bello University

OSHA Technical Manual, Section IV, Chapter 2, Petroleum refining Processes (A publication of the Occupational Safety and Health Administration)

R. R Mohammad, J. Mitra , I. Davood (2013). Progress in catalytic naphtha reforming process. ELSEVIER. 79-93

Ruixia, J; X. zaiku; Z. Chengfang and C. Qingling, (2003). Characterization and Performance of Pd-La/ sonel Catalyst for Preparation of 2,6-diisopropyl aniline. Applied Catalysis A: General, 250: 209-220.

Sinfelt, J.R., Anderson, J.R., Boudart, M., Eds.; Springer-Verlag: Berlin, (1981) Catalytic reforming of hydrocarbons. In Catalysis Science and Technology; Vol. 1, P.257.

Sivasanker, S.; Ratnasamy, P. (1995). Reforming the gasoline and aromatics. In Catalytic Naphtha Reforming; Antos, G.J., Aitani, A.M., Parera, J.M., Eds.; Marcel Dekker: New York,; P. 483 .

Sutton, E.A.; Greenwood, A.R.; Adams, F.H. (1973). A new processing concept for Continuous Platforming. Oil Gas J., 71 (20), P. 136,456.

US Patent 5011805, Dehydrogenation, dehydrocyclization and reforming catalyst (Inventor: Ralph Dessau, Assignee: Mobil Oil Corporation)

Weiszmann, J.A.,Meyers, R.A., Ed.; (1986). Catalytic re-reforming. In Handbook of Petroleum Refining Processes; McGraw-Hill: New York,; P.3-3

William C. baird, Jr.; Paul E. Eberly, Jr.;George J. Balinsky, all of baton Rouge, La (1984) Catalyst regeneration in a catalytic reforming process. US patent 4440667.

X. H. Ren, M. Bertmer, S. Stapf, D.E. Demco, B. Blumich, C. Kern, A. Jess (2002). Deactivation and regeneration of a naphtha reforming catalyst. ELSEVIER. 39-52

Xiao, Z; Laplante, A.R (2004) ‘’Çharacterizing and recovering the platinum group materials-a review’’. Minerals Engineering 17. P. 9-10.

Yasuharu K., Takao K., Yoshio U. and Masatoshi S. (2005); Hydrodesulfurization of thiophene over Platinum supported on metal oxide catalysts. Muroran Institute of Technology. Pg 33-37.

Zharkov, B.B; Maslyanskill, G.N; Bursian, N.R; (2001). Regeneration of platinized alumina reforming catalysts by use of chlorine.

APPENDICES

Appendix A

A1. Calculation of quantity of dichloropropane to be mixed with water at ratio 1:20.

Quantity of DCP ($C_3H_6Cl_2$) - Dichloropropane is as follows:

$$Q = \left(\frac{1.6-x}{100}\right) * \frac{W}{y*d*k}$$ (Axen, 2010)

Where,

Q(l)= Quantity of chloride to be injected.

X(wt %) = Chloride content of catalyst. (1.37 of $C_3H_6Cl_2$)

W(Kg) = catalyst weight loaded.

y = Chloride fraction of chloride. (0.6316 of$C_3H_6Cl_2$)

d(Kg/l) = Specific gravity of chloride. (1.158 of $C_3H_6Cl_2$)

k = fixation rate of chloride of catalyst (0.96 for $C_3H_6Cl_2$)

$$Q = \left(\frac{1.6 - 1.37}{100}\right) * \frac{2}{0.6313 * 1.158 * 0.96}$$

Q= 0.00655L

Q= 6.55mL

For the catalyst density of 0.75 and the design volume of the catalyst to be loaded into the reactor, the quantity of DCP($C_3H_6Cl_2$) to be injected will be 6.55mL.

Table A.1: Catalyst weight loss in decoking presented in weight percentage at 1kg/cm^2, 4 hours and at various temperature range.

	Catalyst weight loss (%)	
Temeprature (^{o}C)	Deactivated A	Deactivated B
400	1.22	1.15
500	1.71	1.54
600	1.45	1.34
700	0.80	0.42
800	0.77	0.62

Table A.2: Catalyst weight loss in decoking presented in weight percentage at optimum temperature 500 ^{o}C, 4 hours and at various air flowrate

	Catalyst weight loss (%)	
Airflowrate pressure (psi)	Deactivated A	Deactivated B
10	1.71	1.54
15	1.80	1.75
20	0.48	0.33
25	0.24	0.17
30	0.08	0.06

Table A.3: Catalyst weight loss in decoking presented in weight percentage at optimum temperature and pressure and at various time range.

	Catalyst weight loss (%)	
Time (HOUR)	Deactivated A	Deactivated B
2	1.80	1.75
4	2.09	2.14
6	1.92	1.90
8	1.96	1.88

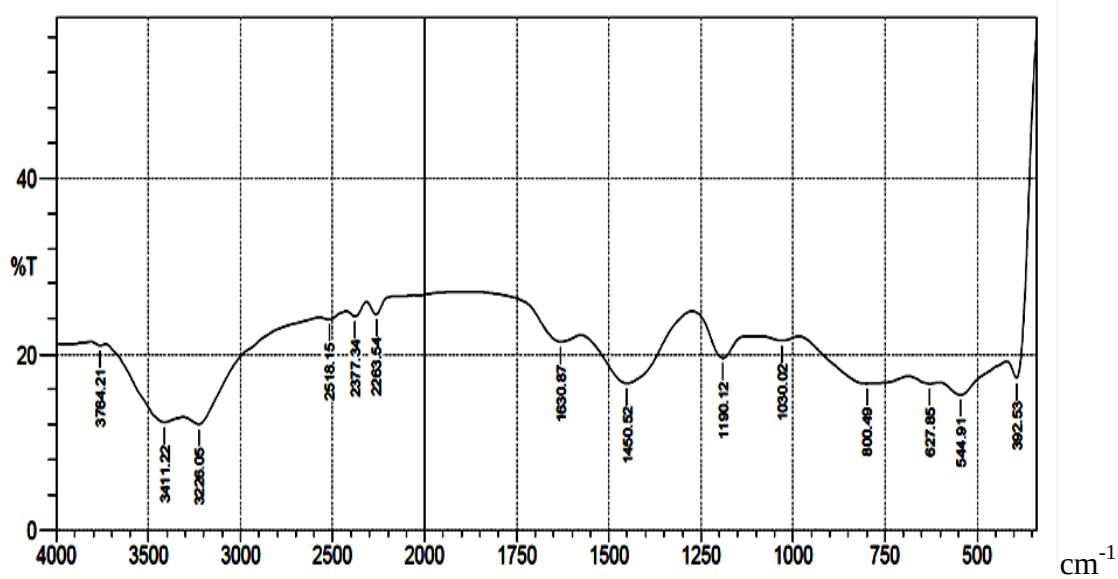


Figure A.1: FT-IR spectroscopy analysis of deactivated A on 400^{o}C calcinations.

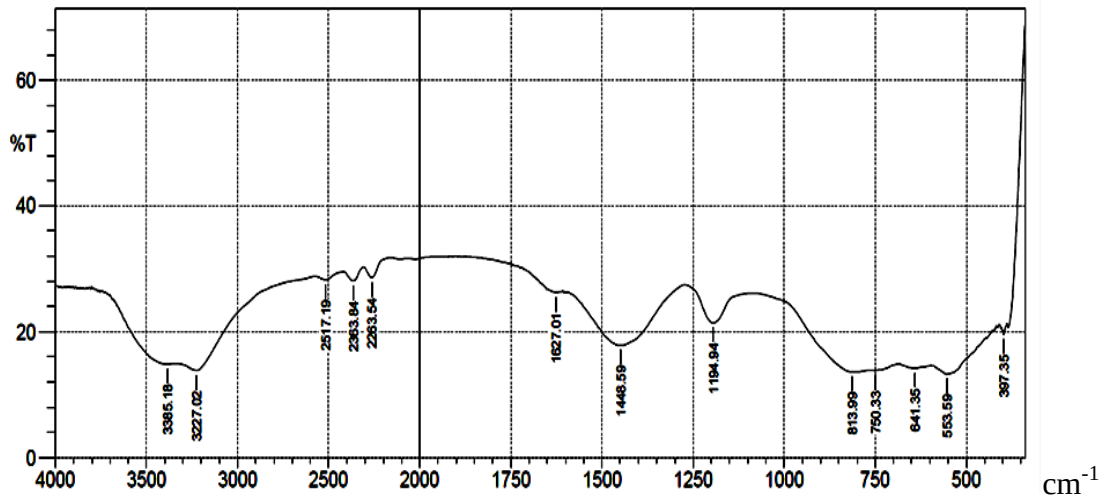


Figure A.2: FT-IR spectroscopy analysis of deactivated B on 400^{o}C calcinations.

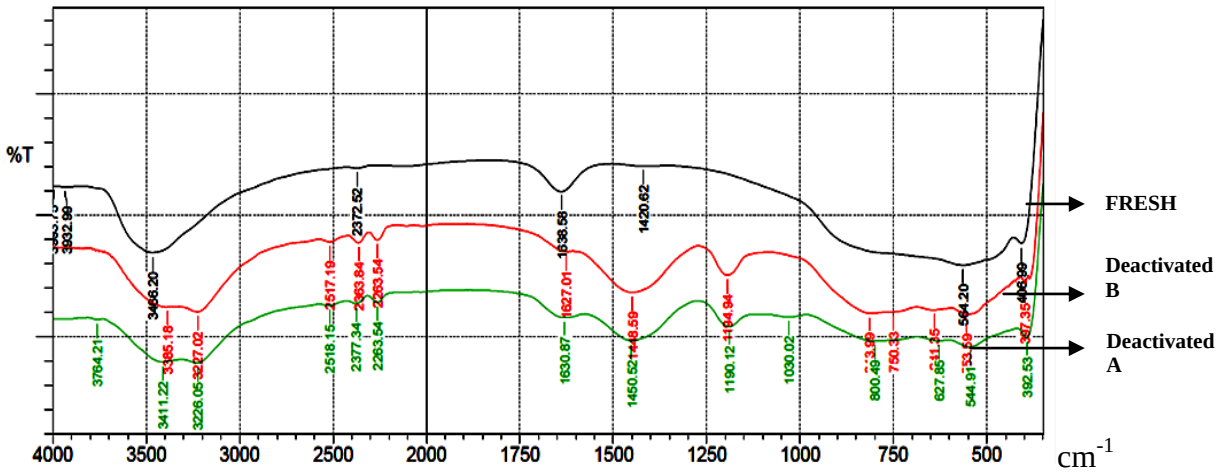


Figure A.3: FT-IR spectroscopy of fresh, deactivated A and deactivated B catalyst at 400^{o}C calcinations

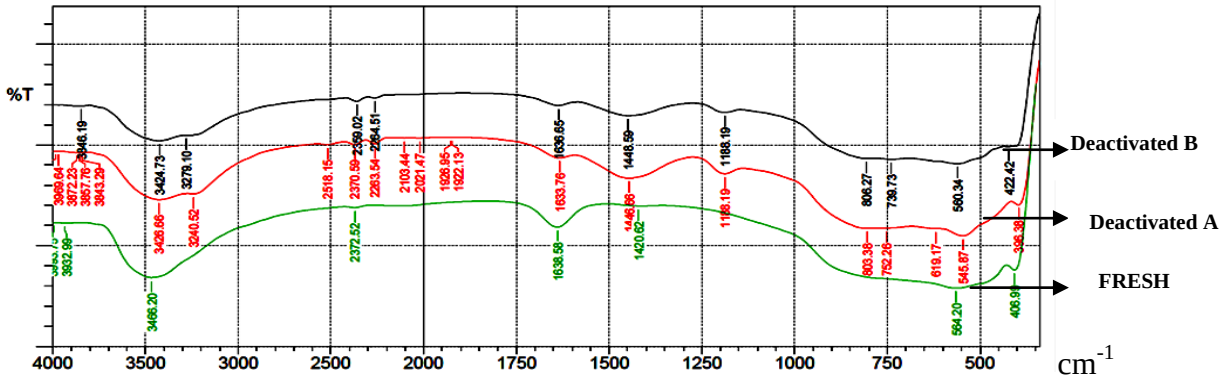


Figure A.4: FT-IR spectroscopy of fresh, deactivated A and deactivated B catalyst at 500^{o}C calcinations

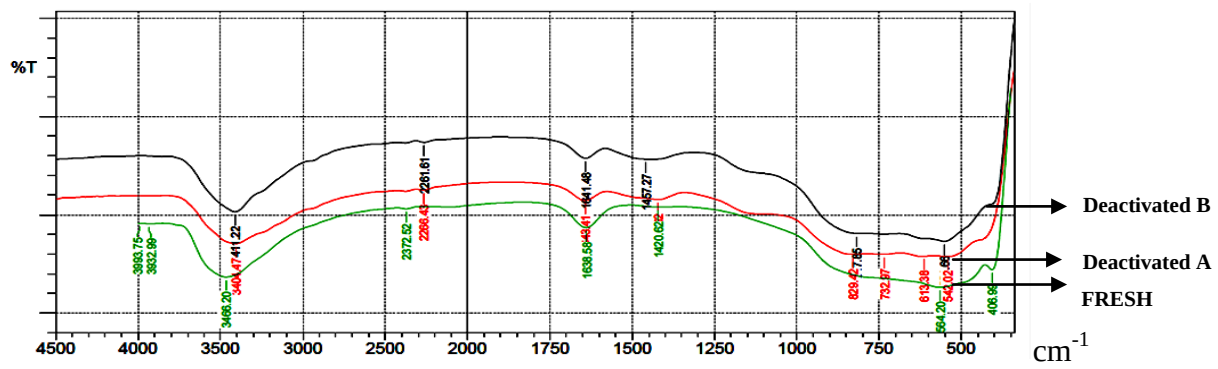


Figure A.5: FT-IR spectroscopy of fresh, deactivated A and deactivated B catalyst at 600^{o}C calcinations

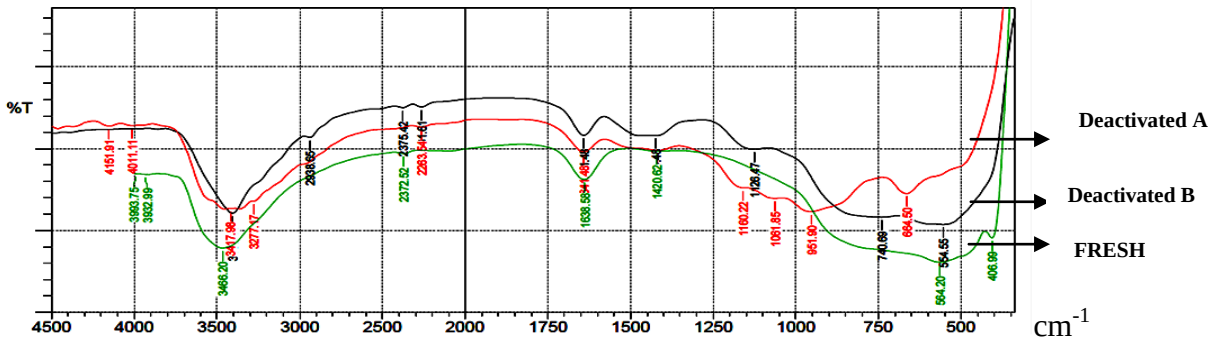


Figure A.6: FT-IR spectroscopy of fresh, deactivated A and deactivated B catalyst at 700^{o}C calcinations

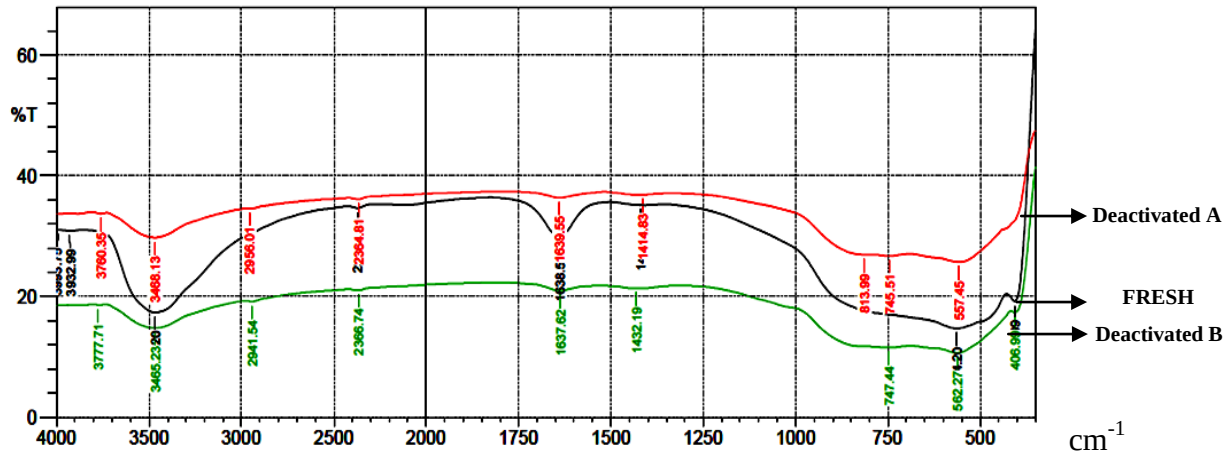


Figure A.7: FT-IR spectroscopy of fresh, deactivated A and deactivated B catalyst at 800^{o}C calcinations

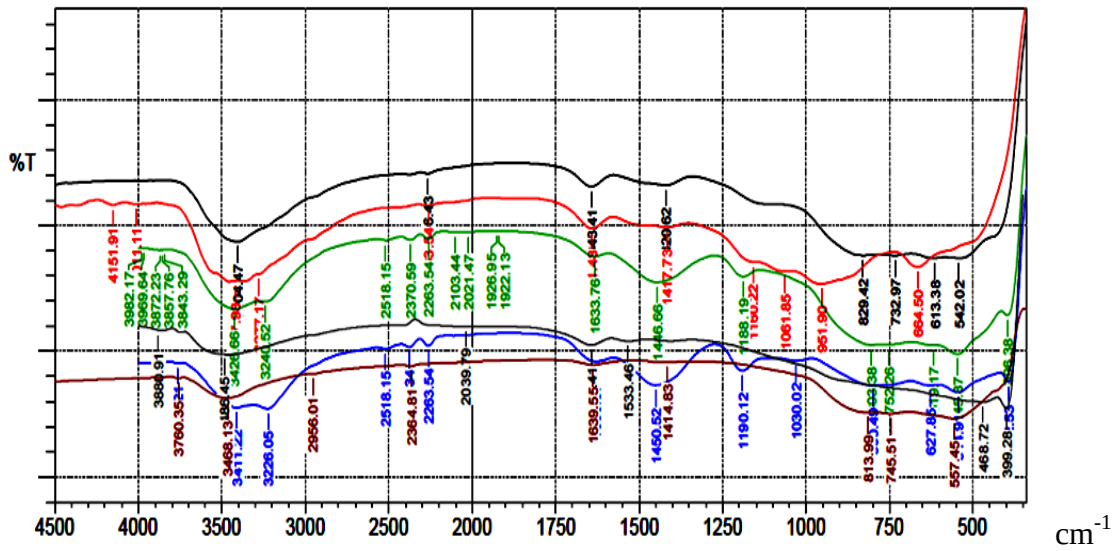


Figure A.8: FT-IR spectroscopy of fresh and deactivated A at 400^{o}C, 500^{o}C, 600^{o}C, 700^{o}C and 800^{o}C calcinations

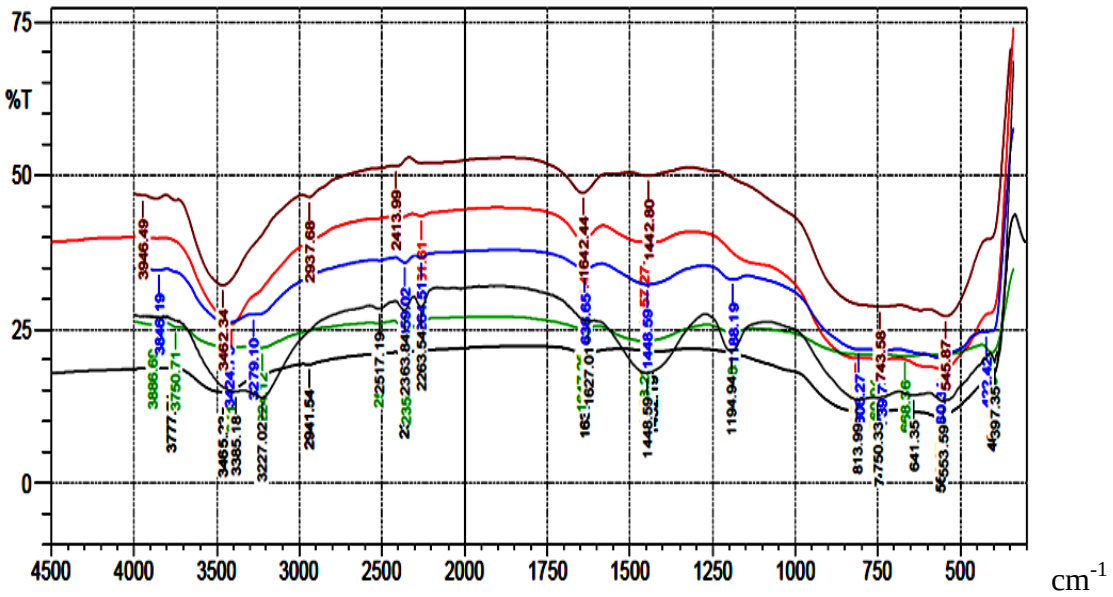


Figure A.9: FT-IR spectroscopy of fresh and deactivated B at 400°C, 500°C, 600°C, 700°C and 800°C calcinations

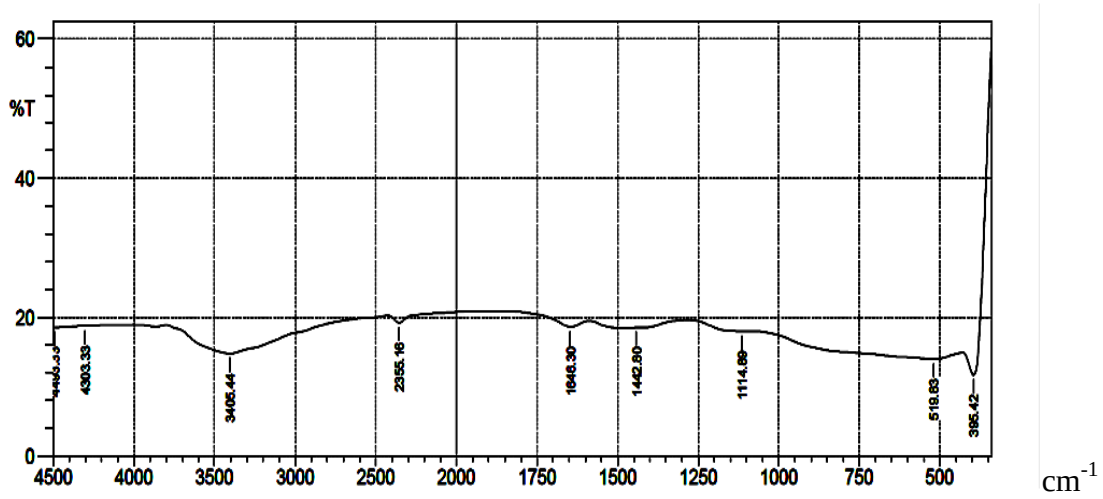


Figure A.10: FT-IR spectroscopy of deactivated A at 500°C for 2 hours calcinations

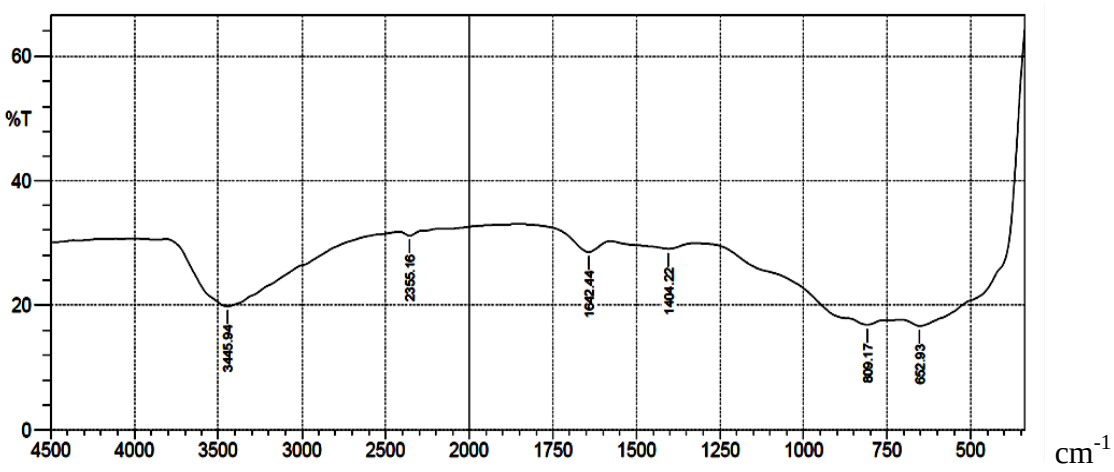


Figure A.11: FT-IR spectroscopy of deactivated A at 500^{o}C for 4 hours calcinations

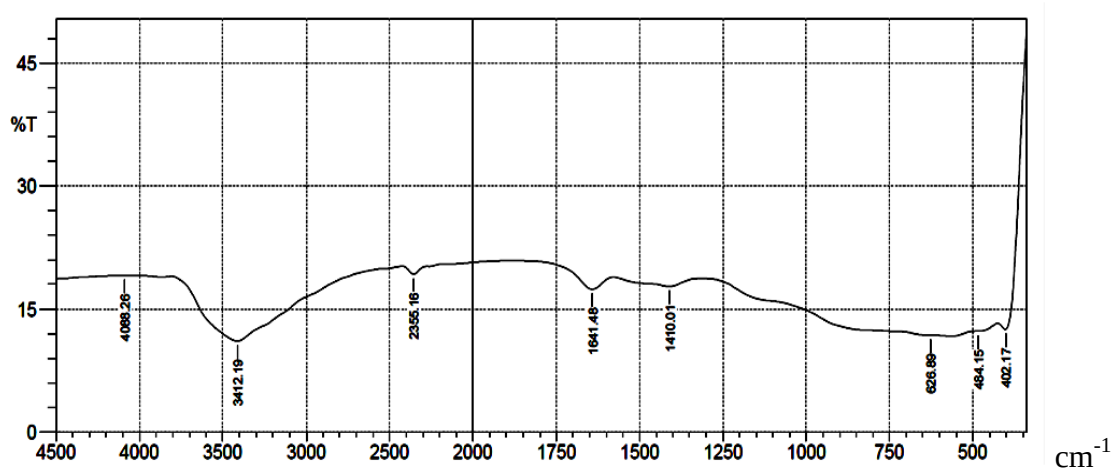


Figure A.12: FT-IR spectroscopy of deactivated A at 500^{o}C for 6 hours calcinations

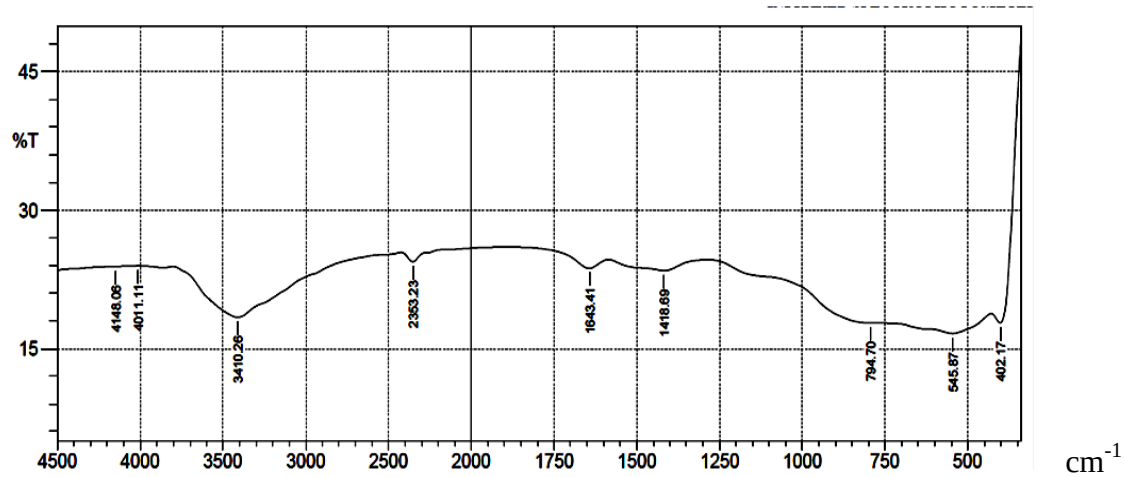


Figure A.13: FT-IR spectroscopy of deactivated A at 500oC for 8 hours calcinations

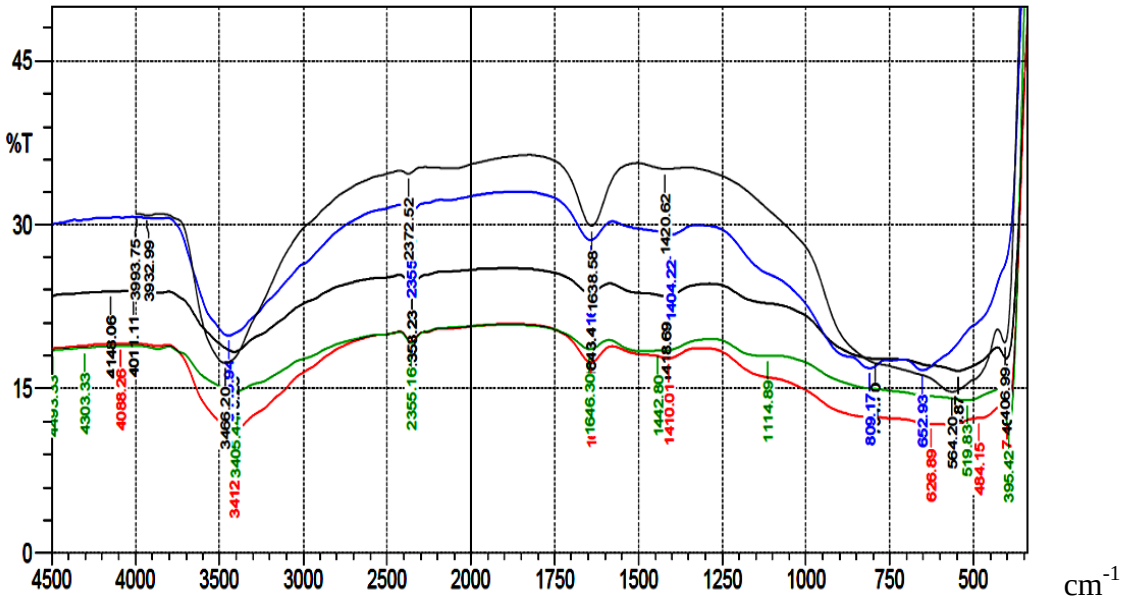


Figure A.14: FT-IR spectroscopy of fresh, deactivated A at 500°C for 2, 4, 6 and 8 hours calcinations.

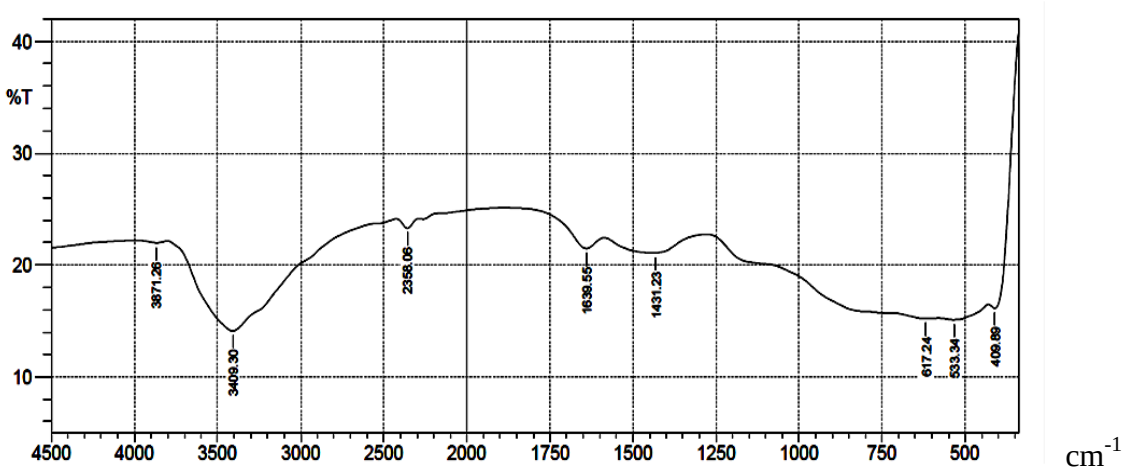


Figure A.15: FT-IR spectroscopy of deactivated B at 500°C for 2 hours calcinations

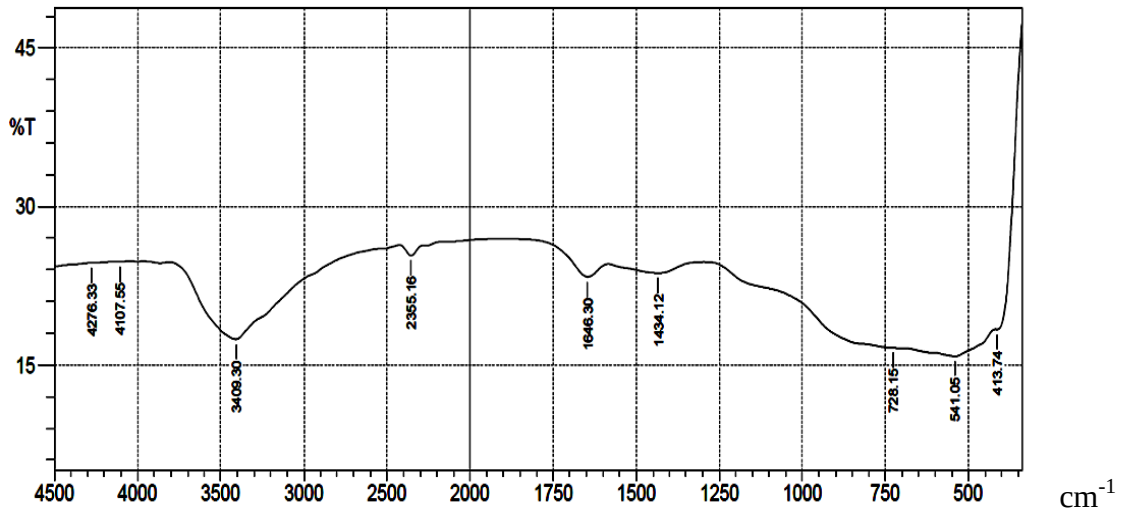


Figure A.16: FT-IR spectroscopy of deactivated B at 500^{o}C for 4 hours calcinations

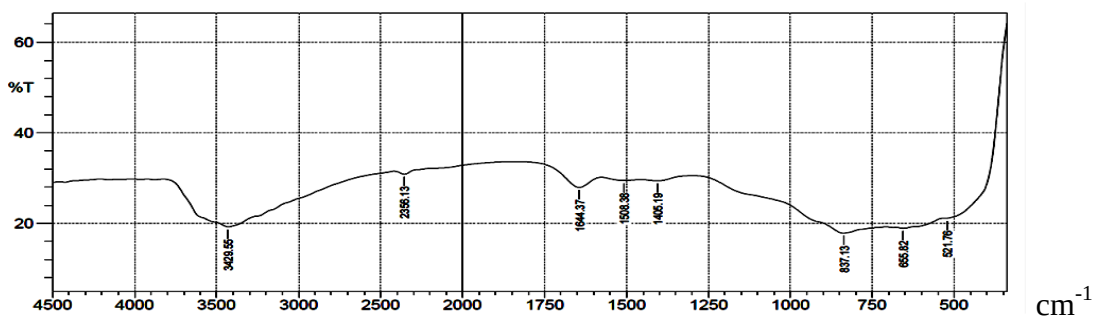


Figure A.17: FT-IR spectroscopy of deactivated B at 500^{o}C for 6 hours calcinations

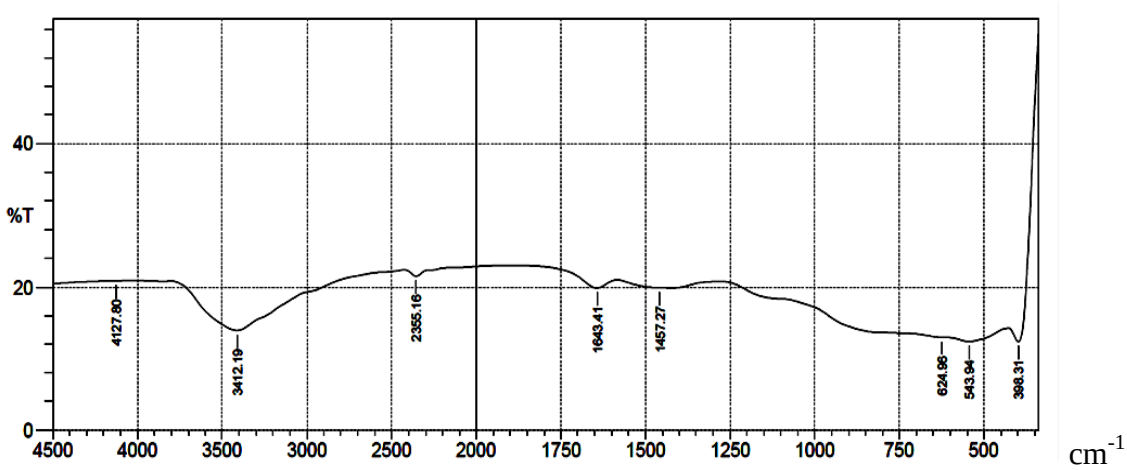


Figure A.18: FT-IR spectroscopy of deactivated B at 500^{o}C for 8 hours calcinations

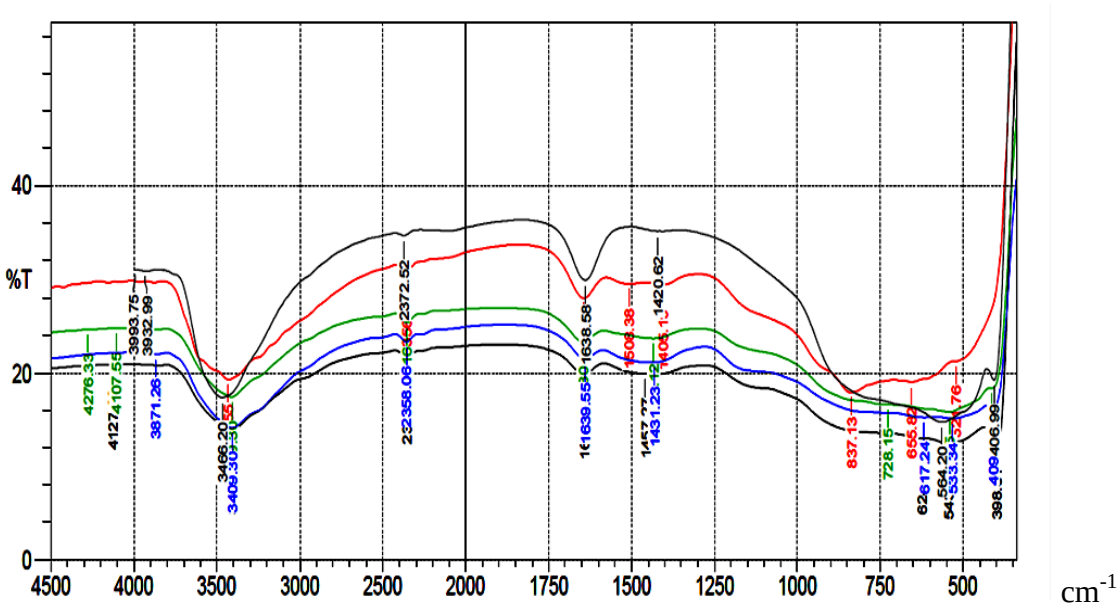


Figure A.19: FT-IR spectroscopy of fresh, deactivated B at 500°C for 2, 4, 6 and 8 hours calcinations

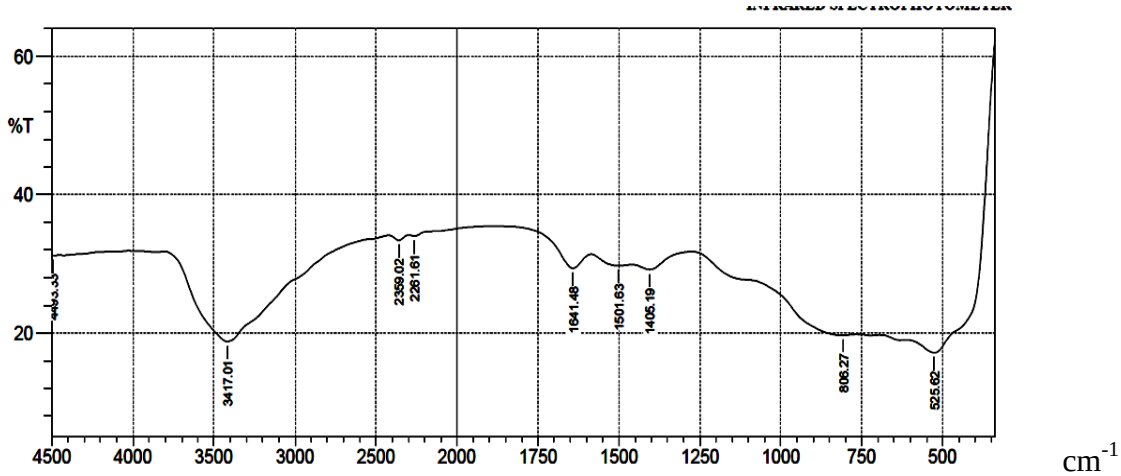


Figure A.20: FT-IR spectroscopy analysis of regenerated deactivated A.

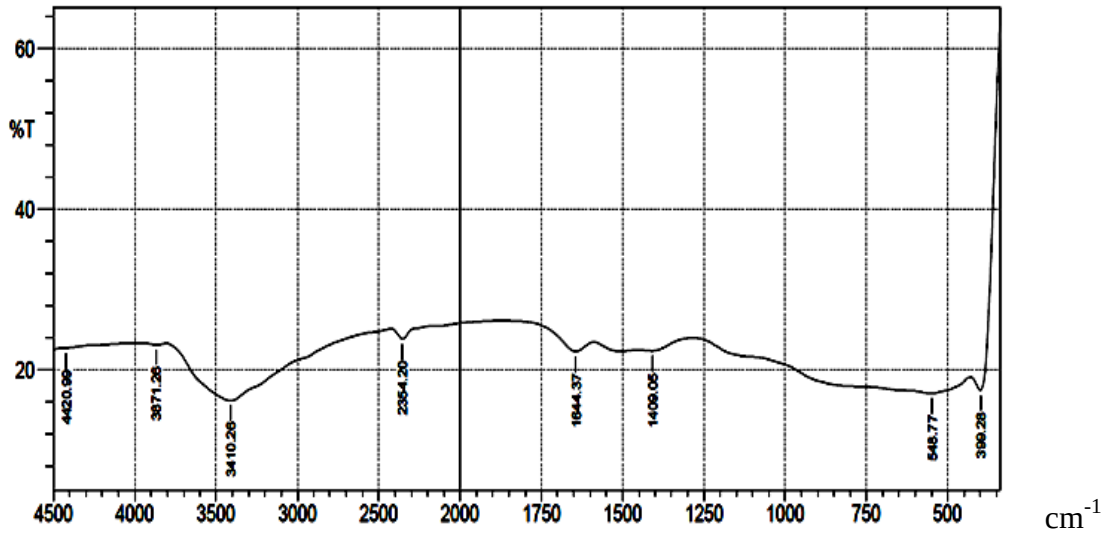


Figure A.21: FT-IR spectroscopy analysis of regenerated deactivated B.

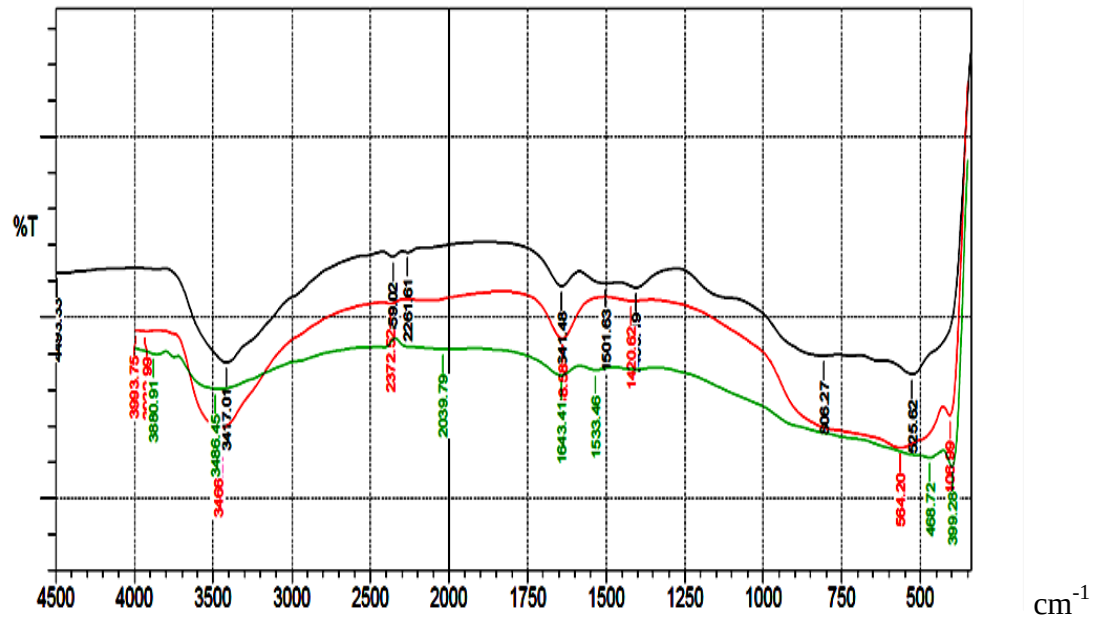


Figure A.22: FT-IR spectroscopy analysis of fresh, deactivated A and regenerated deactivated A catalyst.

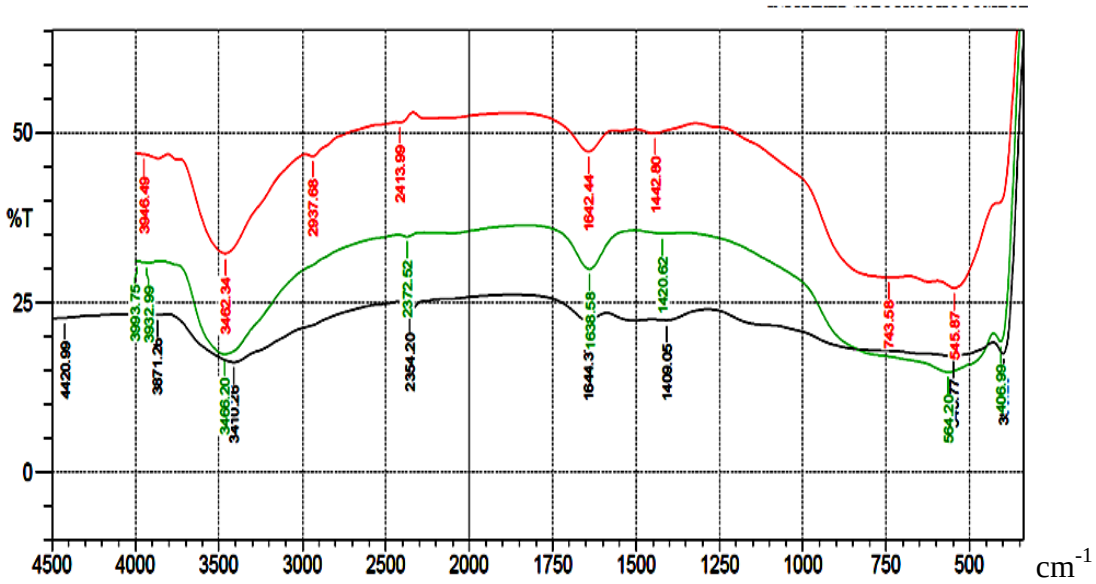


Figure A.23: FT-IR spectroscopy analysis of fresh, deactivated B and regenerated deactivated B catalyst.

Appendix B

B.1 CATALYST PERFORMANCE EVALUATIONS

Tables B. gives the summarized GC-MS results of the reformate samples, with the feed (treated heavy naphtha)

Table B.1: Summarized GC-MS results for the feed (treated heavy naphtha)

Rxn Temp (^oC)	Composition of the reformate as analyzed with a GC-MS Machine					
		Percentage of chromatogram area assigned to component				
	Sample compositions	**Individual (%)**	**Paraffin**	**Total Iso-paraffins (%)**	**Total Aromatics (%)**	**Yield of reformate (%)**
465	Ethyl cyclopentane	0.43	12.48	78.32	8.42	86.74
465	5-methyl-1-heptene	1.61				
465	Cis-1,2-Dimethylcyclopentane	2.28				
465	2-methylheptane	5.08				
465	3-Ethyl-2-methylhexane	1.78				
465	1,2-Dimethyl cyclohexane	2.60				
465	Cis-1-Ethyl-3-methyl cyclopentane	2.31				
465	1-Ethyl-2-methyl cyclopentane	2.47				
465	n-octane	4.07				
465	1,4-dimethyl cyclohexane	1.93				
465	2,2,3-trimethylhexane	1.12				
465	2,4-Dimethylheptane	1.49				
465	Cis-1,2-Dimethylcyclohexane	4.77				
465	1,3,5-trimethylcyclohexane	4.30				
465	Isononane	8.80				
465	3-methyl octane	2.49				
465	Cis-1-Ethyl-4-methyl cyclohexane	4.50				
465	n-nonane	6.83				
	cyclohxylethylalcohol	5.23				
465	Isopropylcyclohexane	4.35				
465	2,6-Dimethyl octane	4.25				
465	2-methyl-3-ethyl alcohol	2.07				
465	5-methyl decane	2.52				
465	2-methyl nonane	3.74				
465	4-methyl-1-decene	2.34				
465	2,3,5,8-tetramethyl decane	5.50				
465	5-ethyl-2-methylheptane	3.74				
465	Isobutylcyclohexane	1.85				
465	1-p-menthene	2.72				
465	P-mentha-1,8-dien-6-ol	0.47				
465	n-Decane	1.58				

Table B.2: Summarized GC-MS results for reactor packed with fresh catalyst

Rxn Temp (^oC)	Composition of the reformate as analyzed with a GC-MS Machine					
		Percentage of chromatogram area assigned to component				
	Sample compositions	**Individual (%)**	**Paraffin**	**Total Iso-paraffins (%)**	**Total Aromatics (%)**	**Yield of reformate (%)**
465	2,2,3-trimethylbutane	1.57	8.72	83.83	6.8	90.63
465	1,2,4-trimethylcyclopentane	1.37				
465	3-methyl-heptene	2.64				
465	4,5-dimethyl octane	5.58				
465	2,3,5-trimethylhexane	2.04				
465	1,2,-dimethylcyclohexane	2.65				
465	1-Ethyl-2-methyl cyclopentane	2.74				
465	n-octane	4.61				
465	P-Dimethylcyclohexanehane	2.40				
465	2,2-Dimethyl heptane	1.51				
465	Isononane	2.10				
465	2,4-Dimethyl decane	5.96				
465	1-cyclopentylpropane	4.31				
465	1,1,3-trimethylcyclohexane	2.27				
465	1,1,5-trimethylcyclohexane	3.24				
465	Nonene	3.55				
465	4-methyl octane	9.23				
465	Isoctane	2.29				
465	1-trans 2,3-trimethylcyclo hexane	2.90				
465	Trans-1-Ethyl-4-methyl cyclohexane	3.29				
465	Isopropylcyclohexane	6.19				
465	1-methyl-3-propylcyclo octane	2.12				
465	3-cyclohexyl-1-propanol	4.15				
465	7-Methyltridecane	3.39				
465	3-methyl nonane	3.10				
465	3-Methyl-3-ethyl heptane	2.07				
465	2,5-dimethyl octane	3.65				
465	1,2,3-trimethyl benzene	2.24				
465	n-Decane	3.79				
465	4-methyl decane	2.14				
465	3-ethyl-o-xylene	0.41				
465	Hendecane	0.32				

Table B.3: Summarized GC-MS results for reactor packed with deactivated A catalyst

Rxn Temp (^oC)	Composition of the reformate as analyzed with a GC-MS Machine					
	Sample compositions	**Percentage of chromatogram area assigned to component Individual (%)**	**Paraffin**	**Total Iso-paraffins (%)**	**Total Aromatics (%)**	**Yield of reformate (%)**
465	Ethyl cyclopentane	0.44	29.28	22.46	3.48	25.94
465	1,2,4-trimethylcyclopentane	1.47				
465	4-methylheptane	0.97				
465	2,2,3-trimethyl butane	2.34				
465	1,4-dimethylcyclohexane	1.05				
465	1-methyl-1-ethylcyclopentane	0.50				
465	1,2,3-Trimethyl cyclohexane	1.30				
465	n-Octane	11.43				
465	cis-1,4-Dimethylcyclohexane	0.87				
465	2-methyloctane	2.09				
465	Iso nonane	6.78				
465	3-methyl octane	1.29				
465	Cis-ethyl-4-methylcyclohexane	1.47				
465	n-nonane	6.96				
465	Bromocycloheptane	1.18				
465	Propylcyclohexane	2.25				
465	n-propylcyclohexane	1.14				
465	2,6-Dimethyl octane	3.45				
465	2-methyl-3-ethylheptane	1.37				
465	4-methyl nonane	1.65				
465	1,2,4-Trimethylbenzene	2.48				
465	n-Decane	4.11				
465	4-methyl decane	0.74				
465	Isobutylcyclohexane	0.26				
465	2-methyl-p-ethyl toluene	0.34				
465	2,7-Dimethyl octane	0.24				
465	5,9-Dimethyl-2-decanone	0.36				

Table B.4: Summarized GC-MS results for reactor packed with deactivated B catalyst

Rxn Temp (^oC)	Composition of the reformate as analyzed with a GC-MS Machine					
		Percentage of chromatogram area assigned to component				
	Sample compositions	**Individual (%)**	**Paraffin**	**Total Iso-paraffins (%)**	**Total Aromatics (%)**	**Yield of reformate (%)**
465	2,2-Dimethylhexane	1.31	22.63	52.07	7.15	59.22
465	2-Ethyl-1-methyl-1-pentene	1.69				
465	1,2-Diethylcyclobutane	3.20				
465	4,5-dimethyl octane	4.04				
465	3,4,5-trimethylheptane	5.72				
465	1,4,-dimethylcyclohexane	3.61				
465	n-octane	12.02				
465	cis-1,4-Dimethylcyclohexane	3.02				
465	3,5,5-trimethyl-1-hexene	1.52				
465	Isononane	2.24				
465	cis-1,2-Dimethylcyclohexane	3.00				
465	Ethylcyclohexane	4.04				
465	3-methyloctane	5.71				
465	1,2-Dimethylbenzene	1.10				
465	n-Nonane	6.80				
465	Hexahydocumene	4.28				
465	Propylcyclohexane	3.20				
465	3-methyl nonane	3.07				
465	2-methyl-3-ethylheptane	2.23				
465	2,2,3,3-tetramethylpentane	3.51				
465	1,2,3-trimethylbenzene	2.35				
465	n-Decane	3.81				
465	4-methyldecane	2.43				
465	Isobutylcyclohexane	0.62				
465	p-xylene	0.52				
465	Tridecane	0.40				

Table B.5: Summarized GC-MS results for reactor packed with regenerated deactivated A catalyst

Rxn Temp (^oC)	Composition of the reformate as analyzed with a GC-MS Machine					
		Percentage of chromatogram area assigned to component				
	Sample compositions	**Individual (%)**	**Paraffin(%)**	**Total Iso-paraffins (%)**	**Total Aromatics (%)**	**Yield of reformate (%)**
465	2,2,3,4-tetramethylpentane	1.42	16.06	50.00	5.68	55.68
465	2-Ethyl-1-hexene	1.20				
465	Isopropyl ketone	1.46				
465	2,3-dimethyl hexane	3.83				
465	3-methylheptane	2.00				
465	1,2,-dimethylcyclohexane	1.74				
465	Cis-2-octene	1.80				
465	n-octane	4.79				
465	Diisobutyl	2.50				
465	1,2,4-trimethylcyclopentane	1.52				
465	Cis-1-Ethyl-2-methylcyclopentane	1.15				
465	2,6-Dimethylheptane	3.08				
465	2-methyl-1-cyclohexanone	1.43				
465	1,2,3-trimethylcyclohexane	1.59				
465	1,2-Dimethylcyclopentane	2.21				
465	Isononane	5.58				
465	3-methyloctane	2.60				
465	Bromocycloheptane	1.76				
465	n-nonane	0.67				
465	Cis-1-Ethyl-,4-methylcyclo hexane	2.09				
465	Propylcyclohexane	2.33				
465	3-methylnonane	2.59				
465	2,6-dimethyloctane	2.46				
465	2-methyl-3-ethyl heptane	2.34				
465	2,5-Dimethyloctane	2.94				
465	1,2,4-trimethylbenzene	0.54				
465	n-Decane	4.23				
465	4-methyl decane	2.50				
465	Isobutylcyclohexane	0.55				
465	3,7-Dimethyl-6-octen-1-yn-3-ol	0.49				
465	n-Tridecane	0.37				

Table B.6: Summarized GC-MS results for reactor packed with regenerated deactivated B catalyst

Rxn Temp (^oC)	Composition of the reformate as analyzed with a GC-MS Machine					
		Percentage of chromatogram area assigned to component				
	Sample compositions	**Individual (%)**	**Paraffin**	**Total Iso-paraffins (%)**	**Total Aromatics (%)**	**Yield of reformate (%)**
465	2,4-Dimethylhexane	0.97	11.88	79.11	9.0	88.11
465	2-Ethyl-1-octene	1.67				
465	1,1,2-trimethylcyclopentene	2.98				
465	4,5-dimethyl octane	5.55				
465	2,3-dimethylheptane	2.92				
465	1,2,-dimethylcyclohexane	2.83				
465	1-Ethyl-2-methyl cyclopentane	2.91				
465	1-methyl-3-ethylcyclopentane	2.71				
465	n-octane	4.13				
465	3,5,5-trimrtyl-1-hexene	1.47				
465	Isononane	2.08				
465	Cis-1,4-Dimethylcyclohexane	5.75				
465	Cis-3,5-Dimethylcyclohexane	4.01				
465	3-methyloctane	2.22				
465	2,3,5-trimethylhexane	3.46				
465	4-methyloctane	9.35				
465	3-methyl octane	2.59				
465	1,3,5-trimethylcyclohexane	2.98				
465	Bromocycloheptane	3.52				
465	n-nonane	6.56				
465	Trans -1-Ethyl-,4-methylcyclo hexane	2.17				
465	n-decane	1.19				
465	n-propylcyclohexane	4.42				
465	Isopropylcyclohexane	3.41				
465	3-Ethyl-2-methylheptane	2.24				
465	4-methyl nonane	3.78				
465	1,2,4-trimethyl benzene	2.08				
465	m-Ethylmethylbenzene	2.43				
465	2,7-dimethyloctane	3.90				
465	4-methyldecane	2.35				
465	Isobytylcyclohexane	0.52				
465	p-xylene	0.48				
465	2,9-Dimethyldecane	0.36				

Tables C are extensions of Tables B.2 to B.6; each with an additional column containing the weight percentage of the dry volatile gases (the byproducts) which could not be captured along with the collected samples. The uniform weight percent (14.5wt %) assigned to the dry gases was referenced from Kalra (2009). Thus, the actual products captured/collected (isoparaffins, aromatics, with the paraffins) were taken (converted) to be 85.5 % of the total products (dry volatile gases inclusive). The values in brackets, in Table C, were the raw data extracted from the GC-MS Results, while the values directly above them were the converted values having included the dry gases in the products' compositions.

Appendix C

Estimated products composition (summarized GC-MS results for the feed and for the reformates got from reactor packed with catalyst)

Table C.1: Summarized GC-MS results for the reformates got from reactor packed with fresh catalyst

Rxn Temp (^oC)	Composition of the products inclusive of the volatile gases							
		Percentage assigned to component						
		Individual (%)	**Total Paraffins (%)**	**Total Iso-paraffins (%)**	**Total Aromatics (%)**	**Net reformate Product (%)**	**Dry volatile gases= X (%)**	**Yield of reformate (%)**
465	2,2,3-trimethylbutane	1.57	7.45	71.67	5.81	77.48	14.5	84.24
465	1,2,4-trimethylcyclopentane	1.37	**(8.72)**	**(83.83)**	**(6.80)**			
465	3-methyl-heptene	2.64						
465	4,5-dimethyl octane	5.58						
465	2,3,5-trimethylhexane	2.04						
465	1,2,-dimethylcyclohexane	2.65						
465	1-Ethyl-2-methyl cyclopentane	2.74						
465	n-octane	4.61						
465	P-Dimethylcyclohexanehane	2.40						
465	2,2-Dimethyl heptane	1.51						
465	Isononane	2.10						
465	2,4-Dimethyl decane	5.96						
465	1-cyclopentylpropane	4.31						
465	1,1,3-trimethylcyclohexane	2.27						
465	1,1,5-trimethylcyclohexane	3.24						
465	Nonene	3.55						
465	4-methyl octane	9.23						
465	Isoctane	2.29						
465	1-trans 2,3-trimethylcyclo hexane	2.90						
465	Trans-1-Ethyl-4-methyl cyclohexane	3.29						
465	Isopropylcyclohexane	6.19						
465	1-methyl-3-propylcyclo octane	2.12						
465	3-cyclohexyl-1-propanol	4.15						
465	7-Methyltridecane	3.39						
465	3-methyl nonane	3.10						
465	3-Methyl-3-ethyl heptane	2.07						
465	2,5-dimethyl octane	3.65						
465	1,2,3-trimethyl benzene	2.24						
465	n-Decane	3.79						
465	4-methyl decane	2.14						
465	3-ethyl-o-xylene	0.41						
465	Hendecane	0.32						

Table C.2: Summarized GC-MS results for the reformates got from reactor packed with deactivated A catalyst

Rxn Temp (^oC)	Composition of the products inclusive of the volatile gases							
		Percentage assigned to component						
		Individ-ual (%)	**Total Paraffins (%)**	**Total Iso-paraffins (%)**	**Total Aromatics (%)**	**Net reformate Product (%)**	**Dry volatile gases= X (%)**	**Yield of reformate (%)**
465	Ethyl cyclopentane	0.44	25.03	19.20	2.98	22.18	14.5	60.47
465	1,2,4-trimethylcyclopentane	1.47	**(29.28)**	**(22.46)**	**(3.48)**			
465	4-methylheptane	0.97						
465	2,2,3-trimethyl butane	2.34						
465	1,4-dimethylcyclohexane	1.05						
465	1-methyl-1-ethylcyclopentane	0.50						
465	1,2,3-Trimethyl cyclohexane	1.30						
465	n-Octane	11.43						
465	cis-1,4-Dimethylcyclohexane	0.87						
465	2-methyloctane	2.09						
465	Iso nonane	6.78						
465	3-methyl octane	1.29						
465	Cis-ethyl-4-methylcyclohexane	1.47						
465	n-nonane	6.96						
465	Bromocycloheptane	1.18						
465	Propylcyclohexane	2.25						
465	n-propylcyclohexane	1.14						
465	2,6-Dimethyl octane	3.45						
465	2-methyl-3-ethylheptane	1.37						
465	4-methyl nonane	1.65						
465	1,2,4-Trimethylbenzene	2.48						
465	n-Decane	4.11						
465	4-methyl decane	0.74						
465	Isobutylcyclohexane	0.26						
465	2-methyl-p-ethyl toluene	0.34						
465	2,7-Dimethyl octane	0.24						
465	5,9-Dimethyl-2-decanone	0.36						

Table C.3: Summarized GC-MS results for the reformates got from reactor packed with deactivated B catalyst

Rxn Temp (^oC)	Composition of the products inclusive of the volatile gases							
		Percentage assigned to component						
		Individual (%)	**Total Paraffins (%)**	**Total Iso-paraffins (%)**	**Total Aromatics (%)**	**Net reformate Product (%)**	**Dry volatile gases= X (%)**	**Yield of reformate (%)**
465	2,2-Dimethylhexane	1.31	19.35	44.52	6.11	50.63	14.5	77.74
465	2-Ethyl-1-methyl-1-pentene	1.69	**(22.63)**	**(69.61)**	**(7.15)**			
465	1,2-Diethylcyclobutane	3.20						
465	4,5-dimethyl octane	4.04						
465	3,4,5-trimethylheptane	5.72						
465	1,4,-dimethylcyclohexane	3.61						
465	n-octane	12.02						
465	cis-1,4-Dimethylcyclohexane	3.02						
465	3,5,5-trimethyl-1-hexene	1.52						
465	Isononane	2.24						
465	cis-1,2-Dimethylcyclohexane	3.00						
465	Ethylcyclohexane	4.04						
465	3-methyloctane	5.71						
465	1,2-Dimethylbenzene	1.10						
465	n-Nonane	6.80						
465	Hexahydocumene	4.28						
465	Propylcyclohexane	3.20						
465	3-methyl nonane	3.07						
465	2-methyl-3-ethylheptane	2.23						
465	2,2,3,3-tetramethylpentane	3.51						
465	1,2,3-trimethylbenzene	2.35						
465	n-Decane	3.81						
465	4-methyldecane	2.43						
465	Isobutylcyclohexane	0.62						
465	p-xylene	0.52						
465	Tridecane	0.40						

Table C.4: Summarized GC-MS results for the reformates got from reactor packed with regenerated deactivated A catalyst

Rxn Temp (^{o}C)	Composition of the products inclusive of the volatile gases							
		Percentage assigned to component						
		Individual (%)	**Total Paraffins (%)**	**Total Iso-paraffins (%)**	**Total Aromatics (%)**	**Net reformate Product (%)**	**Dry volatile gases= X (%)**	**Yield of reformate (%)**
465	2,2,3,4-tetramethylpentane	1.42	13.73	42.75	4.86	47.61	14.5	76.65
465	2-Ethyl-1-hexene	1.20	**(16.06)**	**(50.00)**	**(5.68)**			
465	Isopropyl ketone	1.46						
465	2,3-dimethyl hexane	3.83						
465	3-methylheptane	2.00						
465	1,2,-dimethylcyclohexane	1.74						
465	Cis-2-octene	1.80						
465	n-octane	4.79						
465	Diisobutyl	2.50						
465	1,2,4-trimethylcyclopentane	1.52						
465	Cis-1-Ethyl-2-methylcyclopentane	1.15						
465	2,6-Dimethylheptane	3.08						
465	2-methyl-1-cyclohexanone	1.43						
465	1,2,3-trimethylcyclohexane	1.59						
465	1,2-Dimethylcyclopentane	2.21						
465	Isononane	5.58						
465	3-methyloctane	2.60						
465	Bromocycloheptane	1.76						
465	n-nonane	0.67						
465	Cis-1-Ethyl-,4-methylcyclo hexane	2.09						
465	Propylcyclohexane	2.33						
465	3-methylnonane	2.59						
465	2,6-dimethyloctane	2.46						
465	2-methyl-3-ethyl heptane	2.34						
465	2,5-Dimethyloctane	2.94						
465	1,2,4-trimethylbenzene	0.54						
465	n-Decane	4.23						
465	4-methyl decane	2.50						
465	Isobutylcyclohexane	0.55						
465	3,7-Dimethyl-6-octen-1-yn-3-ol	0.49						
465	n-Tridecane	0.37						

Table C.5: Summarized GC-MS results for the reformates got from reactor packed with regenerated deactivated B catalyst

Rxn Temp (^{o}C)	Composition of the products inclusive of the volatile gases							
		Percentage assigned to component						
		Individual (%)	**Total Paraffins (%)**	**Total Iso-paraffins (%)**	**Total Aromatics (%)**	**Net reformate Product (%)**	**Dry volatile gases= X (%)**	**Yield of reformate (%)**
465	2,4-Dimethylhexane	0.97	10.16	67.64	7.70	75.34	14.5	83.86
465	2-Ethyl-1-octene	1.67	**(11.88)**	**(79.11)**	**(9.00)**			
465	1,1,2-trimethylcyclopentene	2.98						
465	4,5-dimethyl octane	5.55						
465	2,3-dimethylheptane	2.92						
465	1,2,-dimethylcyclohexane	2.83						
465	1-Ethyl-2-methyl cyclopentane	2.91						
465	1-methyl-3-ethylcyclopentane	2.71						
465	n-octane	4.13						
465	3,5,5-trimrtyl-1-hexene	1.47						
465	Isononane	2.08						
465	Cis-1,4-Dimethylcyclohexane	5.75						
465	Cis-3,5-Dimethylcyclohexane	4.01						
465	3-methyloctane	2.22						
465	2,3,5-trimethylhexane	3.46						
465	4-methyloctane	9.35						
465	3-methyl octane	2.59						
465	1,3,5-trimethylcyclohexane	2.98						
465	Bromocycloheptane	3.52						
465	n-nonane	6.56						
465	Trans -1-Ethyl-,4-methylcyclo hexane	2.17						
465	n-decane	1.19						
465	n-propylcyclohexane	4.42						
465	Isopropylcyclohexane	3.41						
465	3-Ethyl-2-methylheptane	2.24						
465	4-methyl nonane	3.78						
465	1,2,4-trimethyl benzene	2.08						
465	m-Ethylmethylbenzene	2.43						
465	2,7-dimethyloctane	3.90						
465	4-methyldecane	2.35						
465	Isobytylcyclohexane	0.52						
465	p-xylene	0.48						
465	2,9-Dimethyldecane	0.36						

Table C.6: Typical product yields in a CRU operation

Products	**Wt %**	**Average Wt %**	**Details**
H_2 Rich gas	6.5-8.0	7.25	X = 7.25+7.25=14.5 %
LPG	2.5-12	7.25	(X = Dry volatile gases: C_1, C_2, C_3, C_4)
Reformate	80-91	85.50	R = Reformate
			f = Converted feed,
			N = Unconverted feed
			Let F be the Treated heavy naphtha fed to the reactor
			Let f be the Treated heavy naphtha consumed.
			$F = f + N = R + X + N$
			$f = R + X$

The first two columns in the above table were extracted from the work of Kalra (2009), while the other columns are deductions made therein.

From Table C, *R, X, N* are the products of reforming. Thus, the yield of the desired product *R* can be quantified as

$$Yield = \frac{R}{f} = \left(\frac{R}{R + X} \right) \times 100\,\%$$

Where $X = 14.50$

The percentage yield (Y_R) of reformates for each run/sample is:

$$Y_R = \frac{R}{\text{Treated heavy naphtha} \quad consumed} \times 100\% = \left(\frac{R}{X + R} \right) \times 100\%$$

For Fresh catalyst

$$Y_R = \left(\frac{77.48}{14.5 + 77.48} \right) \times 100\% = 84.24\%$$

For Deactivated A catalyst

$$Y_R = \left(\frac{22.18}{14.5 + 22.18} \right) \times 100\% = 60.47\%$$

For Deactivated B catalyst

$$Y_R = \left(\frac{50.63}{14.5 + 50.63} \right) \times 100\% = 77.74\%$$

For Regenerated Deactivated A catalyst

$$Y_R = \left(\frac{47.61}{14.5 + 47.61} \right) \times 100\% = 76.65\%$$

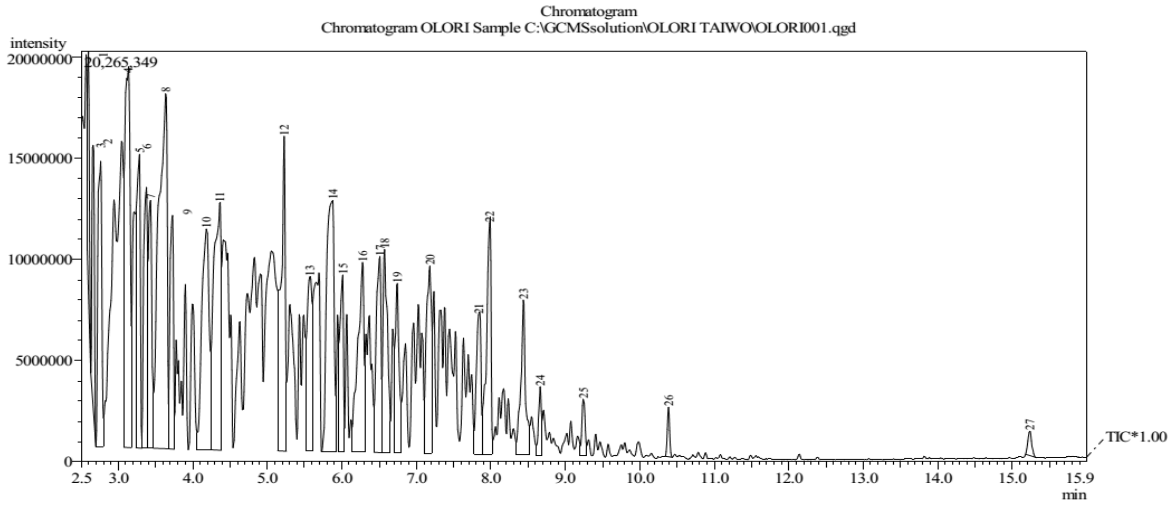
For Regenerated Deactivated B catalyst

$$Y_R = \left(\frac{75.34}{14.5 + 75.34} \right) \times 100\% = 83.86\%$$

GCMS-QP2010 PLUS
SHIMADZU,JAPAN

NARICT, ZARIA
GCMS ANALYSIS

OLORI TAIWO [SAMPLE- SPENT A]



[Comment]

====== Analytical Line 1 ======

[AOC-20i]

# of Rinses with Presolvent	:4
# of Rinses with Solvent(post)	:4
# of Rinses with Sample	:3
Plunger Speed(Suction)	:High
Viscosity Comp. Time	:0.2 sec
Plunger Speed(Injection)	:High
Syringe Insertion Speed	:High
Injection Mode	:Normal
Pumping Times	:5
Inj. Port Dwell Time	:0.3 sec
Terminal Air Gap	:No
Plunger Washing Speed	:High
Washing Volume	:8uL
Syringe Suction Position	:0.0 mm
Syringe Injection Position	:0.0 mm
Use 3 Solvent Vial	:1 vial

[GC-2010]

Column Oven Temp.	:60.0 ℃
Injection Temp.	:150.00 ℃
Injection Mode	:Split
Flow Control Mode	:Linear Velocity
Pressure	:112.8 kPa
Total Flow	:41.2 mL/min
Column Flow	:1.82 mL/min
Linear Velocity	:49.2 cm/sec
Purge Flow	:3.0 mL/min
Split Ratio	:20.0
High Pressure Injection	:OFF
Carrier Gas Saver	:OFF
Splitter Hold	:OFF

Oven Temp. Program

Rate	Temperature(℃)	Hold Time(min)
-	60.0	4.00
10.00	100.0	2.00
15.00	200.0	2.00



Plate A.1: Transducer with a thermocouple wire to check temperature difference.